Silencing of endoglin in rat *hepatic stellate cells*
by RNA interference
identifies endoglin as an important component of the transdifferentiation process

Von der Fakultät für Mathematik, Informatik und Naturwissenschaften der RWTH Aachen University zur Erlangung des akademischen Grades einer Doktorin der Naturwissenschaften genehmigte Dissertation

vorgelegt von

Diplom-Biochemikerin

Wanda Nicolette Vreden

aus Duisburg

Berichter: Privatdozent Dr. rer. nat Christoph Peterhänsel
Universitätsprofessor Dr. rer. nat Ralf Weiskirchen

Tag der mündlichen Prüfung: 24.06.2008

Diese Dissertation ist auf den Internetseiten der Hochschulbibliothek online verfügbar.

Die vorliegende Doktorarbeit wurde in der Zeit vom 15. Februar 2005 bis zum 4. April 2008 im Institut für Klinische Chemie und Pathobiochemie angefertigt und ist in englischer Sprache verfasst.

Referent:
PD. Dr. rer. nat. C. Peterhänsel
Institute for Biology I
Rheinisch-Westfälische Hochschule Aachen (Germany)

Co-Referent:
Prof. Dr. rer. nat. R. Weiskirchen
Institute of Clinical Chemistry and Pathobiochemistry
University Hospital Aachen (Germany)

Co-Referent:
Prof. Dr. rer. nat. F.M. Kreuzaler
Institute for Biology I
Rheinisch-Westfälische Hochschule Aachen (Germany)

Für meine Lieben!

Contents

1 Introduction **1**

1.1 Signal transduction . . . 2

1.1.1 General principles of signal transduction . . . 2

1.1.2 The TGF-β pathway . . . 2

1.2 Endoglin . . . 5

1.2.1 Structure of endoglin . . . 5

1.2.2 Function of endoglin . . . 7

1.3 The Liver . . . 10

1.3.1 Function and anatomy of the liver . . . 10

1.3.2 Function of HSC during liver fibrogenesis . . . 10

1.4 RNAi . . . 14

1.4.1 RNAi as an experimental tool for sequence specific gene silencing 14

2 Materials and methods **18**

2.1 Plastic ware . . . 18

2.2 Equipment . . . 19

2.3 Chemicals . . . 20

2.4 Radioactive materials . . . 23

2.5 Enzymes . . . 23

2.6 Molecular size standards . . . 24

2.7 Cytokines . . . 24

2.8 Multicomponent systems . . . 25

2.9 Antibodies . . . 25

2.9.1 First antibodies . . . 25

2.9.2 Secondary antibodies . . . 26

2.10 Microorganisms . . . 27
2.10.1 Adenoviruses used in this study . . . 27
2.10.2 *E. coli* strains used in this study . . . 27
2.10.3 Eucaryotic cells used in this study . . . 28
2.11 Oligonucleotides . . . 28
2.12 Oligonucleotides for gene silencing . . . 29
2.13 Plasmids . . . 31
2.14 Solutions and buffers . . . 31
2.15 Media for cell culture . . . 36
2.16 Analytical methods . . . 38
2.16.1 Calculation of DNA concentration . . . 38
2.16.2 Calculation of RNA concentration . . . 38
2.16.3 Calculation of adenoviral stock concentration . . . 38
2.16.4 Calculation of protein concentration . . . 39
2.17 Cell culture methods . . . 39
2.17.1 Culture conditions of *E. coli* . . . 39
2.17.2 Culture conditions of COS-7 . . . 39
2.17.3 Coverglass preparation for microscopy . . . 39
2.17.4 Isolation of rat *hepatic stellate cells* . . . 39
2.17.5 Culture conditions of rat *hepatic stellate cells* . . . 40
2.17.6 Stimulation of rat *hepatic stellate cells* . . . 40
2.18 Biochemical methods . . . 41
2.18.1 Preparation of total protein lysate from rat *hepatic stellate cells* . . . 41
2.18.2 SDS polyacrylamide gel electrophoresis . . . 41
2.18.3 Western blot . . . 41
2.18.4 Luciferase assay . . . 42
2.18.5 Proliferation assay . . . 42
2.18.6 Gelatinase assay . . . 42
2.19 Molecular biological methods . . . 43
2.19.1 Isolation of plasmid DNA (Miniprep) . . . 43
2.19.2 Isolation of RNA . . . 43
2.19.3 Formaldehyde agarose gel electrophoresis . . . 43
2.19.4 Northern blot . . . 44
2.19.5 cDNA synthesis . . . 45

2.19.6 Polymerase chain reaction (PCR) . . . 46
2.19.7 DNA sequencing . . . 46
2.19.8 Cloning . . . 47
2.19.9 Transformation . . . 49
2.19.10 Transfection . . . 49
2.19.11 Infection . . . 50
2.20 Adenoviruses . . . 50
2.20.1 Generation of the shRNA expression vector . . . 50
2.20.2 Generation of the $(BRE)_2$ and $(CAGA)_{12}$MLP luciferase shuttle vectors . . . 51
2.20.3 Production and amplification of adenoviral stocks . . . 51
2.20.4 Purification of adenoviral stocks . . . 52
2.20.5 CRP2-adenovirus . . . 53
2.21 Whole rat genome oligo microarray . . . 53
2.21.1 Sample preparation and quality check . . . 53
2.21.2 Hybridization . . . 53
2.21.3 Data analysis . . . 54
2.22 Microscopy . . . 54
2.22.1 Bright field microscopy . . . 54
2.22.2 Immunofluorescence microscopy . . . 55

3 Results **56**
3.1 RNAi - Inhibition of endoglin expression in HSC . . . 57
3.1.1 shRNA virus . . . 58
3.1.2 siRNA oligonucleotides . . . 58
3.1.3 Knock down of endoglin in HSC . . . 62
3.2 Characterization of endoglin deficient HSC . . . 64
3.2.1 Morphology and ECM abundance . . . 64
3.2.2 Cytoskeleton organization . . . 67
3.2.3 Migration . . . 72
3.2.4 Proliferation . . . 73
3.2.5 Whole genome microarray . . . 74
3.2.6 Summary: Characterization of endoglin deficient HSC . . . 81
3.3 α_2-Macroglobulin . . . 82

3.3.1 α_2-Macroglobulin down-regulation through endoglin silencing . 82
3.3.2 Gelatinase and collagenase assay 84
3.3.3 siRNA targeting α_2-macroglobulin 86
3.4 Stimulation Assays 88
3.4.1 TGF-β1 and BMP-7 stimulation experiments 88

4 Discussion **92**
4.1 Down-regulation of endoglin 92
4.2 The impact of endoglin down-regulation on HSC transdifferentiation . . 95
4.3 The role of endoglin in the TGF-β1 and BMP-7 pathways 100

5 Conclusions **103**

Appendix

A Selected candidate gene list **104**

B Vector maps **107**

C Thanks **124**

D List of abbreviations **126**

E Bibliography **129**

F Curriculum Vitae **144**

List of Figures

1.1 General principles of signal transduction 3
1.2 The TGF-β pathway 6
1.3 Structure of endoglin 8
1.4 Normal liver *vs.* liver with advanced fibrosis 11
1.5 Transdifferentiation of HSC 13
1.6 RNAi as an experimental tool for sequence specific gene silencing 15

3.1 Strategy 57
3.2 Testing shRNA 59
3.3 Testing siRNA oligonucleotides 61
3.4 siRNA mediated silencing of endoglin 63
3.5 Endoglin silencing at an early time point of transdifferentiation I 65
3.6 Endoglin silencing at an early time point of transdifferentiation II 66
3.7 Endoglin silencing at later time points of transdifferentiation 68
3.8 Re-arrangement of the cytoskeleton 70
3.9 Re-arrangement of the cytoskeleton in endoglin deficient HSC 71
3.10 Migration assay 72
3.11 BrdU and ^{3}H-thymidine proliferation assay 74
3.12 RNA quality check 76
3.13 Whole genome cDNA microarray 78
3.14 Pathway analysis 80
3.15 Transdifferentiation of HSC *vs.* HSC transfected with siEng 81
3.16 α_2-Macroglobulin in endoglin deficient HSC 83
3.17 Gelatinase assay 85
3.18 Silencing of α_2-macroglobulin 87

3.19 $(CAGA)_{12}$MLP-luciferase and $(BRE)_2$-luciferase tests 89
3.20 Smad1/3 activation 90

B.1 Shuttle vector pENTR/U6 108
B.2 Shuttle vector pENTR/U6 plus shRNA 109
B.3 Shuttle vector pENTR4 110
B.4 Shuttle vector pENTR4 plus $(CAGA)_{12}$MLP-luciferase 111
B.5 Shuttle vector pENTR4 plus $(BRE)_2$-luciferase 112
B.6 Destination vector 113
B.7 Destination vector plus shRNA 114
B.8 Destination vector plus $(CAGA)_{12}$MLP-luciferase 115
B.9 Destination vector plus $(BRE)_2$-luciferase 116
B.10 pGEMT Easy 117
B.11 pGEMT Easy plus insert 118
B.12 pcDNA3.1 119
B.13 pcDNA plus endoglin 120
B.14 pGL3 basic vector 121
B.15 pGL3 plus $(CAGA)_{12}$MLP-luciferase 122
B.16 pGL3 plus $(BRE)_2$-luciferase 123

List of Tables

2.1 Plastic ware . . . 19
2.2 Equipment . . . 20
2.3 Chemicals . . . 23
2.4 Radioactive materials . . . 23
2.5 Enzymes . . . 24
2.6 Molecular size standards . . . 24
2.7 Cytokines . . . 24
2.8 Multicomponent systems . . . 25
2.9 First antibodies . . . 26
2.10 Secondary antibodies . . . 26
2.11 Adenoviral strains used to infect *hepatic stellate cells* . . . 27
2.12 *E. coli* strains used in this study . . . 27
2.13 Eucaryotic cells used in this study . . . 28
2.14 Oligonucleotides used for sequencing . . . 28
2.15 Oligonucleotides used for PCR . . . 29
2.16 Oligonucleotides used to generate the hybridization probes . . . 29
2.17 siRNA oligonucleotides used for gene silencing . . . 30
2.18 Oligonucleotides used to generate the shRNA viruses . . . 30
2.19 Plasmids used in this study . . . 31
2.20 Buffers and solutions . . . 36
2.21 Media for *E. coli* . . . 36
2.22 Media for *hepatic stellate cells* . . . 37
2.23 Microarray hybridization schedule . . . 54

A.1 Selected candidate gene list . . . 106

Zusammenfassung

Primäres Ziel dieser Doktorarbeit war die funktionelle Charakterisierung von Endoglin im Transdifferenzierungsprozess von *Hepatischen Sternzellen* (HSC) zu Myofibroblasten ähnlichen Zellen (MFB). Die Transdifferenzierung von HSC zu MFB spielt eine wichtige Rolle in Wundheilungsprozessen der Leber sowie bei der Entstehung der Leberfibrose. Da Endoglin ein TGF-β Typ III Rezeptor ist und TGF-β1 wiederum das Schlüsselzytokin bei der Initiierung und Aufrechterhaltung der Transdifferenzierung darstellt, drängte sich die Frage auf, ob Endoglin einen Einfluss auf die Transdifferenzierung von HSC und somit auch einen Einfluss auf die Leberfibrose hat.

Um dieser Fragestellung nachzugehen, wurde eine für dieses Labor neue Methode etabliert. Bei dieser Methode handelt es sich um RNA Interferenz, mit der es möglich war, die Expression von Endoglin in *Hepatischen Sternzellen* durch siRNA Oligonukleotide sehr effizient zu inhibieren. Die Endoglin defizienten Zellen sowie die zugehörigen Kontrollzellen wurden anschließend hinsichtlich verschiedener Aspekte der Transdifferenzierung analysiert. Dabei konnte gezeigt werden, dass Endoglin defiziente HSC eine inhibierte Transdifferenzierung aufweisen. Dieses spiegelte sich in einer verminderten Anreicherung von ECM Komponenten, einem veränderten Aufbau des Zytoskeletts und einer verminderten Proliferation wider. Um weitere Mediatoren bestimmen zu können, die durch eine veränderte Expression den Phänotypen der Endoglin defizienten HSC mitbestimmen, wurde ein cDNA Microarray angefertigt. Aus diesem Array gingen u.a. α_2-Macroglobulin und ALK1 hervor, die aufgrund ihrer bekannten Funktionen möglicherweise eine wichtige Rolle bei der Manifestierung des Phänotypens einnehmen. Zuletzt wurde der Einfluss von Endoglin auf den TGF-β und den BMP-7 Signalweg untersucht, denn sowohl TGF-β1 als auch BMP-7 werden von Endoglin gebunden und nehmen eine wichtige Funktion in der Entstehung der Leberfibrose ein. Stimuliert wurde sowohl mit TGF-β1 als auch mit BMP-7. Als *Readout-System* diente der Western Blot und der Reporter-Gen-Assay.

Das Fazit dieser Arbeit ist: Endoglin spielt eine wichtige Rolle in der *in vitro* Transdifferenzierung von HSC zu MFB. Ein knock down von Endoglin führt zur Inhibierung der Transdifferenzierung und zu zahlreichen phänotypischen Veränderungen. Aufgrund dieser Feststellung ist zu vermuten, dass Endoglin ebenfalls eine wichtige Rolle bei der Entstehung der Leberfibrose einnimmt.

Summary

The main purpose of this doctoral thesis was the functional characterization of endoglin in hepatic stellate cells (HSC). This characterization was performed particularly with regard to the impact and the function of endoglin in the transdifferentiation process of HSC into myofibroblast-like cells (MFB). Transdifferentiation of HSC into MFB plays a crucial role in the wound healing process of the liver and is, thus, linked to the development of fibrosis. Endoglin functions as a TGF-β receptor and TGF-β, on the other hand, is a key regulator that initiates and perpetuates the transdifferentiation process. This raises the questions whether endoglin has any impact on the transdifferentiation of HSC and whether endoglin is involved in the process of liver fibrogenesis.

To investigate these questions, RNAi was used for the first time in this laboratory in order to silence endoglin. By transfecting HSC with siRNA oligonucleotides endoglin was down-regulated very efficiently. Subsequently, endoglin lacking HSC were analyzed and compared with the control cells providing a first insight into the function of endoglin in HSC. This analysis revealed an inhibition of the transdifferentiation process in HSC lacking endoglin. Inhibition is represented by a decreased amount of ECM components, by alterations in the organization of the cytoskeleton and by a reduced proliferation. Furthermore, a cDNA microarray was performed in order to designate other mediators, which were differentially expressed in HSC lacking endoglin and consequently influencing the phenotype. This array revealed many presumed candidates amongst them genes such as α_2-macroglobulin and ALK1. Based on their known functions, these candidates might contribute to the phenotype of the endoglin deficient HSC. Finally, stimulation experiments were performed in order to analyze the impact of endoglin on the TGF-β and the BMP pathways. TGF-β1 and BMP-7, which are ligands for endoglin, are important cytokines in the formation and the development of liver fibrosis. Stimulation experiments were performed using TGF-β1 and BMP-7. Reporter gene assay and Western blot analysis were used as read out systems.

Therefore, this research was crucial to demonstrate the importance of endoglin within the process of HSC transdifferentiation. The knock down of endoglin in HSC interferes with the transdifferentiation process and forces phenotypic alteration. Based on these findings it can be assumed that endoglin has an important function within the process of liver fibrogenesis.

Chapter 1

Introduction

The transmission of information is one of the most important processes for every altering organic system.
By the advances of supply chain, transportation and the related information services the world has become a complex network of information traffic. By using this network the mankind is able to act and to influence processes far away from their own localization. Especially nowadays a smooth transmission of information and goods is essential for success.

Signal transduction, which is the transmission of information within a cell, between two cells or within a complex cellular network is unique in its wide range of options. Nevertheless, both structures have some basic principles in common. Starting with the origin of information, followed by transmission and arrival, both result in influencing their destinations. However, the transduction of information within a cell or an organism is the basic of a complex life. Therefore, problems occurring in this process, such as missing or modified components, may result in serious consequences.

Exploring this complex field is essential in order to understand how cells communicate and how single components contribute to the final result. Eventually it will also lead to an advancement in the basic knowledge for drug design.

1.1 Signal transduction

1.1.1 General principles of signal transduction

Signal transduction describes the transfer of information within an organic system and enables cells to communicate. The transfer can be either processed in an endocrine, paracrine, autocrine, synaptical or cell-cell contact dependent manner. Except direct cell-cell interaction through receptors, all the other interactions are mediated through soluble signal molecules such as hormones, growth factors, interleukines, interferones and chemokines.

Signal transduction starts with the specific binding of a ligand to its receptor. Subsequently, the receptor becomes activated, thus, being able to activate down stream components through conformational changes. Conformational changes are normally induced by protein-protein interaction and especially by phosphorylation processes. The activation of down stream components is accompanied by the amplification of the signal. At the same time the receptor activation triggers a feedback circuit that shuts off the receptor or removes it from the cell surface. This is called desensitization and adaptation. Finally, the signal induces a cell response which results in e.g. enzyme production, calcium release, cell migration, proliferation or apoptosis or induces further cell-cell signaling. However, the final cell response is not the result of a single signal, it is rather the integration of many signals. In this way the diversity of cell responses are almost unlimited.

1.1.2 The TGF-β pathway

TGF-β is a multifunctional cytokine and, depending on the cell type, involved in the regulation of many cell features such as proliferation, differentiation and migration. In endothelial cells TGF-β plays a pivotal role in the development of the vessel wall. Furthermore, TGF-β is the key cytokine regulating inflammatory processes as well as fibrotic responses in the liver.

Prior to signaling the TGF-β precursor is cleaved by furin in the golgi membrane [1]. Cleavage results in the small latent complex (SLC), which binds LTBP and forms the large latent complex of TGF-β (LLC) [2]. Next, the large latent complex is secreted and finally activated by proteolytic cleavage, resulting in the mature dimeric TGF-β polypeptide [3] [4]. This TGF-β polypeptide is then able to bind to the TGF-β type II receptor dimer. To this complex a type I receptor dimer is recruited forming a hetero-tetrameric receptor complex [5]. After formation of the hetero-tetrameric receptor com-

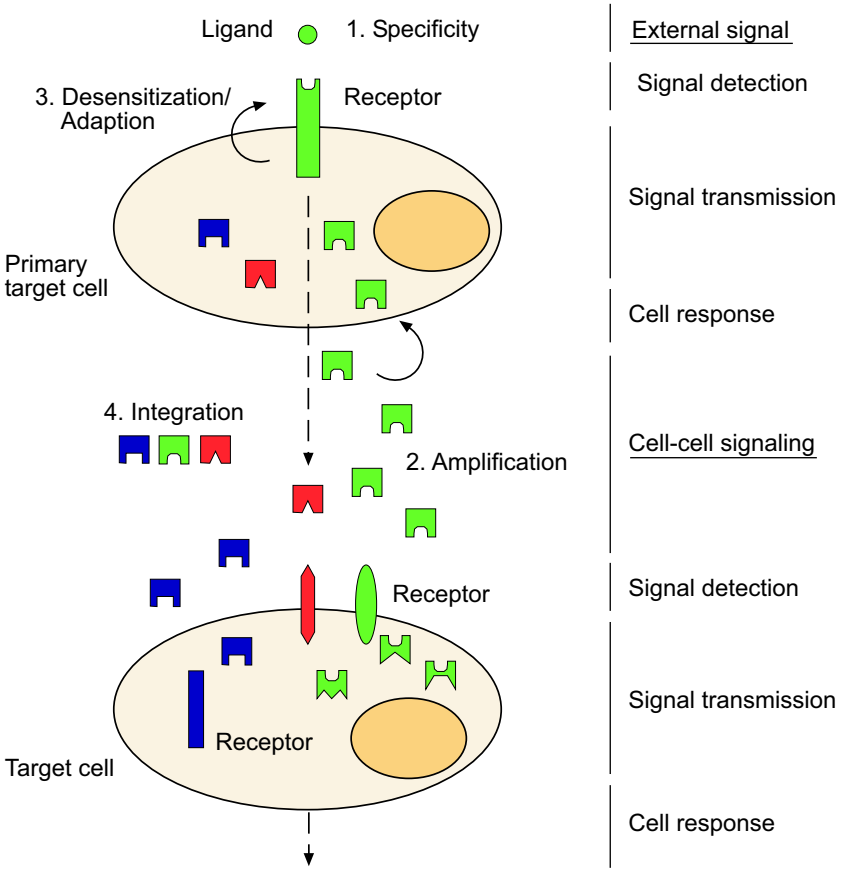


Figure 1.1: General principles of signal transduction. The transduction of a signal enables cells to communicate and to perform adequate and specific cell responses. Cell signaling starts with an external signal, which is received by a receptor, further transmitted inside the cell by e.g. phosphorylation and ends in a cellular response such as enzyme production, calcium release or cell migration. Signal transduction is characterized by 1. ligand-receptor specificity, 2. the amplification of the signal, 3. desensitization/adaptation as a feedback loop to shut off the receptor and 4. the integration of different signal.

plex, the TGF-β type II serine/threonine kinase receptor is able to phosphorylate the TGF-β type I serine/threonine kinase receptor [6]. Two distinct TGF-β type I receptors can be activated by TGF-β, i.e. ALK5 and ALK1. The participation of ALK1 in TGF-β responses has been first inferred from the vascular disease HHT2, which is caused by haplo-insufficiency of ALK1 [7]. Later on the connection of ALK1 and TGF-β has been established in cells derived from the corresponding mouse models [8]. Even though ALK1 and ALK5 trigger opposite cell responses, it is supposed that both receptors are able to cross talk [9]. In most cells TGF-β signaling is mediated via ALK5 activation. Activated ALK5 mediates phosphorylation of Smad2 and Smad3 [11]. Smad2 and Smad3 as well as Smad1, Smad5, Smad7 and Smad8 belong to the receptor regulated Smads (R-Smads). After phosphorylation the R-Smads dissociate from the activated receptor complex, associate with common mediator Smad4 (Co-Smad) and translocate into the nucleus [17]. Nuclear Smad oligomers bind to the DNA and regulate gene expression [12], thus influencing cell proliferation, migration and with respect to the fibrotic response the ECM expression [10] [13] [14]. Signaling via ALK5 is called the "classical" TGF-β pathway. In contrast to ALK5 activation the activation of ALK1 results in phosphorylation of Smad1 and Smad5. This in turn re-gulates cellular responses, which are partially overlapping with ALK5 responses, e.g. proliferation and migration, but are modified in an opposite manner. However, which receptor is activated depends on the ligand concentration and the receptor expression [9] [10] [15]. Signaling via ALK1 is called the "accessory" TGF-β pathway. Last but not least more components such as SARA participate in the TGF-β pathway. SARA is an anchoring protein and recruits the R-Smads [16]. Furthermore, ubiquitin dependent degradation and inhibitory Smad7 (I-Smad) are involved in terminating and fine tuning of the signal [18] [19].

Beside TGF-β the corresponding superfamily encompasses bone morphogenetic proteins, such as BMP-2, BMP-7 and BMP-9. Out of these cytokines BMP-7 is known as an antagonist of the TGF-β1 signaling [20]. Similar to TGF-β, BMP-7 binds to BMP-specific type I and type II membrane receptors, which leads to the activation of Smad1, Smad5 and Smad8 [21]. Therefore, stimulation with TGF-β as well as stimulation with BMP may result in the activation of partially overlapping target genes, but show at least different kinetics [20] [22] [24].

Pathways, which were mentioned above, are not exclusively governed by the essential receptors type I and type II. They are additionally modulated by the accessory type III receptors betaglycan and endoglin (CD105) [15] [20] [23] [26]. Both receptors have - as far as known - a more indirect role in TGF-β signal transduction, since they are

not essential for signal transduction [25] [26]. Betaglycan facilitates the binding of all three TGF-β isoforms to the TGF-β type II receptor, but especially facilitates the binding of TGF-β2, which has a low affinity to the TGF-β type II receptor [26]. Endoglin modulates signaling and binds TGF-β1, TGF-β3 and BMP-7 exclusively in the presence of the type II receptors. [27] [46]. However, the role of betaglycan and endoglin might be underestimated, because both receptors are necessary to maintain proper embryogenesis [28] [29].

1.2 Endoglin

Endoglin is mainly linked to the autosomal dominant disorder hereditary hemorrhagic telangiectasia type 1 (HHT1), also called Rendu-Osler-Weber disease [30]. This disorder is caused by mutations in the endoglin gene and leads to haplo-insufficiency. Patients with HHT1 show telangiectases on skin and mucosa as well as arteriovenous malformations in different organs including brain, lung, and liver [31] [32]. In contrast to haplo-insufficiency the homozygous knock out of endoglin is lethal as demonstrated in various mouse models. These mice show an arrest in the development of the vascular system and die at E11.5 [28]. Due to the strong impact of endoglin on the phenotype and its essential role in development, it is important to challenge the structure and cellular functions of endoglin.

1.2.1 Structure of endoglin

Endoglin is a glycosylated type III TGF-β membrane receptor with a single transmembrane domain of 25 amino acids [33]. The extracellular domain encompasses the ligand binding domain and the proteolytic cleavage side. Endoglin is expressed as a disulfide homodimer and can be monomerized by reducing agents [34] [35] [36]. The very short cytoplasmic domain is serine/threonine-rich and substrate for the TGF-β type I (ALK1, ALK5) and type II (TβRII) kinases [37] [38]. In contrast to other receptors and especially in contrast to the type I and type II TGF-β receptors, endoglin does not possess any kinase activity in its short cytoplasmic domain (CD) [39]. Two serines, which are located at the very end of the C-terminus of endoglin, are supposed to be constitutively phosphorylated by the TGF-βRII and three threonines are supposed to be phosphorylated by ALK1 [37].

The initial mouse mRNA transcript of endoglin is detected as a 3.4-kb single transcript by Northern blotting. To date two splice variants are known, L-endoglin as well

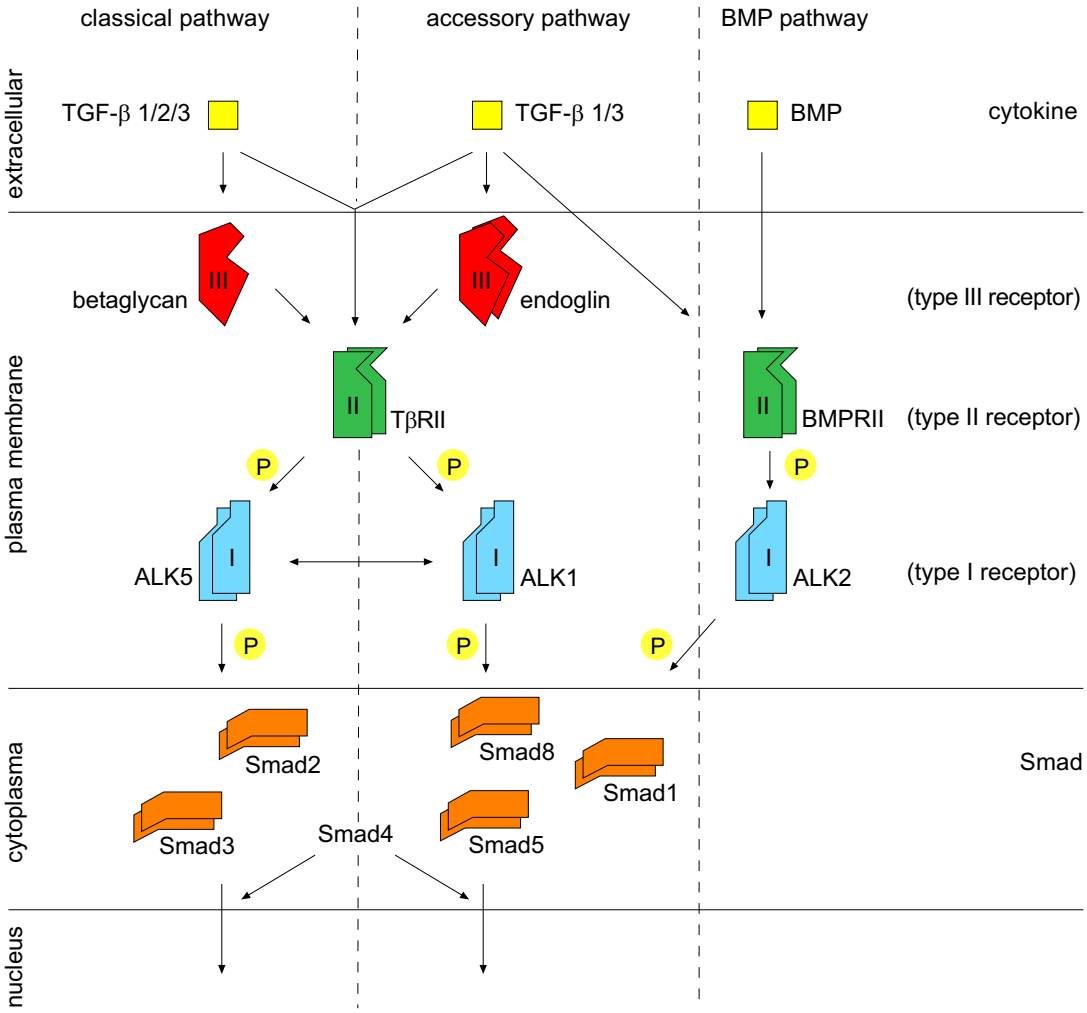


Figure 1.2: The TGF-β and BMP-7 pathways. The "classical" TGF-β pathway is activated through binding of TGF-β to the TβRII. Endoglin as well as betaglycan are able to modulate these binding processes. TβRII phosphorylates ALK5, which in turn phopshorylates either Smad2 or Smad3. This is known as the "classical" TGF-β pathway. The TβRII is also able to phosphorylate ALK1, which in turn phopshorylates either Smad1, Smad5 or Smad8. This is called the "accessory" TGF-β pathway. Phosphorylated Smad1, Smad2, Smad3, Smad5 and Smad8 associate with Co-Smad4, translocate into the nucleus and initiate the expression of specific target genes.
Phosphorylation of Smad1, Smad5 and Smad8 can also be induced by BMP-7. Upon binding of BMP-7 to the BMP type II receptor, ALK2 becomes phosphorylated. Phosphorylated and thus activated ALK2 is able to phosphorylate Smad1, Smad5 and Smad8. These R-Smads are finally translocated into the nucleus.
Whereas betaglycan has been shown to promote the ALK5 pathway, endoglin most likely promotes the ALK1 pathway and inhibits the ALK5 pathway, at least in endothelial cells. In addition it was recently shown that endoglin enhances BMP-7 signaling. However, the exact contribution of endoglin is still under discussion.

as S-endoglin. L-endoglin is the predominantly expressed form of endoglin and consists of approx. 650 amino acids (mouse: 653 aa/ human: 661 aa) [34] [35]. S-endoglin comprises approx. 617 amino acids and in comparison to L-endoglin, S-endoglin lacks 34 amino acids at the very end of the C-terminus. The short intracellular domain of L-endoglin consists of 47 amino acids while the intracellular domain of S-endoglin consists of 14 amino acids. Additional to the splice variants of endoglin, a soluble form of endoglin is also known. Soluble endoglin is the result of shedding and represents the shortest form of endoglin. The putative shedding side is located at amino acid 434-436 in rat endoglin. How this shedding is processed and which components are involved is presently unknown. The molecular weight of endoglin is 95 kDa for the monomeric form and 180 kDa for the dimeric form [34] [40].

Apart from endoglin a second TGF-β type III receptor exists, the so called betaglycan. Betaglycan shows a broader expression pattern compared to endoglin and is expressed on hepatic stellate cells, too. Endoglin and betaglycan share a high homology regarding their structure and regarding their amino acid sequence, especially at their C-termini [36]. Furthermore, they have a single transmembrane domain with a very short intracellular domain and they lack a catalytic domain. However, both receptors comprise many serine and threonine residues and they are both capable of binding to members of the TGF-β superfamily such as TGF-β1 and TGF-β3. One of the main functions of betaglycan is to enhance the affinity of TGF-β2 to bind to the TGF-β type II receptor [26].

1.2.2 Function of endoglin

Endoglin (L-endoglin) is highly expressed on endothelial cells [41], on mesenchymal cells [42] [43] and on stromal cells [44]. Endoglin, as a TGF-β type III receptor, is able to bind at least 6 different cytokines, which are all members of the TGF-β superfamily, i.e. TGF-β1, TGF-β2, BMP-2, BMP-7, BMP-9 and activin [45] [46]. However, endoglin can bind these cytokines only in association with the corresponding type II receptors [46]. According to the ligand spectrum, endoglin modulates a diverse set of cellular responses such as proliferation [23] [47], extracellular matrix (ECM) gene expression [23] [48] and migration [49] [50]. Beside the potential to bind a diverse set of cytokines, direct protein-protein interactions between endoglin and other proteins are described. These interactions may govern the organization of the cytoskeleton in a ligand independent manner [51] [52].

Even though endoglin seems to be involved in many cellular processes, the pre-

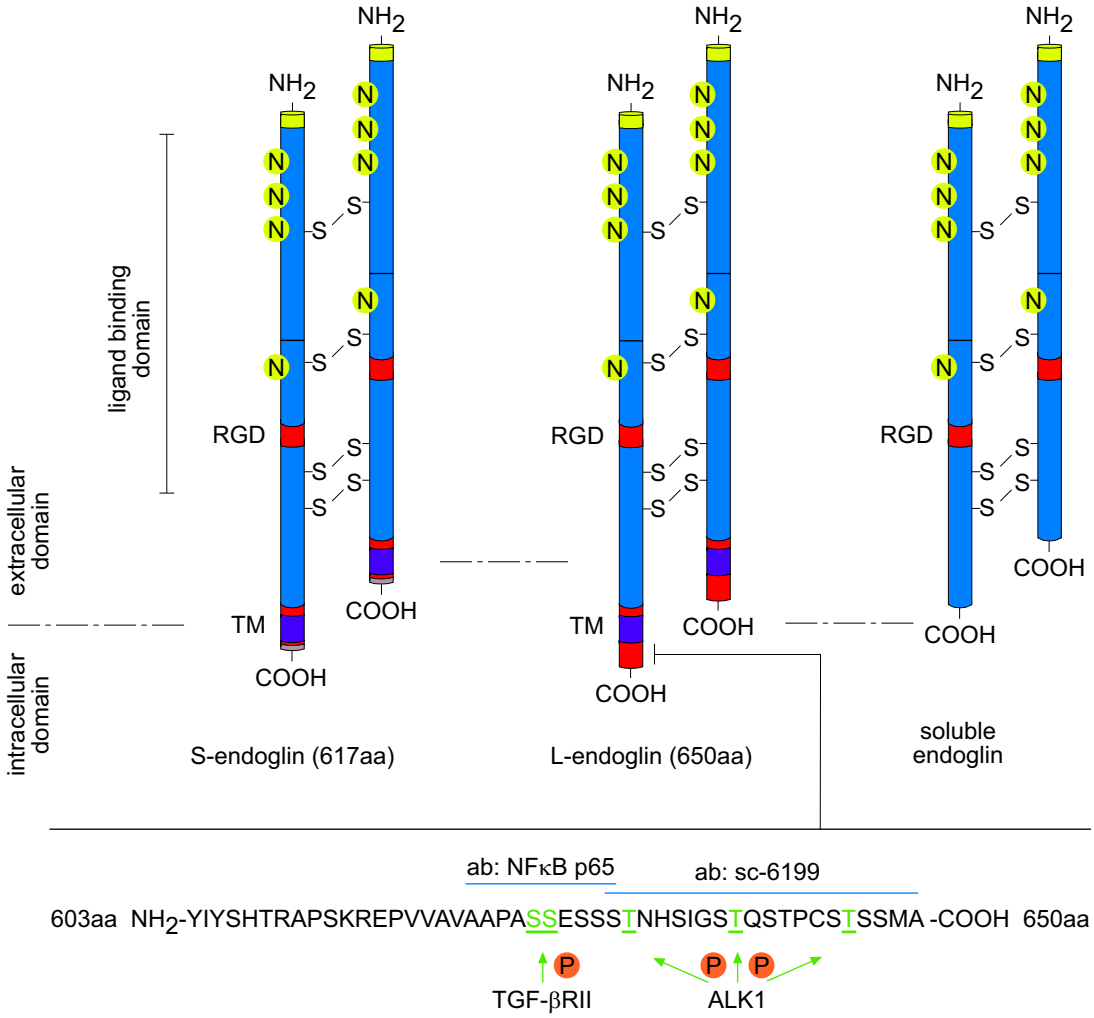


Figure 1.3: The structure of endoglin. S-endoglin and L-endoglin have a single transmembrane domain and are expressed as a disulfide bound homo-dimer at the surface of cells. So far, three variants of endoglin are known at least in human. L-endoglin, as the predominantly expressed form of endoglin, S-endoglin and, finally, soluble endoglin, as the result of a shedding process. Endoglin does not possess any kinase activity in its short cytoplasmic domain. Instead of this, the cytoplasmic domain is serine and threonine-rich and can be phosphorylated by the TGFβ type I (ALK1, ALK5) and type II (TβRII) receptors. Phosphorylation, which is caused by the type II receptor, could be detected by an antibody recognizing a phosphorylation of the NFκB subunit p65. On the other hand the antibody sc-6199, which is directed against the C-terminus of endoglin, only binds when endoglin is not phosphorylated. The extracellular domain possesses the ligand binding domain. Human endoglin additionally contains a RGD domain, which is a key recognition structure in cellular adhesion [34].

cise functionality of endoglin is still poorly understood. The impact of endoglin on the "classical" pathways is putatively mediated by direct interaction of endoglin with the signaling receptors [46] [53] [54] [55]. These interactions are regulated by phosphorylation of the cytoplasmic domain of endoglin [37] [38] [39]. In former studies interactions of endoglin and signaling receptors were investigated. These studies revealed that direct interaction of endoglin and ALK5/Smad2 affects eNOS expression [38] [56], while interaction of endoglin and ALK5/Smad3 affects ECM expression [20] [48] [57] and modulates proliferation and migration [20] [48] [57]. Furthermore, it has been suggested that endoglin is involved in MAP kinase signaling, implicating JNK and ERK1/2 MAP kinases [48] [58]. For example, the interaction of β-arrestin2 with the cytoplasmic domain of endoglin leads to an activation of ERK1/2, thus, regulating endothelial cell migration [59]. In addition, endoglin interacts with LIM-domain proteins. Interaction with LIM-domain proteins such as Zyxin and Zyxin-related protein (ZRP)-1 [51] [52] is necessary for cytoskeletal organization and cellular migration. As described above, endoglin is involved in several cellular processes and is essential for normal cellular behaviour. As a consequence, a dysregulation of endoglin interferes with the normal cellular function. Accordingly, endoglin is related to several pathogenic processes including tumorigenesis and fibrosis [102] [61]. Furthermore, soluble endoglin is a potential tumor marker not only for gastric cancer and prostatic adenocarcinoma [62] [63].

To date the function of soluble endoglin and S-endoglin are less investigated. S-endoglin was cloned from human and mouse [33] [64]. Due to the fact that L-endoglin and S-endoglin differ in the C-terminus, which includes regulatory phosphorylation sites and protein-protein interaction motifs, it was assumed that both splice variants differ in their function [65]. Later on this assumption was experimentally proven [15] [64] [65]. So far soluble endoglin is exclusively found in mammals and is especially elevated in the sera of pre-eclamptic patients [66].

1.3 The Liver

The easiest way to justify the importance and inalienability of every organ is their existence. However, the function of the liver and its involvement in many processes is outstanding.

1.3.1 Function and anatomy of the liver

On the one hand the liver is the central organ of the intermediate metabolism such as glyconeogenesis and glycogenolysis as well as degradation, conversion and assembly of different lipids and the amino acids and protein metabolism. On the other hand the liver stores a multitude of vitamins, especially vitamin B_{12} and metals such as iron and copper and excretes bile, which is an important detergent to emulsify fats. Last but not least the liver is involved in the decomposition of red blood cells and detoxification [67].

In order to perform and hold up this wide range of duties, different cell types are located in the liver and are necessary for proper functionality. Almost 60 - 70% of the liver mass consists of hepatocytes [68]. Hepatocytes are parenchymal cells and most of the metabolic activities in the liver take place in these cells. The other, second cell type, which belongs to the parenchyma is the cholangiocyte. Cholangiocytes modify the composition of the bile. Endothelial cells, Kupffer cells and *hepatic stellate cells* (HSC) represent the non-parenchymal cell types. The sinusoidal endothelial cells are separated from the hepatocytes by the space of Disse and are responsible for the uptake and elimination of macromolecules from the blood. Kupffer cells, which are liver resident macrophages, are attached to the sinusoidal wall and are in contact with the blood flow. As macrophages they are involved in the immune response. HSC, also known as Ito-cells, are fat and retinol (vitamin A) storing cells. They are located within the space of Disse and they are attached to hepatocytes as well as in close interaction with hepatocytes. Furthermore, these cells are mainly responsible for the synthesis of extracellular matrix (ECM) components such as collagen type I, III, and IV [69] [70]. Due to the important function of HSC during liver fibrosis, this cell type will be discussed in more detail in the next subsection.

1.3.2 Function of HSC during liver fibrogenesis

HSC as a non-parenchymal cell type of the liver and TGFβ as an autocrine and paracrine regulator of HSC physiology are intrinsically tied to the initiation process and the de-

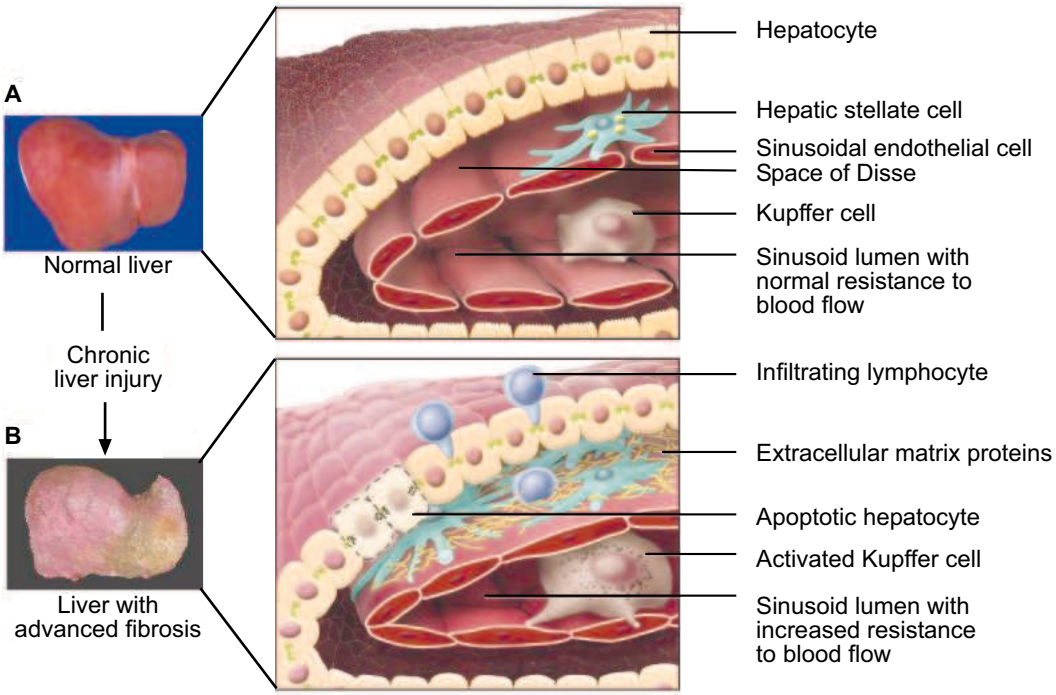


Figure 1.4: Architecture of a normal liver *vs.* liver with advanced fibrosis. The sinusoidal endothelial cells are separated from the hepatocytes by the space of Disse. In the normal liver HSC are localized within the space of Disse and Kupffer cells are attached to the sinusoidal wall on the luminal side of the sinusoid. Upon noxae of different etiologies, Kupffer cells become activated and produce fibrogenic mediators. Furthermore, hepatocytes become apoptotic and release TGFβ and other fibrogenic mediators. Activated HSC transdifferentiate into myofibroblast-like cells, migrate and accumulate at the site of tissue repair and synthesize ECM components such as collagen type I and III. Additionally, inflammatory lymphocytes infiltrate the hepatic parenchyma. With the loss of the fenestration character of the sinusoidal endothelial cells the resistance to the blood flow increases and liver function decreases.

velopment of liver fibrosis.

Liver fibrosis is the preliminary stage before liver cirrhosis and is associated with the loss of liver function [72] [73]. In contrast to the traditional view, recent studies indicate that even advanced fibrosis is reversible [74]. The loss of liver function is characterized by hypertension, which is caused by a higher resistance to blood flow, and a reduced exchange capacity of the sinusoid and the parenchyma, which is caused by the loss of fenestration. This in turn is due to a massive formation of collagen and other ECM components, which leads to an increase of connective tissue in the affected organ [73]. HSC are the main source of ECM components such as collagen type I, III, IV and fibronectin. Therefore, HSC are the key regulator of ECM synthesis during liver fibrogenesis.

However, synthesis of ECM components is moderate in quiescent HSC. Prior to ECM production, quiescent HSC need to be activated. Activation of HSC can either be induced by cytokines, which originate from hepatocytes, Kupffer cells or sinusoidal endothelial cells (paracrine stimulation) or by infiltrating lymphocytes, thrombocytes and leukocytes. One of the most important cytokine for the initial activation process is TGFβ. TGFβ is normally stored in hepatocytes and released in response to cell damage [75]. After activation, HSC transdifferentiate into contractile, pro-inflammatory and fibrogenic myofibroblast-like cells (MFB) [76] [77] [78] and migrate towards the traumata. There they participate in the wound healing process by secreting ECM components, thus forming the scar tissue. The formation of scar tissue is further supported by a decreased ECM degradation [88] [89]. ECM degradation is caused by matrix metalloproteinases and their inhibition is due to an increased expression of the tissue inhibitors of matrix metalloproteinases (TIMPs) [79] [80].

HSC once activated produce and secrete TGFβ resulting in an autocrine stimulation of HSC and apoptotic hepatocytes. These reciprocal effects are the basis for a deregulated wound healing process [81] [82]. However, a single noxis is insufficient to induce a deregulated wound healing process. Instead of this many recurring persistent stimuli have to occur, which lead to a deregulated wound healing process and finally to liver fibrosis and cirrhosis [83] [84] [87].

In vitro the activation of HSC and transdifferentiation into MFB can be experimentally induced. Activation and transdifferentiation *in vitro* is associated with the modification of distinctive cell features/attributes. These modifications are comparable to the modifications that occur in the *in vivo* situation (Figure 1.5) .

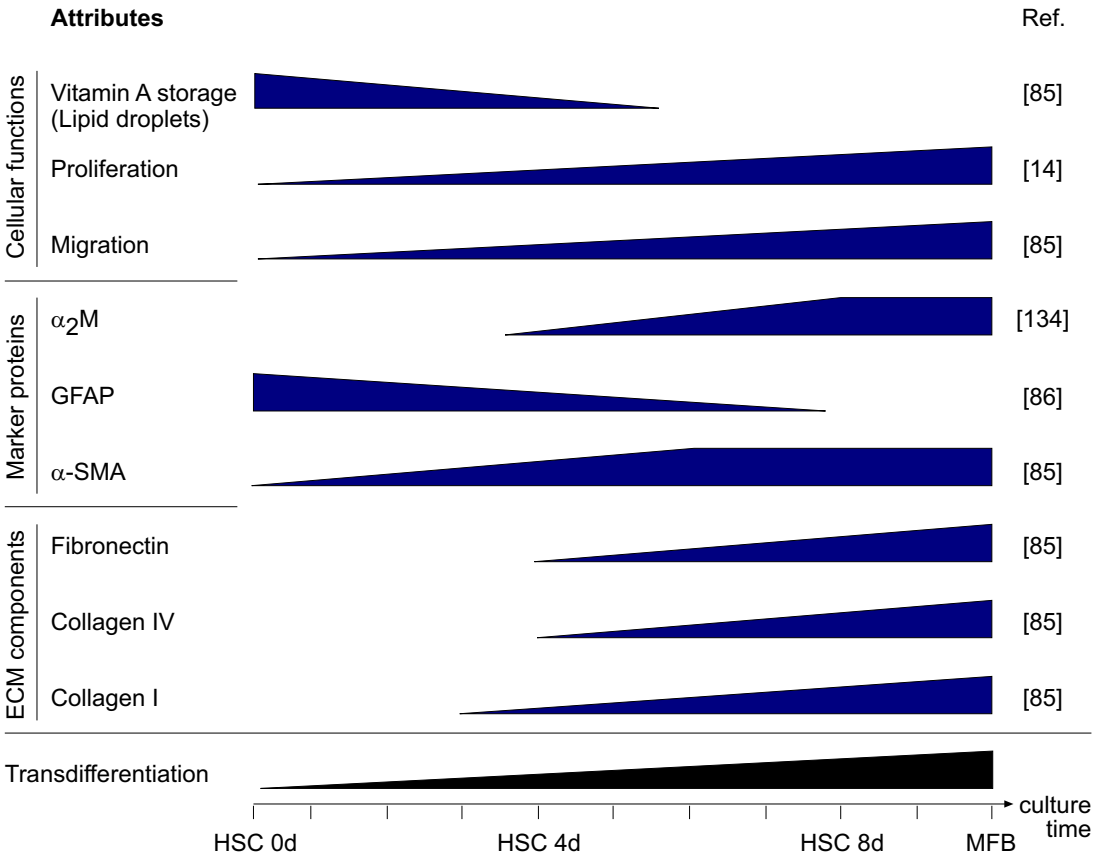


Figure 1.5: Modification of distinctive cell features/attributes during *in vitro* transdifferentiation of HSC. The arrows describe the changes of cell attributes as they occur in HSC during transdifferentiation *in vitro*. X-axis: day of culture; Y-axis: attributes, which are modified during transdifferentiation. While the number of lipid droplets and the amount of GFAP (glial fibrillary acidic protein) is decreased during transdifferentiation the potential to proliferate and migrate is increased. Furthermore, activation of HSC is accompanied by the induction of ECM (extracellular matrix) components, α_2-macroglobulin and α-SMA (alpha smooth muscle actin) synthesis. Therefore, the expression of ECM components, the expression of marker proteins as well as cellular function characterize the transdifferentiation process and they are helpful tools to determine the stage of transdifferentiation.

1.4 RNAi

In 2006 Andrew Z. Fire and Craig C. Mello were honored with the Nobel Prize in Physiology and Medicine for their discovery of "RNA interference - gene silencing by double-stranded RNA". Due to the immense and immediate impact of RNAi on biomedical research Andrew Z. Fire and Craig C. Mello got the Nobel Prize - in contrast to most of the other Nobel laureates - shortly after their first publication. Additionally, the potential transfer of this method to novel medical applications in future emphasizes the importance of this method.

1.4.1 RNAi as an experimental tool for sequence specific gene silencing

In 1998 Fire and co-workers were performing gene silence experiments with *Caenorhabditis elegans* and antisense oligonucleotides (ASOs), when they found out that dsRNA is more efficient for gene silencing than the corresponding antisense oligonucleotides [90]. Although observations in former studies were obviously caused by RNA interference, this observation by Fire and co-workers was finally the birth of RNAi. Due to the fact that dsRNA interferes with the function of the target gene this new technology was named RNA interference.

Even though the knowledge about RNAi is new, the mechanism itself is evolutionary conserved. This highly conserved character is due to the important biological function of siRNA such as the protection of cells against viruses and repetitive DNA elements [91]. Furthermore, RNAi is involved in a wide variety of cellular processes such as the regulation of development, growth, differentiation, apoptosis and cancer [92] [93]. However, for this thesis it might be sufficient to provide a short overview about siRNA as an experimental tool for gene silencing *in vitro*. The starting point for RNA interference is normally a double-stranded RNA (dsRNA) of approximately 100 nucleotides. This dsRNA is recognized and digested by the Dicer into small interfering siRNA of 21-23 nucleotides [94]. In case RNA interference is used as an experimental tool, cells are directly transfected with either synthetic siRNA of 21-23 nucleotides or with a vector, that allows stable expression of shRNA molecules (Figure 1.6). While synthetic siRNA of 21-23 nucleotides are not processed by the Dicer, shRNA (short hairpin RNA) is recognized and need to be digested by the Dicer. The Dicer is a RNAse type-III enzyme, holding a dual catalytic domain and additional RNA helicase and PAZ motif (putative protein-protein interaction domain) [95]. After digestion the siRNA enters the RNA-induced silencing complex (RISC). For the incorporation of siRNA into

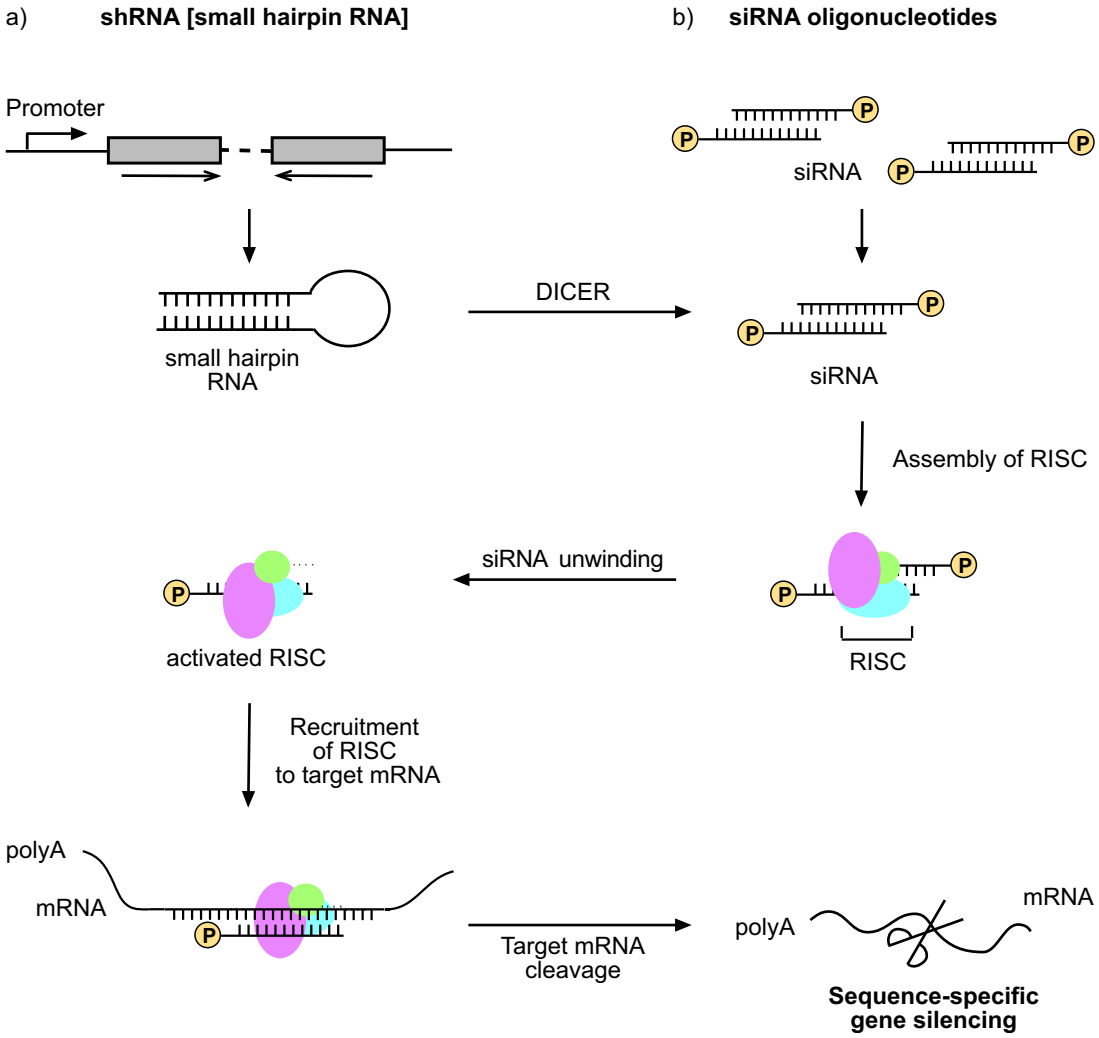


Figure 1.6: RNAi as an experimental tool for sequence specific gene silencing. Cells are directly transfected with either b) synthetic siRNA of 21-23 nucleotides or with a) a vector, that allows stable expression of shRNA molecules. While synthetic siRNA of 21-23 nucleotides are not processed by the Dicer, shRNA (short hairpin RNA) is recognized and digested by the Dicer into siRNA of 21-23 nucleotides. siRNA of 21-23 nucleotides finally enter the RNA-induced silencing complex (RISC) and become unwinded. Unwinding in turn activates the RISC complex and guides the siRNA to the complementary target mRNA. After binding the target mRNA is digested by the RISC complex. In this way RNA interference is able to silence genes in a sequence-specific manner.

the RISC complex the double-stranded feature and the two-nucleotides 3'-overhangs and 5'-phosphate termini of the siRNA are functionally important [96] [97]. Incorporation is followed by unwinding of the siRNA [97] through the Piwi-Argonaute-Zwille (PAZ) domain of Argonaute 2 [98]. This in turn activates the RISC complex and guides the siRNA to the complementary target mRNA. Identification of the target mRNA is due to Watson-Crick basepairing [99] and is followed by mRNA cleavage, which is performed by the RNaseH-like structure of the argonaute 2 protein [98]. This cleavage is endonucleolytic and occurs - at least in Drosophila - only in the region, which is homologous to the siRNA [100]. In this way RNA interference is able to silence genes in a sequence-specific manner.

Nevertheless, there are several challenges that can occur by working with siRNA. First of all partial sequence homology of the siRNA with other than the intended target mRNA might lead to an inhibition of translation. This is comparable to the inhibition of translation caused by miRNA [60] [101]. Furthermore, an interferon response might lead to a shutdown of the global protein expression [103]. Such an interferon response is normally restricted to oligonucleotides ≥ 30 [104], but might also occur by the use of shorter siRNA, e.g. siRNA of 21 oligonucleotides [105]. These unintended effects are called off-target effects.

Last but not least RNAi is also involved in the regulation of gene expression due to its impact on heterochromatin assembly - at least in *S. pombe* - [106] [107]. Genes, which are localized within the heterochromatin are transcriptionally silenced. Assembly and spreading of heterochromatin in *S. pombe* is induced by histone H3 lysine 9 deacetylation, which is followed by methylation processes. Deacetylation and the following methylation process can be initiated by the RITS complex (RNAi-induced transcriptional silencing complex), which contains both a chromatin-associated protein and a RNAi-associated protein [108]. The targeting of the RITS complex to heterochromatin regions for inactivation requires siRNA binding [108]. In *S. pombe* most of the chromatin modifications were restricted to known heterochromatic loci. However, recent investigations in mammalian cells revealed that chromatin modifications can also occur at loci, which are normally euchromatic [109]. In this case synthetic siRNA targeting CpG islands induces DNA methylation, which in turn results in an repressed gene expression at the transcriptional level [109].

Aim of this study

The aim of this study was to investigate the function of endoglin in primary rat *hepatic stellate cells*, especially with respect to the activation and transdifferentiation process. For this purpose siRNA was used to down regulate endoglin. Subsequent endoglin deficient cells were characterized and different aspects of the transdifferentiation process such as ECM components, marker proteins and cellular features were analyzed.

Chapter 2

Materials and methods

2.1 Plastic ware

Plastic ware	Company
Cell culture 6 well plates	Sarstedt, Germany
Cell culture 12 well plates	BD Bioscience, USA
Cell culture 96 well plates	BD Bioscience, USA
Microtest^{TM} 96-well Assay plate	BD Bioscience, USA
Cell culture Dishes ∅ 60 mm	Sarstedt, Germany
Cell culture Dishes ∅ 100 mm	Sarstedt, Germany
Culture Slides 4 wells	BD Bioscience, USA
CryoTubes	Sarstedt, Germany
Falcon 50 ml	Greiner, Germany
Gloves, powder free	Sempermed, Austria
Immuno Module F16 Maxi Sorp	NUNC, Germany
Immuno 96 Microwell Plates	NUNC, Germany
Pipette tips 10 μl	Eppendorf, Germany
Pipette tips 200 μl	Eppendorf, Germany
Pipette tips 1000 μl	Eppendorf, Germany
Safeseal pipette tips 10 μl	Biozym, Germany
Safeseal pipette tips 200 μl	Biozym, Germany
Safeseal pipette tips 1000 μl	Biozym, Germany
Tissue Culture Flasks ∅ 550 ml	Cellstar®, Germany
Tubes 1.5ml	Sarstedt, Germany
Tubes 2 ml	Sorenson Bio Science Inc., USA

Tubes low binding 0.5 ml	Eppendorf, Germany
UltraClear^{TM}Tubes 7/16 x 2 3/8 11 x 60 mm	Beckman Coulter, USA

Table 2.1: Plastic ware

2.2 Equipment

Equipment	Company
ABI 310 Genetic Analyzer	Applied Biosystems, USA
Agarose gel electrophoresis system	Febikom, Germany
Axiovert 135 M Microscope	Zeiss, Germany
Beckman Avanti^{TM}J-15 Centrifuge	Beckman Coulter, USA
Beckman Optima L-70k Ultracentrifuge	Beckman Coulter, USA
Biometra WT16 (Rocking platforms)	Biometra, Germany
Biometra T3 (Thermocycler)	Biometra, Germany
Biofuge pico centrifuge	Heraeus Instruments, Germany
Biofuge 15R centrifuge	Kendro Products, Germany
Cell Culture Incubator	Heraeus, Germany
Gene Quant	Pharmacia Biotech, USA
Ice machine	Ziegra, Germany
INTAS DNA-Gel-documentation Imager	INTAS, Germany
Leica DMLB Microscope	Leica, Germany
Lumi-Imager ECL	Boeringer, Germany
MicroBeta Jet 1450 Scintillation and Luminescence Counter	PerkinElmer, USA
Microprocessor pH-Meter	WTW, Germany
MilliQ Water Purification System	Millipore S.A., France
Pipetman 10 μl	Eppendorf, Germany
Pipetman 20 μl	Eppendorf, Germany
Pipetman 100 μl	Eppendorf, Germany
Pipetman 200 μl	Eppendorf, Germany
Pipetman 1000 μl	Eppendorf, Germany
Power PAC 300	BioRad, USA

Sartorius 1364MP (analytical balance)	Sartorius, Germany
Sartorius 1212MP (analytical balance)	Sartorius, Germany
Thermomixer 5436	Eppendorf, Germany
Victor 1420 Multilabel Counter	Wallac, Finland
Vortex Genie2	Fisher Scientific, USA
XCell SureLock^{TM} Mini-Cell	Invitrogen, USA
XCell II Blot Module	Invitrogen, USA

Table 2.2: Equipment

2.3 Chemicals

Chemicals	Company
Acetic acid	Merck, Germany
Aceton	Merck, Germany
Agarose seaKem®	Cambrex, USA
Bacto^{TM} Agar	BD Bioscience, USA
Bacto^{TM} Peptone	BD Bioscience, USA
Bacto^{TM} Yeast Extract	BD Bioscience, USA
Bicin	AppliChem, Germany
Biotin Blocking Solution	DakoCytomation, USA
Bis-Tris	AppliChem, Germany
BrdU	
BSA (Albumin, bovine serum)	Sigma, Germany
Calcium chloride	Merck, Germany
Caesium chloride	MP Biomedicals, USA
Centrisep Spin Columns	Princeton Separation, USA
ChemMate Peroxidase-Blocking Solution	DakoCytomation, USA
Chlorobutanol	Fluka, Austria
Chloroform	Sigma, Germany
Chromatography paper 3MM	Whatman, England
Collagen, Type 1 (rat tail)	B&D, USA
Complete protease inhibitor cocktail	Roche, Germany
DAPI	Molecular Probes, USA
DMEM	Cambrex, Belgium

(Dulbecco's Modified Eagle's Medium)	
DMSO (Dimethylsulfoxide)	Fluka, Austria
DPBS	Cambrex, Belgium
(Dulbecco's Phosphate Buffered Saline)	
DTT (1,4-dithiothreitol)	Sigma, Germany
dNTP's	Roche, Germany
EDTA (ethylenediaminetetra acetic acid)	Merck, Germany
Ethanol	Roth, Germany
Ethidium bromide	Sigma, Germany
Fast Red Tablets	Roche, Germany
FCS (fetal calf serum)	Perbio, Switzerland
Ficoll	Amersham, Sweden
Fluorescent Mounting Medium	DakoCytomation, USA
Formaldehyde ($\geq$ 36,5 %)	Roth, Germany
Formamide	Fluka, Switzerland
FuGene^{TM}6 (Transfection Reagent)	Roche, Germany
Gelatin	Sigma, Germany
Glycerin	Sigma, Germany
Guanidinthiocyanate	Merck, Germany
HEPES	Roth, Germany
Hybond-N membrane	Amersham, Sweden
HiPerFect (Transfection Reagent)	Qiagen, Germany
Isopropanol	Roth, Germany
L-Glutamine	Cambrex, Belgium
Lipofectamine®2000 (Transfection Reagent)	Invitrogen, USA
Lithium chloride	Merck, Germany
Magnesium chloride	Merck, Germany
MES	Roth, Germany
(2-(N-morpholino)ethanesulfonic acid)	
Methanol	Roth, Germany
2-Mercaptoethanol	Roth, Germany
MOPS	Roth, Germany
(3-(N-morpholino)propanesulfonic acid)	
Mounting Medium Faramount	DakoCytomation, Denmark

Nanofectin I (Transfection Reagent)	PAA, Austria
Nycodenz	Nyegaard, Norway
Nitrocellulose Membrane	Schleicher & Schuell, Germany
NuPage BisTris Gels 4-12 %	Invitrogen, Germany
NuPage BisTris Gels 10 %	Invitrogen, Germany
NuPage TrisAcetate Gels 3-8 %	Invitrogen, Germany
NuPage LDS-sample-Buffer (4x)	Invitrogen, Germany
NP-40 (Nonidet P40)	Roche, Germany
Paraformaldehyde	Merck, Germany
Penicillin/Streptomycine	Cambrex, Belgium
Phenol	Roth, Germany
Phosphatase Inhibitor Cocktail 2	Sigma, USA
PEG (Polyethylenglycol)	Fluka, Switzerland
Potassium Phosphate (Dibase/Monobase)	Merck, Germany
Poly-L-Lysine Solution	Sigma, Germany
Potassium Chloride	Merck, Germany
PVP (Polyvinylpyrrolidon)	Sigma, Germany
RotiszintEcoplus Szintillator	Roth, Germany
Sodium acetate	Merck, Germany
Sodium azide	Merck, Germany
Sodium carbonate	Merck, Germany
Sodium chloride	Roth, Germany
Sodium citrate	Merck, Germany
Sodium hydrogen carbonate	Merck, Germany
Sodium hydrogen phosphate monohydrate	Merck, Germany
Sodium Hydroxide	Merck, Germany
SDS (Sodium dodecyl Sulfate)	Roth, Germany
Skimmed milk powder	Roth, Germany
SuperSignal®West Dura Extended Duration Substrate	Pierce Biotechnology, USA
SYBR Green	Roche, Germany
TCA (Trichloracetic Acid)	Roth, Germany
Trizma®Hydrochloride	Roth, Germany
Tricine	Roth, Germany

Triton X-100	Roth, Germany
Tween20 (polyoxyethylenesorbitan monolaureate)	Roth , Germany
T4-Ligase Buffer	Roche, Germany
X-ray film BioMax XAR	Kodak, USA
Xylol	Merck, Germany

Table 2.3: Chemicals

2.4 Radioactive materials

Material	Company
$[\alpha^{32}P]$-dCTP	Amersham Bioscience, England
^{3}H-thymidine	NEN Life Science Products, Germany

Table 2.4: Radioactive materials

2.5 Enzymes

Enzymes	Company
Omniscript®Reverse Transcriptase	Qiagen, Germany
*Bam*HI	NEB, USA
DNase type II	Roche, Germany
*Eco*RI	NEB, USA
*Hind*III	NEB, USA
Gateway®LR Clonase^{TM}II Enzyme Mix	Invitrogen, USA
Klenow-Fragment	Roche, Germany
*Kpn*I	NEB, USA
*Mlu*I	NEB, USA
*Not*I	NEB, USA
*Pac*I	NEB, USA
ProteinaseK	Sigma, Germany
Taq DNA Polymerase	Roche, Germany
Trypsin (10x)	PAA Laboratories, Austria
T4-DNA-Ligase	Roche, Germany

RNase	Roche, Germany
*Sal*I	NEB, USA
*Xba*I	NEB, USA
*Xho*I	NEB, USA

Table 2.5: Enzymes

2.6 Molecular size standards

Standards	Company
GeneRuler 100 bp DNA Ladder Plus	Fermentas GmbH, Germany
*Hind*III ladder	NEB, USA
SeeBlue Plus2 Pre-Stained Standard	Invitrogen GmbH, Germany

Table 2.6: Molecular size standards

2.7 Cytokines

Cytokines	Company
BMP-7 recombinant human	R&D Systems, USA
TGF-β1 recombinant human	R&D Systems, USA

Table 2.7: Cytokines

2.8 Multicomponent systems

Multicomponent systems	Company
Adeno-X- rapid Titer Kit	BD Bioscience Clontech, USA
Annexin-V-FLUOS Staining Kit	Roche, Germany
BigDye Terminator Cycle Sequencing Ready Reaction Kit	Applied Biosystems, USA
BLOCK-IT Adenoviral RNAi Expression System	Invitrogen, USA
DC Protein Assay	BIO-RAD, Germany
Expand high fidelity PCR Systems	Roche, Germany
EnzChek Gelatinase/Collagenase Assay Kit	Invitrogen, USA
pGM®-T and pGEM®-T Easy Vector System	Promega Corporation, USA
QIAquick Gel Extraction Kit	Qiagen, Canada
RNeasy Mini Kit	Qiagen, Germany
Steady Glo Luciferase Assay system	Promega, Germany
SuperScript Reverse Transcriptase AMV	Roche, Germany

Table 2.8: Multicomponent systems

2.9 Antibodies

Antibodies used in this study are listed in the table below. The antigen-antibody complexes in Western blot analysis were detected by Supersignal®West Dura Extended Duration Substrate.

2.9.1 First antibodies

Antibody	Source	Company
p-Smad3/1 (♯9514)	rabbit polyclonal	Cell signaling, USA
human α_2-macroglobulin (♯15942)	goat polyclonal	Rockland, USA
rat α_2-macroglobulin (R2M-25A-Z)	rabbit polyclonal	ICL, USA
rat Endoglin N-terminus (PPabE1)	rabbit polyclonal	Davids Biotechnologie, Germany
rat Endoglin C-terminus (sc-6199)	goat polyclonal	SantaCruz, USA
β-Actin N-terminus (A5441)	mouse monoclonal	Sigma, Germany
human α-smooth muscle	rabbit polyclonal	Abcam, UK

Actin N-terminus (ab5694)		
rat Collagen IV full length (ab6586)	rabbit polyclonal	Abcam, UK
rat Collagen I full length (PS065)	rabbit polyclonal	Monosan, The Netherlands
rat Fibronectin full length (AB1954)	rabbit polyclonal	Chemicon Int., Germany
HSP70 C-terminus (sc-1060)	goat polyclonal	SantaCruz, USA
phospho-NF-κB p65 Ser468 (♯3039)	rabbit polyclonal	Cell signaling, USA

Table 2.9: First antibodies

2.9.2 Secondary antibodies

Antibody	Source	Company
rat IgG-HRP (sc-2006)	goat polyclonal	SantaCruz, USA
rabbit IgG-HRP (sc-2007)	goat polyclonal	SantaCruz, USA
mouse IgG-HRP (sc-2055)	donkey polyclonal	SantaCruz, USA
goat IgG-HRP (sc-2056)	donkey polyclonal	SantaCruz, USA
goat IgG-HRP (sc-2922)	rabbit polyclonal	SantaCruz, USA

Table 2.10: Secondary antibodies

2.10 Microorganisms

2.10.1 Adenoviruses used in this study

Virus	Source
Ad5-$(BRE)_2$-luciferase	this thesis
Ad5-$(CAGA)_{12}$MLP-luciferase	this thesis
Ad5-P_{U6}-siEng	this thesis
Ad5-P_{U6}-si*LacZ*	this thesis
Ad5-CMV-CRP2-GFP	Prof. Weiskirchen
Ad5-CMV-CRP2	Prof. Weiskirchen

Table 2.11: Adenoviral strains used to infect *hepatic stellate cells*

2.10.2 *E. coli* strains used in this study

Strain	Genotype	Source
JM105	F'*traD36 lacl*^{q}Δ (LacZ)*M15proA*$^+$*B*$^+$*/thi rpsL (Str*^{r}*endA sbcB15 sbcC? hsdR4* (r_K^- m_K^+)Δ(*lac-proAB)*	NEB, USA
One Shot®TOP10 Chemically Competent	F$^-$*mcr*AΔ(*mrr-hsd*RMS- *mcr*BC)ϕ80*lac*ZΔM15Δ *lac*X74*rec*A1*ara*D139Δ(ara-leu)7697*gal*U*gal* K*rps*L (Str^R) *end*A1*nup*G	Invitrogen, USA

Table 2.12: *E. coli* strains used in this study

2.10.3 Eucaryotic cells used in this study

Strain	Description	Source
COS-7	African Green Monkey SV40-transformed kidney fibroblast cell line	ATCC, USA
293A	established from primary embryonal kidney transformed with sheared humen Ad5 DNA	Invitrogen, USA
rHSC	male Sprague-Dawley rat *hepatic stellate cells*	this laboratory
mHSC	male C57BL/6J mouse *hepatic stellate cells*	this laboratory

Table 2.13: Eucaryotic cells used in this study

2.11 Oligonucleotides

Oligonucleotides used for sequencing

Gene	Acc. No	Fragment	Primer
pAd-Block-iT	-	-	WV009 5′-(GAC TTT GAC CGT TTA CGT GGA GAC)-3′for WV010 5′-(CCT TAA GCC ACG CC ACA CAT TTC)-3′rev
pENTR4	-	-	WV013 5′-(GGA ACC AAT TCA GTC GAC TG)-3′for WV014 5′-(GTA ACA TCA GAG ATT TTG AGA C)-3′for

Table 2.14: Oligonucleotides used for sequencing

Oligonucleotides used for PCR and Sequencing

Gene	Acc. No	Fragment	Primer
eng	AY562420	535 bp	SM010 5′-d(CAG GCA TCC AAC ACC ATA G)-3′for SM011 5′-d(CGA TGC TGT GGT TGG TAC)-3′rev
rzyxin	XM216124	523 bp	SM171 5′-d (CCT GCT TCA CTT GTC ATC)-3′for SM172 5′-d (GGT GTG GAA GGA GGT CC)-3′rev
rzrp-1	AF120109	520 bp	SM173 5′-d (GTC TGG AGT GGA GCA ACC)-3′for SM174 5′-d (CGG TAG CAT AAG AGG CTG)-3′rev

rS6	NM017160	383 bp	rS6s 5′-d(GAC TGA CAG ATA CCA CTG TGC CT)-3′for rS6r 5′-d(TTA TTT TTG ACT GGA CTC AGA T)-3′rev

Table 2.15: Oligonucleotides used for PCR

Oligonucleotides used to generate the hybridization probes for Northern blotting

Gene	Acc. No	Fragment	Primer
Eng	AY562420	815 bp	SM014 5′-d(CCA AGG CTG CCA CTT GG)-3′for SM015 5′-d(TGC TCA CCT GTA CGA AGC)-3′rev
r$\alpha_2 M$	NM012488	570 bp	WV022 5′-d(GTT GTC CGC AAT GCC CTC)- 3′for WV023 5′-d(CAG GCA CAG TCG GCA ATG)-3′rev
rColIα 2	NM053356	787 bp	WV026 5′-d(GCT CAG TAT TCT GAC AAA GG)- 3′for WV027 5′-d(GAC CAG TGG CAC CAG CAG)-3′rev
rFn	NM019143	604 bp	WV028 5′-d(GCT GTG ACC CAG ACT TAC)-3′for WV029 5′-d(CCG AAG CAG GTA CAG TTC)-3′rev
rAlk1	L36088	835 bp	SM032 5′-d(CTA TCT CCA AGG ACC ATG ACC)-3′for SM034 5′-d(GCT GCG TGC TGG AGT TCC G)-3′rev
rMMP10	NM133514	500 bp	WV020 5′-d(CTC ATG CCT ACC CAC CTG)- 3′for WV021 5′-d(CTG CCC AGA ACT GAC TTC C)- 3′rev

Table 2.16: Oligonucleotides used to generate the hybridization probes

2.12 Oligonucleotides for gene silencing

siRNA oligonucleotides (Qiagen)

Gene	Acc. No	Order no.	Oligonucleotide
Control Fluo	NONE	siRNA Alexa Fluor 488	r(UUC UCC GAA CGU GUC ACG U)dtdt sense r(ACG UGA CAC GUU CGG AGA A)dtdt antisense
Control	NONE	AllStar siRNA	Proprietary

$\alpha_2 M$	NM012488	Rn_A2m_6_HP	r(CCA UAA CCA AAC UAU CAU U)dtdt sense
			r(AAU GAU AGU UUG GUU AUG G)dtdt antisense
$\alpha_2 M$	NM012488	Rn_A2m_7_HP	r(CCA ACU CGA ACA UCC GUA A)dtdt sense
			r(UUA CGG AUG UUC GAG UUG G)dtdt antisense
Eng	AY562420	Rn_Eng_1_HP	r(CCA UAU AUU UAC CAA UAA A)dtdt sense
			r(UUU AUU GGU AAA UAU AUG G)dtdt antisense
Eng	AY562420	Rn_Eng_2_HP	r(CAC UGC ACU UGG UCU ACA A)dtdt sense
			r(UG UAG ACC AAG UGC AGU G)dtdt antisense

Table 2.17: siRNA oligonucleotides used for gene silencing

Oligonucleotides used to generate the shRNA viruses

Gene	Acc. No	Order no.	Oligonucleotide
Eng	AY562420	siRNA 12	5′-d(CAC CGC ACC CTC AGT TGC AAC TTA
			GCG AAC TAA GTT GCA ACT GAG GGT GC)-3′
			5′-d(AAA AGC ACC CTC AGT TGC AAC TTA
			GTT CGC TAA GTT GCA ACT GAG GGT GC)-3′
Eng	AY562420	siRNA 34	5′-d(CAC CGA AAG TCA GGC CTG TGA
			TGG TGC GAA CAC CAT CAC AGG CCT GAC)-3′
			5′-d(AAA AGT CAG GCC TGT GAT GGT
			GTT CGC ACC ATC ACA GGC CTG ACT TTC)-3′
Eng	AY562420	siRNA 56	5′-d(CAC CGA ATA GAT GTA CCA CAG
			TGC AGC GAA CTG CAC TCT GGT ACA TCT A)-3′
			5′-d(AAA ATA GAT GTA CCA GAG TGC
			AGT TCG CTG CAC TCT GGT ACA TCT ATT C)-3′
LacZ		si*LacZ*	5′-d(CAC CGC TAC ACA AAT CAG CGA
			TTT CGA AAA ATC GCT GAT TTG TGT AG)-3′
			5′-d(AAA ACT ACA CAA ATC AGC GAT
			TTT TCG AAA TCG CTG ATT TGT GTA GC)-3′

Table 2.18: Oligonucleotides used to generate the shRNA viruses

2.13 Plasmids

Vector	Description	Source
CAGA	$(CAGA)_{12}$MLP in pGL3-Basic Vector	Dennler *et al.*, [110]
BRE	$(BRE)_2$ in pGL3-Basic Vector	Korchynskyi *et al.*, [111]
pENTR4	pENTR^{TM}4 2,7kb	Invitrogen, USA
pAd-Block-it	pAd/BLOCK-iT^{TM}-DEST 34864bp	Invitrogen, USA
Mouse Endoglin	mouse endoglin in pCMV-Sport6	RZPD, Germany
Rat Endoglin	rat endoglin in pcDNA 3.1(+)	Meurer *et al.*, [36]

Table 2.19: Plasmids used in this study

2.14 Solutions and buffers

ddH_2O was used as a solvent throughout this thesis.

Buffer/Solution	Concentration
Ampicillin	
ampicillin	10% (w/v)
	in PBS (pH 7.4)
Blocking Solution Western blot	
skim milk	5%
	in TBST
Blocking Solution Immunohistochemistry	
fish gelatin	0.1% (w/v)
BSA	1% (w/v)
	in PBS (pH 7.4)
Collagen stock solution	
acetic acid	0.1% (w/v)
collagen, Type 1 rat tail (2 mg/ml)	2.5% (w/v)
	in ddH_2O
CsCl-Buffer	
CsCl	5,7 M
NaOAc (pH 6.0)	25 mM
	in ddH_2O

Denhardt's solution		
	BSA	1% (w/v)
	PVP	1% (w/v)
	Ficoll 400	1% (w/v)
		in ddH_2O
dNTPs		
	dATP	10 mM
	dTTP	10 mM
	dGTP	10 mM
	dCTP	10 mM
		in ddH_2O
GIT-Buffer		
	Guanidinthiocyanate	4 M
	NaOAc	25 mM
	NaCl	100 mM
	Mercaptoethanol	0,835% (v/v)
	EDTA (pH 8.0)	1 mM
		in ddH_2O
HBSS		
	NaCl	0.137 M
	KCl	5.4 mM
	Na_2HPO_4	0.25 mM
	K_2HPO_4 (pH 7.5)	0.44 mM
	$CaCl_2$	1.3 mM
	$MgSO_4$	1 mM
	$NaHCO_3$	4.2 mM
		in ddH_2O
Hybridization solution I		
	Formamid	50 % (v/v)
	SSC 20x (pH 7.4)	30% (v/v)
	EDTA	5 mM
	Denhardt's solution 50x	10% (v/v)
	SDS	0.5% (w/v)
		in ddH_2O (pH 7.4)

MEN-Buffer 10x		
	MOPS	200 mM
	NaOAc	50 mM
	EDTA	10 mM
		in ddH_2O (pH 7,0)
Herring sperm DNA		
	Herring sperm DNA	10 mg/ml
	solved for 8 h at 4°C	in ddH_2O
MOPS SDS-Running-Buffer		
	MOPS	50 mM
	Tris-HCl (pH 7.7)	50 mM
	SDS	3.47 mM
	EDTA	1.025 mM
		in ddH_2O
PBS		
	NaCl	137 mM
	KCl	2.7 mM
	Na_2HPO_4	8 mM
	K_2HPO_4 (pH 7.5)	50 mM
		in ddH_2O pH 7.3
Permeabilization buffer 10x		
	Triton X-100	0.1% (v/v)
	KCl	2.7 mM
		in PBS
4% PFA		
	Paraformaldehyde	4% (w/v)
	adjusted with NaOH	2M
		in PBS (pH 7.4)
Potassium phosphate buffer		
	K_2HPO_4	1 M
	KH_2PO_4	1 M
		in ddH_2O

RIPA lysis buffer		
	Tris	20 mM
	NaCl	150 mM
	NP-40	2% (v/v)
	SDS	0.1% (w/v)
	DOC	0.5% (w/v)
	adjusted with HCl	2M
		in ddH_2O (pH 7.2)
RNA running buffer		
	Formaldehyde	4% (v/v)
		in MEN-buffer 1x
RNA sample buffer		
	Formaldehyde	6% (v/v)
	Formamide	70% (v/v)
	Bromphenol Blue	0.03% (v/v)
	Ficoll 400	1% (v/v)
store at -20°C		in MEN-Buffer 1x
Solution I		
	Glucose	50 mM
	EDTA	10 mM
	Tris-HCl	25 mM
		in ddH_2O (pH 8.0)
Solution II		
	SDS	1%
	NaOH	0.2 M
		in ddH_2O
Solution III		
	KOAc	3 M
	acetic acid	5.75% (v/v)
		in ddH_2O
SSC (20x)		
	NaCl	3 M
	tri-Sodiumcitrate	300 mM
		in ddH_2O

DNA sample buffer (5x)		
	EDTA	20 mM
	Glycerin	30% (v/v)
	SDS	0.5% (v/v)
	Bromphenol blue	0.1% (w/v)
		in ddH_2O
TBS (10x)		
	Tris-HCl (pH 8.0)	100 mM
	NaCl	1.5 M
		in ddH_2O
TBS-T		
	Tris-HCl (pH 8.0)	100 mM
	NaCl	1.5 M
	Tween-20	0.1% (v/v)
		in ddH_2O
TBE-Buffer		
	Tris Base	89 mM
	Boric acid	89 mM
	EDTA	1 mM
		in ddH_2O
Transfer-Buffer (Western blot)		
	Bicine	25 mM
	Bis-Tris	25 mM
	EDTA	1 mM
	Chlorobutanol	0.05 mM
	Methanol	10% (v/v)
		in ddH_2O
Tris-Acetate Running-Buffer (Western blot)		
	Tris-HCl (pH 7.7)	50 mM
	Tricin	50mM
	SDS	0.1% (w/v)
		in ddH_2O

Wash solution I (Northern blot)		
	SSC (20x)	10% (v/v)
	EDTA	1 mM
	SDS	0.1% (w/v)
		in ddH_2O
Wash solution II (Northern blot)		
	SSC (20x)	2% (v/v)
	EDTA	1 mM
	SDS	0.1% (w/v)
		in ddH_2O

Table 2.20: Buffers and solutions

2.15 Media for cell culture

Media for *E. coli*		
LB		0.5% yeast extract
		1% tryptone
		0.5% NaCl
	final pH 7.5; use NaOH	
LB-Amp		LB
	add Ampicillin to a final conc.	50 μg/ml
LB-Kan		LB
	add Kanamycin to a final conc.	50 μg/ml
SOC		1x SOB-media
	after autoclaving	20 mM glucose

Table 2.21: Media for *E. coli*

Media for *hepatic stellate cells*	
DMEM 10% FCS (Culturing)	DMEM media 10% fetal calf serum 100 mg/ml Streptomycin 100 U/ml Penicillin 4 mM L-Glutamine
DMEM 0.5% FCS (Starvation)	DMEM media 0.5% fetal calf serum 100 mg/ml Streptomycin 100 U/ml Penicillin 4 mM L-Glutamine
DMEM 0.2% FCS (Stimulation)	DMEM media 0.2% fetal calf serum 100 mg/ml Streptomycin 100 U/ml Penicillin 4 mM L-Glutamine

Table 2.22: Media for *hepatic stellate cells*

2.16 Analytical methods

2.16.1 Calculation of DNA concentration

The concentration and purity of DNA was determined by measuring the absorbance at 260 nm using a spectrophotometer.

$$c(dsDNA)\ in\ \frac{\mu g}{ml} = OD_{260} \cdot dilution\ factor \cdot 50 \tag{2.1}$$

$$c(ssDNA)\ in\ \frac{\mu g}{ml} = OD_{260} \cdot dilution\ factor \cdot 33 \tag{2.2}$$

Pure DNA solution has a ratio of OD_{260nm} and OD_{280nm} between 1.8 and 2.0.

2.16.2 Calculation of RNA concentration

The concentration and purity of RNA was determined by measuring the absorbance at 260 nm using a spectrophotometer.

$$c(ssRNA)\ in\ \frac{\mu g}{ml} = OD_{260} \cdot dilution\ factor \cdot 40 \tag{2.3}$$

Pure RNA solution has a ratio of OD_{260nm} and OD_{280nm} between 1.9 and 2.1.

2.16.3 Calculation of adenoviral stock concentration

After cloning, amplification and purification of the adenoviral stock (chapter 2.20), 40 μl of the viral stock was diluted 1:25 in ddH_2O and the OD_{260nm} was measured. As a reference 40 μl of formulation buffer was also diluted with 960 μl of ddH_2O. Based on OD_{260nm} the concentration of viral particles was calculated as followed:

$$\frac{Particles}{ml} = OD_{260} \cdot 1.1 \cdot 10^{12} \cdot 25 = \frac{x \cdot 10^{12} Particles}{ml} \tag{2.4}$$

"Particle" include intact and infectious viruses as well as damaged, non-infectious viruses. Therefore, the concentration of plaque forming units have to be further determined. The conversion of particle to plaque forming units (Pfu) was based on the experience value of the technician, meaning 4 particles correlate with approximately 1 Pfu.

2.16.4 Calculation of protein concentration

The protein concentration was determined using the DC protein assay. The concentration of standard samples have been between 0.6 $\mu g/\mu l$ and 1.8 $\mu g/\mu l$. The DC protein assay was performed according to the manufacturer's instructions. The absorbance was measured in a 96-well plate at 690 nm using the Victor 1420 Multilabel Counter.

2.17 Cell culture methods

2.17.1 Culture conditions of *E. coli*

E. coli cells were cultured either in LB medium at 37°C and 180 rpm or on LB agar plates at 37°C. Depending on the plasmid and it's resistance gene antibiotics were added to the LB medium and to the LB agar plates with a final concentration of 50 μg/ml for ampicillin and kanamycin. Positive transformants were selected on these plates.

2.17.2 Culture conditions of COS-7

COS-7 cells were cultured at 37°C in a CO_2 incubator with a concentration of 5% CO_2 and 100% relative humidity.

Culturing of COS-7 cells was performed in DMEM, enriched with 10% (v/v) FCS, L-glutamine (4 mmol/liter), penicillin (100 IU/ml) and streptomycin (100 μg/ml)

2.17.3 Coverglass preparation for microscopy

For microscopy of cultured *hepatic stellate cells*, cells were seeded onto cover glass. Prior to the experiment cover glasses were incubated in 25% hydrochloric acid for 8 h at 37°C, washed with MilliQ and stored in 70% EtOH at 4°C. One day before seeding cover glasses were shortly heated up in order to vaporize EtOH, placed in one well of a 6-well-plate and covered with DMEM containing 10% FCS. The next day medium was removed and cells were seeded and cultured as described below.

2.17.4 Isolation of rat *hepatic stellate cells*

Isolation of HSC was performed by a technician. Briefly, HSC were isolated from male Sprague-Dawley rats by the Pronase-collagenase method followed by a density centrifugation on a Nycodenz gradient. Livers were perfused with Hanks' buffered saline solution (HBSS) and subsequently with 0.35% (w/v) Pronase E and 0.015% (w/v) collagenase, both in HBSS. Afterwards, the liver was dissected in HBSS supplemented with

DNase type II (100 μg/ml) and filtered through a nylon mesh. The resulting cell suspension was centrifuged, and cells were washed in ice-cold HBSS containing 0.25% (w/v) bovine serum albumin. HSC were further purified on 8.25% (w/v) Nycodenz gradients. The mean purity was estimated by vitamin A autofluorescence. The yield ranged from 20 to 50 x 10^6 HSC/liver. According to the growth area the number of cells was adjusted as listed below. Cells were initially cultured in HEPES-buffered Dulbecco's modified Eagle's medium supplemented with L-glutamine (4 mmol/liter), penicillin (100 IU/ml), streptomycin (100 μg/ml), and 20% FCS [113].

growth area	number of cells
64 cm^2	2.5-3 $\cdot 10^6$
28 cm^2	0.8-1 $\cdot 10^6$
10 cm^2	0.3-0.5 $\cdot 10^6$
12 well	0.09-0.15 $\cdot 10^6$
24 well	0.05-0.08 $\cdot 10^6$

2.17.5 Culture conditions of rat *hepatic stellate cells*

Hepatic stellate cells were cultured at 37°C in a CO_2 incubator with a concentration of 5% CO_2 and 100 % relative humidity.

Culturing of HSC was performed in DMEM, enriched with 10% FCS, L-glutamine (4 mmol/liter), penicillin (100 IU/ml) and streptomycin (100 μg/ml) as described in 2.22. Medium was renewed every second day with prewarmed medium. Prior to stimulation experiments, cells were starved in DMEM enriched with 0.5% FCS for 16 h. Stimulation itself took place in DMEM enriched with 0.2% FCS. Throughout starvation and stimulation medium was enriched with L-glutamine, penicillin and streptomycin. The only exception was transfection using Lipofectamine as described in 2.19.10. In this case DMEM without additives was used.

2.17.6 Stimulation of rat *hepatic stellate cells*

Stimulation of *hepatic stellate cells* was performed in DMEM enriched with 0.2% FCS, L-glutamine, penicillin and streptomycin. Before stimulation cells were starved in DMEM enriched with 0.5% FCS, L-glutamine and penicillin for 16 h. Cells were stimulated for 8-12 h with either TGF-β1 or BMP-7 with a concentration of 1 ng/ml or of 50 ng/ml, respectively. Afterwards, cells were harvested and according to the experimental procedure further processed.

2.18 Biochemical methods

2.18.1 Preparation of total protein lysate from rat *hepatic stellate cells*

Hepatic stellate cells were washed twice in ice-cold PBS. According to the size of the culture dish, cells were lysed in 200 μl - 600 μl RIPA buffer. RIPA buffer contained the complete protease inhibitor cocktail and depending on the experiment RIPA buffer was enriched with a Phosphatase inhibitor cocktail (1:100). Lysis was supported by additional shearing through a 0.4 x 19 mm needle and the lysate was further incubated on ice for 30 minutes. Afterwards, the lysate was centrifuged at 4°C and 13 000 rpm in a table top centrifuge. The pellet was discarded and the supernatant was used for SDS polyacrylamide gel electrophoresis and Western blot analysis.

2.18.2 SDS polyacrylamide gel electrophoresis

SDS polyacrylamide gel electrophoresis was used to separate denatured proteins according to their molecular weight. To determine the weight of the proteins molecular weight markers (2.3) were used. Protein concentration was determined as described in 2.16.4. Equal amounts of protein were diluted with 4 x LDS electrophoresis sample buffer (2.3). Depending on the experiment DTT was added as a reducing agent (final concentration 10 mM). After incubation for 10 min at 70°C proteins were separated on either 4-12% Bis-Tris gradient gels (2.3) using MOPS-SDS running buffer or alternatively on 3-8% Tris-Acetate gradient gels (2.3) using Tris-Acetate SDS running buffer. Depending on the experiment 10 μg or 20 μg of protein was loaded on the gel and separated at 140 V for about 2.5 h.

2.18.3 Western blot

Immunoblotting was performed using a wet transfer system. Proteins were transferred onto a nitrocellulose membrane at 55 V for 3 h. To reduce non-specific binding of antibodies the nitrocellulose membrane was initially blocked for 20 min with 5 % skim milk powder in TBS-T, followed by over night incubation with the primary antibody. Primary antibodies were detected with horseradish-peroxidase (HRP)-conjugated secondary antibodies. The secondary antibody was incubated for 5-6 h. Before and after incubation with the secondary antibody the nitrocellulose membrane was washed three times with TBS-T. Finally, the secondary antibody was detected with the SuperSignal West Dura Extended Duration Substrate. All antibodies were diluted in 5% (w/v) skim milk powder in TBS-T.

2.18.4 Luciferase assay

HSC were either transfected with $(BRE)_2$-Luc and $(CAGA)_{12}$MLP-Luc in pGL3 as described in 2.19.10 or infected with the corresponding $(BRE)_2$-Luc and $(CAGA)_{12}$MLP-Luc adenovirus as described in 2.19.11. After transfection or infection, the cells were cultured for at least 24 h. Prior to stimulation with TGF-β1 or BMP-7 cells were starved in DMEM containing 0.5% of FCS instead of 10% FCS. After stimulation for 6 h or 12 h cells were washed twice with PBS. Cell lysis buffer, which was supplied with the Steady-Glo-Luciferase Assay system was diluted 1:5 with ddH_2O. 350 μl of cell lysis buffer was added to the HSC and incubated for 1 minute. Cells were scraped off using a rubber policeman and further homogenized using a 0.4 x 19 mm needle. The samples were centrifuged in a table top centrifuge at maximal speed at 4°C for 15 minutes. The supernatant was transferred to a new reaction tube.

LAR substrate was diluted 1:2 with ddH_2O. 100 μl LAR was filled in one well of a black 96 well plate. 20 μl of the cell lysate was added and mixed by pipetting. Fluorescence was determined using the MicroBeta Jet 1450 Scintillation and Luminescence Counter.

2.18.5 Proliferation assay

HSC were seeded onto 12-well plates and cultured in DMEM containing 10% FCS. One day after initial plating, cells were transfected with siRNA as described in 2.19.10. On day 2 of culture the medium was renewed. One day later the medium was replaced again with 1 ml of DMEM containing 10% FCS and cells were exposed to 75 kBq/ml [methyl^{3}H]-thymidine for a 24 h labelling period. In case of BrdU, medium was renewed on day 4 and afterwards cells were exposed to BrdU for a 48 h labelling period. Radioactivity incorporated into DNA was measured using the Microbeta 1450 Jet Scintillation and Luminescence counter. BrdU incorporation was measured by a colorimetric BrdU cell proliferation ELISA according to the manufacturer's instructions (Roche).

2.18.6 Gelatinase assay

HSC were cultured in 96-well plates and DMEM containing 10% FCS. One day after initial plating, cells were transfected with siRNA on day 1 as described in 2.19.10. On day 4 the gelatinase/collagenase assay was initiated and fluorescence was measured at 530 nm at the indicated time points according to the manufacturer's instructions.

2.19 Molecular biological methods

2.19.1 Isolation of plasmid DNA (Miniprep)

E. coli were grown over-night in 2-3 ml LB medium containing the corresponding antibiotics. The next day cells were pelleted by centrifugation for 1 minute at 13 000 rpm in a table top centrifuge. The supernatant was discarded. The cell pellet was resolved by vortexing in 100 μl solution I and incubated at room temperature for 5 minutes. To lyse cells 200 μl of solution II was added and the reaction tube was inverted for a couple of times until the solution became clear. After incubation for additional 5 minutes on ice 150 μl of solution III was added and again incubated for 5 minutes on ice. Precipitation of protein started. After incubation 100 μl of chloroform was added, vortexed and centrifuged for 10 minutes at room temperature and 13 000 rpm in a table top centrifuge. After centrifugation the sample contained two phases. The upper, aqueous layer contained the DNA. This aqueous layer was transferred to a new reaction tube, 1 ml of ice cold abs. ethanol was added and incubated for 5 minutes on ice. Samples were centrifuged for 10 minutes at 13 000 rpm and 4°C in a table top centrifuge. The supernatant was discarded, 1 ml of 70% ethanol was added to the pellet and again centrifuged for 10 minutes at 13 000 rpm and 4°C in a table top centrifuge. The supernatant was discarded, the pellet was air dried for 15-30 minutes and finally resolved in 50-100 μl ddH_2O. The DNA concentration was determined as described in 2.16.1.

2.19.2 Isolation of RNA

For isolation and purification of total RNA from *hepatic stellate cells* the RNeasy Mini Kit from Qiagen was used. Briefly, cells were washed twice with ice cold PBS and depending on the number of cells 300 μl or 500 μl of RLT buffer containing 1% (v/v) β-Mercaptoethanol were added. Cells were scraped off using RNase free tissue cell rubber policeman. Cells were then homogenized using a 0.4 x 19 mm needle and the QIAshredder spin columns. The samples were further processed as described in the instruction manual. Finally RNA was eluted in 30 μl RNase free ddH_2O. The concentration of the total RNA was determined as described in 2.16.2. RNA was stored at -80°C.

2.19.3 Formaldehyde agarose gel electrophoresis

Isolation of total RNA was performed as described before (2.19.2). Because Ribonucleases (RNases) are very stable and active enzymes possible RNase contaminations were

eliminated as followed. Glassware was washed and oven baked at 180°C over-night. Electrophoresis tanks, gel slides and other hard plastic components were treated with 2% SDS solution for 3-4 h. MilliQ water that was used to set up buffers was autoclaved in RNase free glassware. Furthermore, sterile, disposable polypropylene plastic ware was used. Throughout the experiment gloves were worn.

To separate total RNA a formaldehyde agarose gel containing 2% (w/v) agarose and 17% (v/v) formaldehyde in 1 x MEN-buffer was prepared as followed. 146 ml water and 2 g agarose were heated in a microwave until agarose was completely dissolved. Prior to adding 20 ml of 20 x MEN-buffer and 34 ml of formaldehyde the solution was cooled down to 65°C and finally poured onto a gel support. 5 μg or 10 μg of total RNA were diluted with 1.5 volumes of RNA sample buffer and incubated for 10 min at 70°C. 1 μl of ethidium bromide was added to the sample. The sample was loaded onto the gel. The gel was run at 30 V until the bromphenol blue band had passed three-quarter of the gel. Prior further processing images were taken under UV light.

2.19.4 Northern blot

To transfer RNA from agarose gel to a nitrocellulose membrane a plastic dish, slightly larger than the agarose gel was used as electrophoresis tank. The tank was filled with 20 x SSC transfer buffer. A plastic plate was arranged on the edges of the plastic dish. Whatmann paper, which was soaked with 20 x SSC, were placed on the plastic plate touching the transfer buffer and mediating the buffer flow. Air bubbles were removed by rolling a 10 ml sterile plastic pipet over the surface of the whatman papers. Afterwards the gel was placed upside down on the whatman papers and topped with a nitrocellulose membrane. It was important to avoid bubbles at this step. In order to maintain that the buffer pass through the gel, the gel was surrounded with strips of plastic wrap.

Three more whatman papers were placed on the nitrocellulose. Air bubbles were removed using a sterile plastic pipet. Finally, a big layer of paper towels and a glass plate were placed on top. To ensure good contact between the gel and nitrocellulose and to hold everything in place a weight was placed on the glass plate. The transfer was performed over-night.

The next day paper towels and whatman papers were removed. The position of wells, the direction of sample loading as well as 18S and 28S RNA were marked. The membrane was placed in between two whatman papers and air dried for at least 30 minutes. The RNA was immobilized by baking at 80°C for 2 h. The membrane was either

immediately used or stored at -80°C.

Labelling of DNA probes

DNA probes used for RNA detection were either obtained by restriction digestion or by PCR using the corresponding pGEMT-easy vector. DNA was purified by agarose gel extraction as described before (2.19.8). Approximately 100 ng of double-stranded DNA were diluted with water to a final volume of 10 μl. Samples were heated for 3 minutes in boiling water and transferred on ice. Primer (5 μl), buffer solution (10 μl), MilliQ (18 μl), 5 μl [α^{32}P] dCTP ($\sim$ 3000 Ci/mmol) and Klenow fragment (2 U) were added and incubated for 2 h at 37 °C. Non incorporated nucleotides were separated from the DNA probe by a G50-Sephadex column. The column consists of a Pasteur pipette and a glass ball slightly sealing the Pasteur pipette. The Pasteur pipette was filled with G50-Sephadex. TES was used as running buffer and for equilibrating the column. The labelling sample was loaded onto the G50-Sephadex column and eluted with TES. The fractions (1st fraction: 600 μl next fractions 200 μl each) were collected. 1 μl of each fraction was counted in a liquid scintillation counter. Fraction 2 + 3, which contained the radioactive labelled probe, were pooled, denatured for 10 minutes at 95°C and used for the hybridization.

Hybridization

The nitrocellulose membrane was placed in a hybridization tube. 1 ml Hybridization solution I per cm^2 supplemented with herring sperm DNA (final concentration: 100 μg/ml) were added and incubated for 3 h at 37°C and 60 Upm. The Hybridization solution I was replaced by 1 ml Hybridization solution I per 5 cm^2. Radioactive labelled DNA probe was added to the hybridization tube to a final concentration of 1 million counts/ml and incubated for 16 h at 37°C and 60 Upm. Afterwards the membrane was washed once with wash solution I for 20 minutes at 55°C, followed by washing twice with wash solution II for 20 minutes at 50°C. Finally autoradiography was performed.

2.19.5 cDNA synthesis

cDNA synthesis was performed according to the instruction manual using the Superscript II Reverse Transcriptase Kit (Invitrogen). Briefly, 1 μg of total RNA, 1 μl random primer (250 ng/μl) and 1 μl dNTPs (10 mM) were diluted with H_2O to a final volume of 13 μl. To avoid regions of double-stranded RNA sample was heated for 5 minutes

at 65°C. After heating the reaction tube was immediately transferred on ice and 4 μl of 5 x buffer and 2 μl of DTT 0.1 M were added and carefully mixed. Prior to adding 1 μl of super script II reverse transcriptase the sample was incubated for 2 minutes at 25°C. After adding reverse transcriptase the sample was incubated for 10 minutes at 25°C, followed by 1 h at 42°C and 15 minutes by 70°C. For long term storage cDNA samples were kept at -20°C.

2.19.6 Polymerase chain reaction (PCR)

Polymerase chain reaction was used to amplify DNA sequences for cloning or sequencing. 100-200 ng of Plasmid or cDNA, 1 μl of forward and reverse primer (0.1 $\mu g/\mu l$), 2.5 μl of 10 x buffer, 0.5 μl dNTPs (10 nM), 1 μl of *Taq* DNA Polymerase were diluted with ddH_2O to a final volume of 25 μl.

Depending on the lengths of DNA fragments and the relation between purines and pyrimidines a program similar to the program shown below was set up in a Robocycler.

1	Denaturing	5 min	95°C		
2	Denaturing	30 s	95°C		
3	Annealing	30 s	54°C		
4	Elongation	90 s	72°C		
				Step 2-4	25-35 cycles
5	Holding temperature	unlimited	4°C		

To perform a semi-quantitative PCR the number of cycles and the amount of cDNA were reduced as much as possible.

2.19.7 DNA sequencing

For sequence validation of PCR and cloning products DNA sequencing was performed. During the sequencing reaction fluorescent dye labelled dideoxynucleotides were introduced into the sequence. This caused an arrest of the extension and resulted in fragments of different sizes, containing an end labelled dideoxynucleotide. For each reaction 8 μl Terminator Ready Reaction Mix, 400 ng DNA and 40 ng sequencing primer were diluted with H_2O to a final volume of 20 μl. Because the Terminator Ready Reaction Mix does contain the polymerase each step was performed on ice. The sequencing reaction program was set up as follows:

1	Denaturing	5 min	95°C		
2	Denaturing	30 s	95°C		
3	Annealing	20 s	50°C		
4	Elongation	4 min	60°C		
				Step 2-4	50 cycles
5	Holding temperature	unlimited	4°C		

The sequencing products were purified using Centrisep Spin Columns. Prior to purification 800 μl of H_2O was loaded onto the column and incubated for at least 3 h. Afterwards, the top and bottom lid was removed, the column was placed in a reaction tube and centrifuged for 2 min at 750 g. The column was transferred to a new reaction tube, the sequencing reaction was loaded onto the column and again centrifuged for 2 min at 750 g. The flow through contained the purified sequencing products and was further processed by drying in a vacuum centrifuge for 20 minutes. The sample was resolved by a technician and analyzed using ABI 310 Genetic Analyzer or stored at -20°C before sequencing.

2.19.8 Cloning

Agarose gel electrophoresis

Agarose gel electrophoresis was used to separate DNA fragments of different sizes. Depending on the DNA fragment size the percentage of agarose varied between 0.7% and 2.0%. Agarose was dissolved in TBE-buffer and heated up in a microwave until agarose was completely dissolved. 2-4 μl EtBr were added. The gel solution was mixed, poured onto a gel support and run at 75 V for 2-3 h. DNA/EtBr complexes were visualized by UV light and images were taken.

Isolation of DNA fragments by gel extraction

DNA fragments were separated by agarose gel electrophoresis. DNA fragments of interest were excised with a scalpel and purified using the QIAquick Gel Extraction Kit (Qiagen). The gel extraction was performed as recommended by the manufacturer. Finally DNA was eluted with 30 μl - 50 μl ddH_2O.

Digestion of DNA

For cloning strategies plasmids and DNA fragments were specifically cut using restriction enzymes. According to the restriction enzyme the buffer-system as recommended and supplied by the manufacturer was used. The total volume of the reaction was 20 μl, containing 0.5 - 2 μg DNA, 2 μl 10x buffer, 1 U of Enzyme and if recommended 0.1% BSA. Incubation time was 1-3 h at 37°C. After digestion DNA fragments were separated on an agarose gel. DNA of interest was gel extracted as described in 2.19.8.

Klenow reaction

The Klenow enzyme was used for complete filling of 3' recessed DNA ends. 3' recessed DNA are the product of some restriction enzymes, which produce sticky ends. The standard reaction mix contained 1 μg DNA, 1 μl of NTPs (10 mM), 4 μl 10 x filling buffer (M-restiction buffer) and 2 μl Klenow enzyme (2 U/μl). ddH_2O was added to a final volume of 40 μl. The sample was incubated for 60 minutes at 37°C followed by inactivation at 65°C for 10 minutes.

Dephosphorylation of plasmid-DNA

In order to avoid self-ligation of single cut DNA fragments phosphate groups were removed from the 5'-end of the DNA using calf intestinal alkaline phosphatase (CIP) as recommended by the manufacturer. Briefly, dephosphorylation reaction contained 1 μg DNA, 4 μl 10 x dephosphorylation buffer, 2 U of alkaline phosphatase and was diluted with water to a final volume of 40 μl. The reaction was incubated for 60 minutes at 37°C followed by inactivation of the enzyme at 65°C for 10 minutes.

Ligation of DNA fragments

Ligation reactions were performed in a total volume of 20 μl. The ligation reaction contained 2 μl of 10 x T4-DNA-Ligase-buffer, 1 μl of T4 DNA-Ligase and the digested and eventually dephosphorylated vector DNA as well as the DNA fragment of interest in a molar ratio of 1:3. The reaction was incubated over-night at 16°C or for 1-2 h at room temperature. *E.coli* were directly transformed with the ligation reaction as described in 2.19.9.

2.19.9 Transformation

Heat shock transformation of *E. coli*

E. coli (DH5α cells) were transformed with DNA using the heat shock method. Cells were thawed on ice, 0.5-2 μg of DNA was added, mixed and kept on ice for 30 minutes. *E. coli* were heat-shocked at 42°C for 60 - 90 sec, immediately placed on ice and kept in LB-medium for 30-60 min at 37°C. For selection *E. coli* were spread on LB plates containing the appropriate antibiotics and grown over-night at 37°C. Single colonies were then grown in LB media containing the appropriate antibiotics. Plasmids were isolated as described in 2.19.1.

2.19.10 Transfection

Transfection of 293A cell line

Plasmid transfection into 293A cells was exclusively part of adenovirus production and is described in detail in 2.20.3.

Transfection of COS-7

COS-7 cells were seeded onto 6 well plates (150 000 cells/well). The next day medium was renewed one hour before the transfection was performed.

For each well 1 μg of DNA was placed in a reaction tube. In a second reaction tube 3 μl FuGene (for each μg of DNA) was diluted with 100 μl DMEM, gently vortexed, centrifuged and incubated for 15 minutes at room temperature. After incubation the FuGene solution was added to the DNA and incubated for 15 minutes. Finally the solution was drop-wise added to the medium and incubated for 24 h before medium was exchanged.

Transfection of *hepatic stellate cells*

HSC were isolated and seeded on 6-well plates. The next day medium was replaced with DMEM supplemented with L-glutamine (4 mmol/liter), penicillin (100 IU/ml), streptomycin (100 μg/ml) and 10% FCS (v/v). Medium was renewed every second day and additional 2-3 h prior to transfection. For each well 1 μg of DNA was diluted with 100 μl 150 mM NaCl, gently vortexed and briefly centrifuged. In a second reaction tube 6 μl Nanofectin (for each μg of DNA) was also diluted with 100 μl 150 mM NaCl,

gently vortexed and briefly centrifuged. Afterwards the Nanofectin solution was transferred to the DNA solution, mixed by tapping and incubated for 30 minutes at room temperature. Finally the solution was added drop-wise to the medium and incubated for 24 h before medium was changed.

Transfection of *hepatic stellate cells* with siRNA

HSC were isolated and seeded onto 12-well plates, 6-well plates or 60 mm dishes. The next day medium was replaced with DMEM supplemented with L-glutamine (4 mmol/liter), penicillin (100 IU/ml), streptomycin (100 μg/ml) and 10% FCS (v/v) and incubated for 4 h. After incubation cells were transfected according to the manufacturer's instruction with a final siRNA concentration of 5 nM unless otherwise indicated. The ratio of siRNA (20 μM) and HiPerFect was 1:20 (v/v). Depending on the experimental procedure, medium was renewed every 48 h. Specific siRNAs targeting rat endoglin (SI01509963, SI01509970) or rat α_2-macroglobulin (SI03028361,SI03108518) or siRNA control (1027281) were used. After establishing this method every experiment was performed using SI01509970 in case of endoglin and SI03028361 and SI03108518 in case of α_2-macroglobulin.

2.19.11 Infection

Depending on the experimental setup *hepatic stellate cells* were infected with adenovirus between day 1 and day 3 of culturing. Unless otherwise indicated, the cells were infected with $1 \cdot 10^8$ Pfu/ml in DMEM containing 10% FCS. The medium was renewed 12 h after infection. Depending on the experiment cells were starved for 16 h and stimulated as described in 2.17.6 or further cultured and processed for Western blot analysis.

2.20 Adenoviruses

As part of this thesis adenoviruses for reporter gene assays and adenoviruses for gene silencing were constructed, produced, amplified and purified.

2.20.1 Generation of the shRNA expression vector

For creating the shRNA expression vector the instruction manual was followed accurately. Briefly, two complementary oligonucleotides encoding shRNA of interest were annealed to create a double-stranded oligo and directly ligated into the pENTR^{TM}/U6

vector. The pENTR^{TM}/U6 vector represents the shuttle vector. *E. coli* was transformed with this shuttle vector and selected for recombinant clones. The functionality of the shuttle vector was tested in COS-7 cells.

The recombinant viral vector was generated by performing LR recombination reaction using the shuttle vector pENTR^{TM}/U6 containing shRNA and the pAd/Block-it^{TM}Dest vector. Top10 *E. coli* were transformed with the LR reaction mixture and selected for expression clones.

2.20.2 Generation of the $(BRE)_2$ and $(CAGA)_{12}$MLP luciferase shuttle vectors

For generating the $(BRE)_2$ luciferase and $(CAGA)_{12}$MLP luciferase shuttle vector the pGL3-Basic vector containing either $(CAGA)_{12}$MLP Luc or $(BRE)_2$ Luc (see Appendix for plasmid maps) were double digested with *Bam*HI and *Kpn*I. pENTR4 was digested with *Eco*RI and both digestion reactions were seperated on a 1% agarose gel. DNA fragments were isolated as described in 2.19.8. The 3‘ recessed DNA ends of both DNA fragments were filled using the Klenow enzyme as described in 2.19.8. The pENTR4 fragment was additionally dephosphorylated and the ligation was performed overnight with the corresponding insert as described in 2.19.8. *E. coli* were transformed with the ligation reaction and selected for recombinant clones.

The recombinant viral vector was generated by performing LR recombination reaction using the shuttle vector pENTR4 containing either $(CAGA)_{12}$MLP Luc or $(BRE)_2$ Luc and the pAd/Block-it^{TM}Dest vector. The LR reaction mixture were transformed into Top10 *E. coli* and selected for recombinant clones.

2.20.3 Production and amplification of adenoviral stocks

293A cells were used to produce the adenovirus. The adenoviral expression vectors were cut with *Pac* I. 293A cells were transfected with the digested epression vector using Lipofectamine 2000 as transfection reagent. Prior to transfection cells were seeded in a 6-well plate and cultured in normal growth medium containing 10% FCS. Cells were grown until a confluence of 80% was reached. Transfection of the expression vector in different concentrations but with a fixed ratio of 1:3 (Vector (μg) : Lipofectamine 2000 (μl)) was performed according to the manufacturer’s instructions. The next day medium was replaced and one day later cells were trypsinized and seeded onto a 10 cm culture plate. Every second day medium was replaced and cells were thoroughly monitored until regions of cytopathic effects were visible. Cytopathic ef-

fects were indicated by patches of rounding, dying cells. When cytopathic effects were visible, the medium was either partly replaced or fresh medium was added. When approximately 90% of the cells showed the cytopathic effect, cells were harvested and a crude viral lysate was prepared by three freeze/thaw cycles in liquid nitrogen followed by centrifugation for 20 minutes at 4°C and 3 000 g. The supernatant contained the crude viral lysate.

The crude viral lysate was diluted and used to infect 16 flasks of 293A cells. After 2-3 days most of the cells had a round shape and were floating within the medium. The medium, which contains the floating cells was transferred to a falcon tube. Attached cells were harvested, added to the falcon tube and centrifuged for 20 minutes at 4°C and 900 g. The supernatant was discarded and the pellet was further purified as described next.

2.20.4 Purification of adenoviral stocks

The pellet enriched with infected 293A cells was resuspended in DMEM to a total volume of 14.7-14.8 ml. Cells were lysed by three freeze/thaw cycles in liquid nitrogen followed by centrifugation for 20 minutes at 4°C and 3 000 g. The supernatant contained the viral lysate. The lysate (14.7-14.8 ml) was mixed with 8 g of CsCl and 4 x 4.1 ml were transferred to a centrifuge tube. The CsCl gradients were ultra centrifuged for 22-24 h at 4°C and 40 000 rpm using a SW60Ti rotor. *Via* ultra centrifugation three different bands were visible in the gradient. The top band contained debris of cells and medium, the middle faint band contained damaged virus and the lowest band contained intact virus. The CsCl solution containing the debris and damaged virus was removed using a syringe. The CsCl solution enriched with intact virus was afterwards removed using a fresh syringe and further purified using the Adeno-X-rapid Titer Kit.

Two filter steps are applied when the Adeno-X-rapid Titer Kit is used. Since the virus was already purified by using the CsCl gradient the bottle top filter was skipped. Furthermore, Benzonase was not used. Except this modifications the purification was performed according to the instruction manual. Briefly, the Adeno-X syringe-filter was washed with 50 ml PBS, loaded onto the Adeno-X syringe-filter, washed with wash buffer and eluted with 3 ml 1 x elution buffer. The eluate was centrifuged for 30 min at 12 000 rpm and 4°C. The supernatant was discarded and the pellet was resolved in a total volume of 1260 μl Formulation buffer. The adenoviral titer was determined as described in 2.16.3.

2.20.5 CRP2-adenovirus

Adenoviral vectors expressing the cysteine rich protein 2 (CRP2) or a green fluorescent protein (GFP)-tagged version of CRP2 were cloned using standard procedures and were provided by Prof. R. Weiskirchen. Briefly, expression cassettes directed under transcriptional control of the CMV promoter were cloned into shuttle vector pΔE1sp1A (Microbix Biosystems Inc., Ontario, Canada) and subcloned into the adenoviral backbone vector pJM17 (Microbix Biosystems) by homologous recombination in 293A cells. Recombination, amplification and purification of respective adenoviral particles was performed as described above.

2.21 Whole rat genome oligo microarray

Gene expression analysis of different rat mRNAs using agilent whole genome oligo microarrays was performed by Miltenyi Biotec GmbH. Isolation of total RNA and parts of the final data analysis was performed independently from Miltenyi as a part of this thesis.

2.21.1 Sample preparation and quality check

HSC were isolated and seeded on 6 mm cell culture dishes. On day 1 of culture cells were transfected with siRNA as described in 2.19.10. On day 8 of culture total RNA was isolated (2.19.2) and the concentration of RNA was determined as described in 2.16.2. Silencing of endoglin on the level of mRNA was demonstrated by semi quantitative PCR as described in 2.19.6. Out of these samples 18 vials (6 groups each consisting of Control, siEndoglin and siControl samples) were shipped to Miltenyi on dry ice for further quality checks using the agilent 2100 bioanalyzer platform. For more detail information see: www.miltenyibiotec.com. Finally four groups were chosen to perform the hybridization (see table 2.23).

2.21.2 Hybridization

Before hybridization three different groups -each group consists of Control, siEndoglin and siControl samples- were pooled. One group was further processed without pooling. The selection of oligo(dT)-positive mRNAs, sample labelling and microarray hybridization was performed by Miltenyi Biotech according to the *agilent 60-mer oligo mi-*

crorray processing protocol using the *agilent gene expression hybridiztion kit*. The hybridization schedule was as followed:

Exp No.	Cy5 / Cy3	Array No.
1	1 (Con) / 3 (siCon)	251487910880_1
2	2 (siEng) / 3 (siCon)	251487910880_2
3	Pool 1 (Con) / Pool 3 (siCon)	251487910880_3
4	Pool 2 (siEng) / Pool 3 (siCon)	251487910880_4

Table 2.23: Microarray hybridization schedule

2.21.3 Data analysis

The fluorescence signals of the agilent oligo microarray were detected using agilent's DNA microarray scanner and further processed with the agilent Feature Extraction Software. The complete raw data set and a putative candidate gene list were obtained from Miltenyi. The putative candidate gene list contained genes with a fold change ≥ 2 and p-value ≤ 0.01. Additional to these basic information Miltenyi performed pathway gene analysis.

The putative candidate gene list was further processed as part of this thesis. Genes which were differentially expressed in hybridization no.1 (single) and no.3 (pool) were excluded from hybridization no.2 (single) and no.4 (pool). In this way genes, which were differentially expressed by the transfection itself, were skipped. Genes were also skipped, if they were differentially expressed in only one of the hybridization no.2 (single) or no.4 (pool). The remaining genes of hybridization no.2 (single) and no.4 (pool) were defined as differentially expressed as a result of endoglin silencing.

2.22 Microscopy

2.22.1 Bright field microscopy

For bright field microscopy, cells were seeded on plastic dishes and cultivated as described in 2.17.5. Cells were washed with PBS and images were taken using a 10 x objective and a 10 x ocular lens. Documentation of representative eye fields was performed with a HV-C20 digital camera (HITACHI Denshi Ltd., Tokyo, Japan) or a KY-F75U digital camera (HITACHI) and the DISKUS software package version 4.14 (Hilgers, Königswinter, Germany).

2.22.2 Immunofluorescence microscopy

For immunofluorescence microscopy, the cells were seeded onto cover slides and cultivated for the appropriate time period. Cells were once washed with PBS, fixed for 20 min in 4% PFA, permeabilized for 5 min with 0.1% Triton X-100 in phosphate buffer and twice washed with PBS. The Alexa Fluor 488 Phalloidin stock solution was diluted 1:50 with PBS. PBS was removed and cells were stained for 40 min using 200 μl of the diluted Phalloidin solution. Cells were washed three times with PBS. Nuclei were counterstained with DAPI (1 μg/ml) for 1 min and washed with PBS and water. Finally, cells were mounted in antifade mounting medium (DAKO) and the cover slide was placed on a glass slide.

When GFP-tagged proteins such as CRP2-GFP were visualized no permealization was performed. Cells were directly counterstained, washed and mounted. Images were taken using 10 x objective, a 20 x objective or a 40 x objective and a 10 x ocular lens. Documentation of representative eye fields was performed as described above.

Chapter 3

Results

In order to characterize HSC, which express less endoglin compared to wild type HSC, heterozygous knock out mice were initially analyzed. (Homozygous knock out of endoglin is lethal during early embryogenesis [28].) First experiments revealed only marginal changes in the quantity of endoglin in heterozygous knock out mice compared to wild type mice. In addition preparation of HSC from endoglin deficient animals was difficult to accomplish, because of the vascular malformation. This malformation leads to a disruption of vessels during the perfusion procedure. Therefore, it was not possible to keep on working with heterozygous knock out mice. Instead, it was necessary to search for an alternative method to knock down endoglin *in vivo* and *in vitro*, respectively. The most promising method was the use of RNA interference. For *in vivo* experiments an adenovirus, carrying the genetical information for shRNA targeting mouse endoglin, was generated. For *in vitro* experiments primary rat HSC were transfected with siRNA oligonucleotides targeting rat endoglin. Due to the fact that *in vivo* experiments are very time-consuming they have not been performed yet. However, based on a very efficient and sustained knock down of endoglin *in vitro* it was possible to investigate the function of endoglin in HSC.

This thesis can be roughly divided into two sections. Experiments of the first section analyze the function of endoglin under normal growth conditions (10% FCS). These experiments revealed changes in morphology, in ECM abundance, in organization of the cytoskeleton, in proliferation and in the gene expression pattern of HSC lacking endoglin. Experiments of the second section analyze the involvement of endoglin in the TGF-β1 and BMP-7 pathway after cell starvation (0.5% FCS) and stimulation (0.2% FCS). Due to the fact that primary HSC are very difficult to transfect, but easy to infect, a $(CAGA)_{12}$MLP-luciferase virus and a $(BRE)_2$-luciferase virus were generated. Beside

Western blot analysis these viruses were used as an additional read out system for TGF-β1 and BMP-7 stimulation experiments.

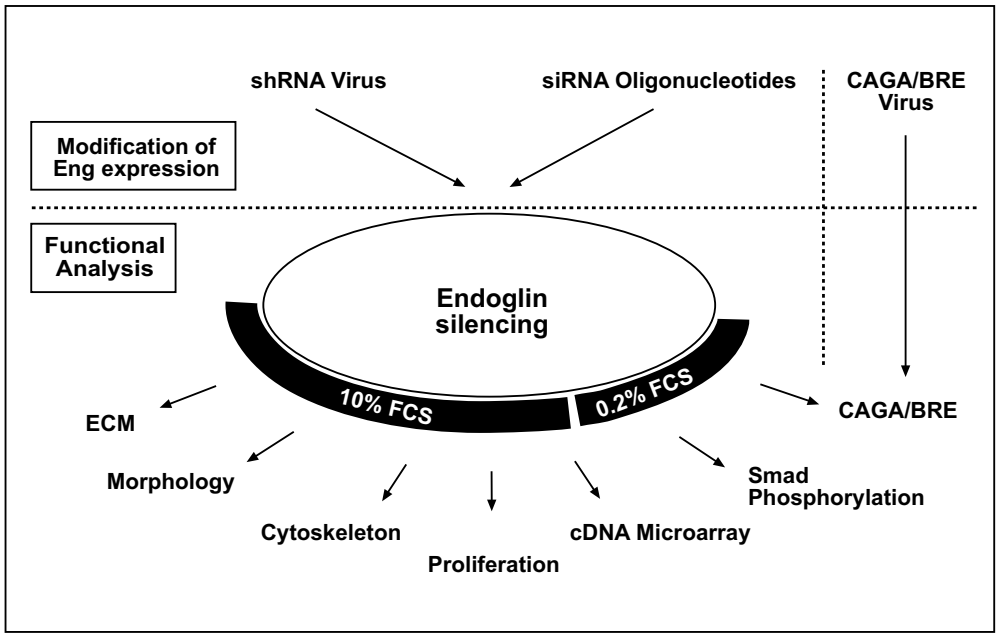


Figure 3.1: The cartoon gives a short overview of the main experiments, which were performed in this thesis.

Please note: Unless otherwise indicated, all experiments were performed with primary rat *hepatic stellate cells* (HSC). All time data indicate the day after initial plating of HSC.

3.1 RNAi - Inhibition of endoglin expression in HSC

RNA interference (RNAi) describes the inhibition of eukaryotic gene expression by double-stranded RNA (dsRNA). Inhibition of gene expression is due to a degradation of messenger RNA (mRNA) complementary to the dsRNA. *In vivo* dsRNA is processed into 21-23 nucleotide double-stranded short interfering RNA (siRNA). siRNA leads to specific degradation of complementary mRNA. Short hairpin RNA (shRNA) is an artificial designed dsRNA. This dsRNA is processed to siRNA which in turn leads to a specific degradation of mRNA.

3.1.1 shRNA virus

In order to perform *in vivo* experiments three shRNA viruses were generated. For this purpose, different double-stranded oligonucleotides encoding shRNA targeting mouse endoglin were ligated into the pENTR^{TM}/U6 vector (shuttle vector). These three constructs were termed shRNA 12.1, shRNA 34.1 and shRNA 56.1. As a negative control double-stranded oligonucleotides encoding shRNA targeting LacZ were used. Prior to homologous recombination the ability of these shRNAs to silence mouse endoglin was tested in COS-7. COS-7 do not express endogenous endoglin. Therefore, COS-7 were (double) transfected with the shRNA shuttle vector construct and additionally with an expression vector encoding mouse endoglin. After transfection, cells were cultured for 4 days. Western blot analysis was performed and revealed shRNA 12.1 as the construct, which down regulates mouse endoglin most efficiently (Fig. 3.2 a). Double transfection of either shRNA 12.1 and shRNA 34.1 or shRNA 12.1 and shRNA 56.1 did not increase gene silencing compared to shRNA 12.1 applied alone.

Subsequent to COS-7 experiments, shRNA 12.1 and shRNA 34.1 were subcloned by homologous recombination into the pAd/Block-*it*^{TM}-Dest vector. After subcloning adenoviruses were amplified and the crude viral lysates were tested. Mouse HSC were infected on day 2, cultured and harvested on day 7. Western blot analysis was performed. Endoglin and α-SMA were detected using specific antibodies. As expected, mouse HSC infected with shRNA *LacZ* did not show any decrease in endoglin expression (Fig. 3.2 b). Single infection of mouse HSC with a virus encoding shRNA 34.1 as well as double infection with a virus encoding shRNA 34.1 and shRNA 12.1 resulted in a decrease in endoglin expression. Depending on the virus concentration down-regulation of endoglin was more efficient at higher concentration. α-SMA expression as a marker for transdifferentiation was not affected in any sample analyzed. Single infection with the adenovirus encoding shRNA 12.1 had no impact on endoglin expression. This is contrary to the results obtained in COS-7 experiments. While in COS-7 endoglin was sufficiently silenced using shRNA 12.1 (Fig. 3.2 a) in mouse HSC, endoglin is unaffected using shRNA 12.1 (Fig. 3.2 b). Therefore, the adenovirus carrying shRNA 34.1 is appropriate for endoglin down-regulation and suited for *in vivo* experiments.

3.1.2 siRNA oligonucleotides

In order to perform *in vitro* experiments siRNA oligonuclotides targeting rat endoglin were used. First of all the transfection efficiency of primary HSC with siRNA oligonucleotides was determined using fluorescence-labelled siRNA oligonucleotides and HiPer-

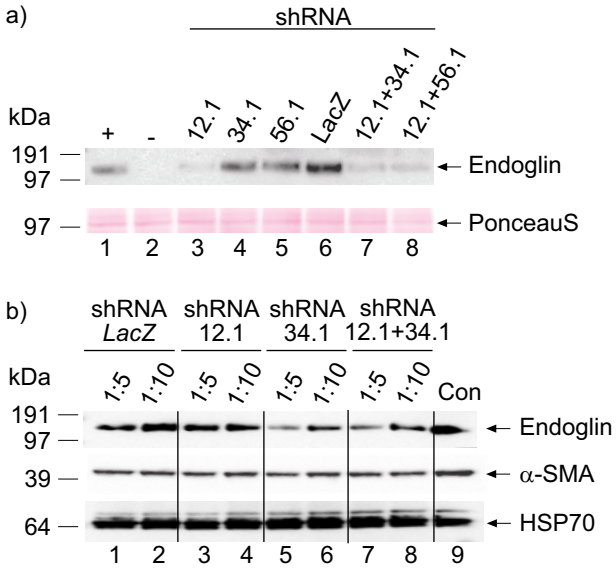


Figure 3.2: shRNA testing in COS-7 and HSC. (a) Western blot analysis of COS-7 transfected with three different shRNAs in pENTR^{TM}/U6 was performed. 20 μl protein lysate were loaded onto a 4-12% Bis-Tris gel. COS-7 were single transfected with an expression vector encoding mouse endoglin were used as positive control (lane 1). Untransfected COS-7 were used as negative control (lane 2). COS-7 were double transfected with an expression vector encoding mouse endoglin and with the shuttle vector containing either shRNA 12.1, shRNA 34.1, shRNA 56.1 or shRNA *LacZ* (lane 3-6). COS-7 were triple transfected with an expression vector encoding mouse endoglin in combination with the shuttle vectors shRNA 12.1 and shRNA 34.1 or shRNA 12.1 and 56.1 (lane 7-8). shRNA 12.1 down regulates endoglin most efficiently compared to the other shRNA constructs. PonceauS staining was used as a loading control. (b) Western blot analysis of mouse HSC infected with different shRNA constructs on day 2 and harvested on day 7 was performed. 20 μl protein lysate were loaded onto a 4-12% Bis-Tris gel. After dilution of the crude viral lysates (1:10 or 1:5) mouse HSC were either single infected with shRNA *LacZ* virus, with shRNA 12.1 virus, with shRNA 34.1 virus (lane 1-6) or double infected with shRNA 12.1 virus and shRNA 34.1 virus (lane 7-8). As an internal control uninfected mouse HSC were used (lane 9). To investigate the transdifferentiation process α-SMA expression was analyzed. Protein standard size markers are indicated in the left margin. HSP70 was used as a loading control.
shRNA 34.1 virus silenced endoglin most efficiently. There were no differences towards the double infection. shRNA 12.1 virus did not down regulate endoglin in mouse HSC. Downregulation of endoglin in HSC was more efficient when HSC were infected with higher concentrations of virus.

Fect as transfection reagent (Fig. 3.3 a). HSC were transfected with different concentrations (5 nM, 10 nM, 15 nM) of fluorescence-labelled siRNA oligonucleotides. HiPerFect was used as transfection reagent. The next day, medium was renewed and images of HSC were taken under UV-light. Untransfected HSC (Con) were used as negative control. HSC successfully transfected with fluorescence-labelled siRNA showed little spots of green fluorescence. Number and intensity of green spots increased with an increase in siRNA concentration. This experiment revealed that transfection of primary HSC with siRNA is realizable using HiPerFect as transfection reagent.

Next, three aspects regarding the silencing efficiency were tested, i.e. concentration (Fig. 3.3 b), double *vs.* single transfection (Fig. 3.3 c) and detection of first silencing effects (Fig. 3.3 d). Two different siRNAs targeting endoglin were obtained by Qiagen and used for double transfection experiments. Unless otherwise mentioned, a mixture of 2 siRNA oligonucleotides targeting endoglin was used. On day 1 HSC were transfected with different concentrations of siRNA. The final concentration of siRNA oligonucleotides in the culture medium was either 0.16 nM, 0.31 nM, 0.63 nM, 1.25 nM, 2.5 nM or 5 nM. The ratio of siRNA to HiPerFect was constant. HSC transfected with scrambled siRNA (siCon) and untransfected HSC (Con) were used as negative controls. Knock down efficiency increased constantly when the concentration of siRNA was raised. In order to test the ability of each siRNA to down regulate endoglin, HSC were single transfected on day 1 (Fig. 3.3 c). Untransfected HSC (Con) were used as a control. siRNA 2 targeting endoglin was able to down regulate endoglin more efficiently than siRNA 1 targeting endoglin. Double transfection of both siRNA oligonucleotides did not enhance the efficiency of siRNA 2. Finally, down-regulation of endoglin during the first two days after transfection was analyzed (Fig. 3.3 d). HSC were transfected on day 1 with two different concentrations of siRNA oligonucleotides targeting endoglin. Subsequent to transfection of siRNA endoglin expression was unaffected, but 24 h after transfection endoglin expression was already significantly reduced. At that time suppression of endoglin was more efficient when siRNA was applied in higher concentrations. In HSC harvested 48 h after transfection endoglin was almost abolished. At that time endoglin suppression was reduced independent of the initial siRNA concentration.

Parameters for optimizing HSC transfection with siRNA oligonucleotides were determined by the experiments described above. Based on these results, the remaining experiments were performed with a final concentration of 5 nM siRNA using siRNA oligonucleotide 2 targeting endoglin (Rn_Eng_2_HP Qiagen). For simplification siRNA

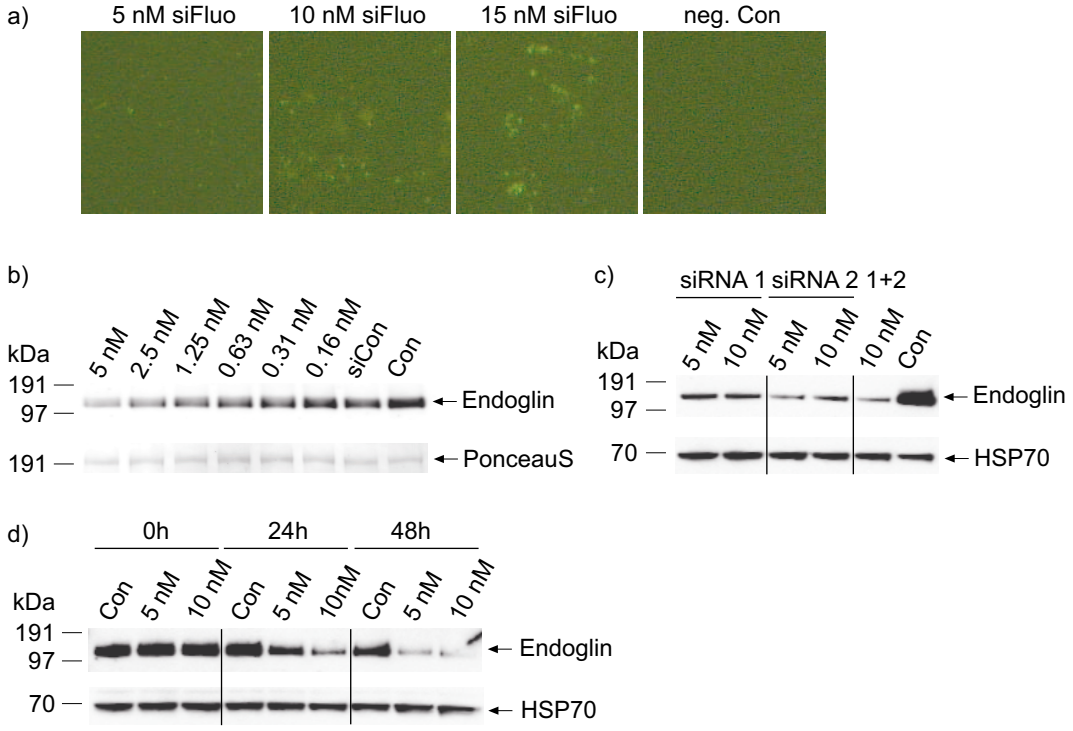


Figure 3.3: Determination of the transfection efficiency of fluorescence-labelled siRNA oligonucleotides as well as analysis of the knock down efficiency of siRNA oligonucleotides targeting endoglin. (a) Transfection efficiency was tested using increasing concentrations (5 nM, 10 nM and 15 nM) of fluorescence-labelled siRNA. Therefore, HSC were transfected with siRNA oligonucleotides on day 3. On day 4 pictures were taken under UV-light. Untransfected HSC (Con) were used as control. (b, c, d) Western blot analysis was performed to analyze down-regulation of endoglin. (b, d) On day 1 HSC were transfected with a mixture (1:1) of two different siRNA oligonucleotides targeting endoglin. (b) The ability of siRNA oligonucleotides to down regulate endoglin was tested using different concentrations (0.16 nM, 0.31 nM, 0.63 nM, 1.25 nM, 2.5 nM, 5 nM) of siRNA. Untransfected HSC (Con) and HSC transfected with scrambled siRNA (siCon) were used as negative controls. PonceauS stain was used as a loading control. (c) siRNA oligonucleotides 1 and 2 were transfected separately on day 1. As negative control a protein sample of untreated HSC was analyzed. (d) The ability of each siRNA to silence endoglin was analyzed at different time points after transfection. HSP70 was used as loading control (c, d). Protein standard size markers are indicated in the left margin (b, c, d).
Green spots of fluorescence-labelled siRNA became visible at a concentration of 10 nM. Significant changes in endoglin expression were first observed at a final concentration of 0.63 nM siRNA. Down-regulation of endoglin was maximal at a final concentration of 5 nM. siRNA 2 revealed a stronger down-regulation of endoglin compared to siRNA 1. Immediately after transfection of HSC on day 1, the expression of endoglin was unaffected. However, suppression of endoglin reached a value of 50-70% after 24 h and a value of 95-98% after 48 h.

oligonucleotide 2 targeting endoglin will be termed "siEng" and scrambled siRNA will be termed "siCon" in the following paragraphs.

3.1.3 Knock down of endoglin in HSC

Silencing of endoglin using siRNA was further examined with respect to following questions. How long remains endoglin down regulated? Is the inhibition of endoglin expression due to a degradation of messenger RNA or due to disturbance of the translational process?

To determine how long endoglin remains silenced, HSC were transfected on day 1 and harvested on the days 2, 6, 11 and 17. Cell lysates were analyzed by Western blotting using a specific antibody against endoglin (Fig. 3.4 a). Endoglin was found to be silenced at least until day 17. No recovery of endoglin expression was detected in any experiment. Therefore, this method is appropriate to mediate a very strong and long lasting knock down of endoglin. To determine, if inhibition of endoglin expression is due to degradation of mRNA, HSC were transfected on day 1 and harvested on day 4. mRNA was isolated and cDNA was synthesized. Comparative RT-PCR was performed for endoglin and for specific transcripts of the ribosomal S6 protein (Fig. 3.4 b). Additional to comparative RT-PCR, Northern blot analysis was performed. For Northern blot analysis 5 μg of total RNA, which was obtained from HSC harvested on day 8, were loaded onto each lane and analyzed with probes specific for endoglin and *GAPDH* (Fig. 3.4 c). *GAPDH* was used as a loading control. In accordance with Western blot analysis comparative RT-PCR as well as Northern blot analysis showed a very efficient reduction of endoglin mRNA in HSC transfected with siEng. Therefore, endoglin down-regulation is due to degradation of mRNA.

To exclude apoptosis as the reason for the sustained knock down a TUNEL test was performed (Fig. 3.4 d). Subsequent to isolation, HSC were seeded on glass slides and transfected with siRNA on day 1. On day 8 HSC were fixed with 4% PFA and incubated with the TUNEL reaction mixture. As a positive control, cells were treated with recombinant DNase I. Images were taken at 200 x magnification. No differences in degradation of DNA among untransfected HSC (Con), HSC transfected with siEng or HSC transfected with siCon were determined using the TUNEL assay. Degradation of DNA is one parameter of apoptosis. These results confirmed that cells transfected with siEng are viable (not apoptotic).

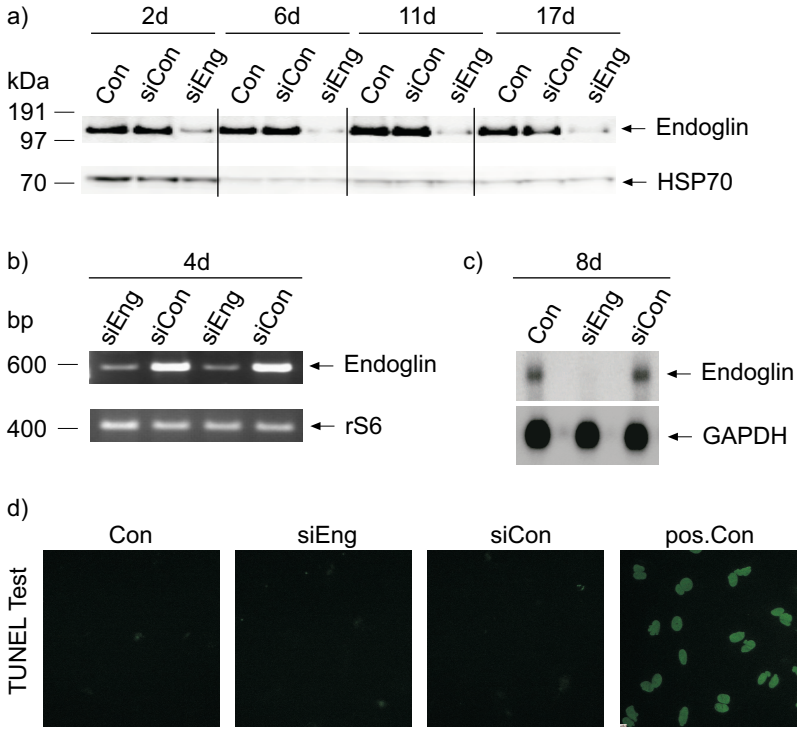


Figure 3.4: siRNA mediated silencing of endoglin in HSC. HSC were transfected with siRNA on day 1. Silencing of endoglin on the level of protein was analyzed by (a) Western blotting at the indicated time points. 20 μg protein were loaded onto a 4-12% Bis-Tris gel. Silencing of endoglin on the level of mRNA was examined either by (b) comparative RT-PCR or by (c) Northern blot analysis. mRNA for comparative RT-PCR was isolated from HSC harvested on day 8 and reverse transcribed to cDNA. mRNA for Northern blot analysis was isolated from HSC harvested on day 8. For Northern blot analysis 5 μg of total RNA were loaded onto a formaldehyde agarose gel. (a) HSP70, (b) rS6 and (c) GAPDH were used as loading controls. (d) HSC were seeded on glass slides and transfected with siRNA on day 1. On day 8 HSC were fixed with 4% PFA and incubated with the TUNEL reaction mixture. As a positive control, HSC were treated with recombinant DNase I. Images were taken at 200 x magnification. (a, b, c, d) Untransfected HSC (Con) and HSC transfected with scrambled siRNA (siCon) were used as negative controls. Protein (a) and nucleic acid (b, c) standard size markers are indicated in the left margin.
Treatment of HSC resulted in a very strong and sustained knock down of endoglin on the level of mRNA as well as on the level of protein. Furthermore, siRNA treatment did not induce apoptosis.

3.2 Characterization of endoglin deficient HSC

The use of siRNA oligonucleotides resulted in a very efficient and sustained knock down of endoglin in HSC. This knock down provides a stable basis to analyze the effects of a reduced endoglin expression on activation and transdifferentiation of HSC.

3.2.1 Morphology and ECM abundance

HSC start to transdifferentiate into myofibroblast-like cells as soon as they are seeded on tissue culture dishes. This transdifferentiation is associated with changes in cellular morphology, with the loss of lipid droplets and with the development of cell-cell contacts. Therefore, morphological features of HSC transfected with siEng were analyzed.

Transfection of HSC on day 1 of culture

HSC were transfected with siRNA on day 1. Morphology of HSC during transdifferentiation was analyzed using bright field microscopy (a). Images were taken on the days 4, 5 and 6 (Fig. 3.5 a) as well as on the days 7, 8 and 9 (Fig. 3.6 a). Untransfected HSC (Con) and HSC transfected with scrambled siRNA (siCon) were used as negative controls. Bright field microscopy revealed alterations in morphology during transdifferentiation. Although HSC were transfected on day 1, which leads to a maximal down-regulation of endoglin on day 3, these alterations became first visible on day 5. Morphological transdifferentiation is accompanied by a loss of lipid droplets and the development of cell-cell contacts. Transfection of HSC with siEng led to an inhibition of this morphological transdifferentiation (Fig. 3.5 a and Fig. 3.6 a). HSC transfected with siEng did not lose their circular arranged lipid droplets and form less or no cellular contacts to their neighbor cells.

Beside changes in cellular morphology (morphological transdifferentiation), transdifferentiation is also accompanied by specific up-regulation of ECM genes and by up-regulation of α-SMA. Therefore, the quantity of ECM components and of α-SMA as a marker of transdifferentiation, was analyzed. Western blot analysis of HSC transfected with siRNA on day 1 was performed (Fig. 3.5 b and Fig. 3.6 b). Antibodies specific for ECM components and for α-SMA were used. Western blot analysis of HSC transfected with siEng showed a reduced amount of collagen type I, collagen type IV, and fibronectin when compared to control cells. The reduced amount of collagen type I became visible on day 5 and remained decreased at least until day 9. Even though collagen type I is not completely abolished, the total amount of collagen type I is sig-

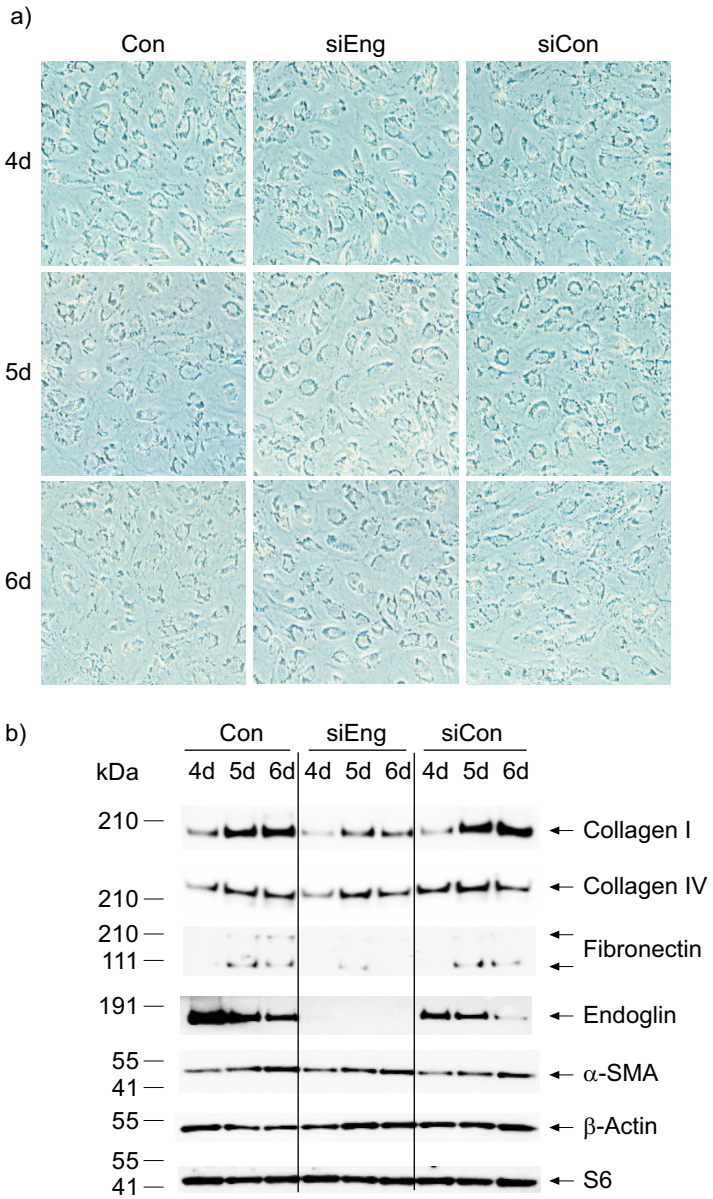


Figure 3.5: Morphology and ECM expression of HSC on the days 4, 5 and 6 of culture. HSC were transfected with siRNA on day 1. At indicated time points the morphology was analyzed by (a) bright field microscopy (200 x magnification) and protein lysates were analyzed by (b) Western blotting. For Western blot analysis 20 μg or 5 μg protein were loaded onto a 4-12% Bis-Tris gel in order to analyze the expression of endoglin and α-SMA, respectively. Additionally, 10 μg protein were loaded onto a 3-8% Tris-Acetate gel in order to analyze the expression of ECM components. Untransfected HSC (Con) and HSC transfected with scrambled siRNA (siCon) were used as negative controls. S6 and β-Actin were used as loading controls. Protein standard size markers are indicated in the left margin.
Western blot analysis revealed a reduced amount of ECM components. In contrast, the expression of the transdifferentiation marker α-SMA is unaffected.

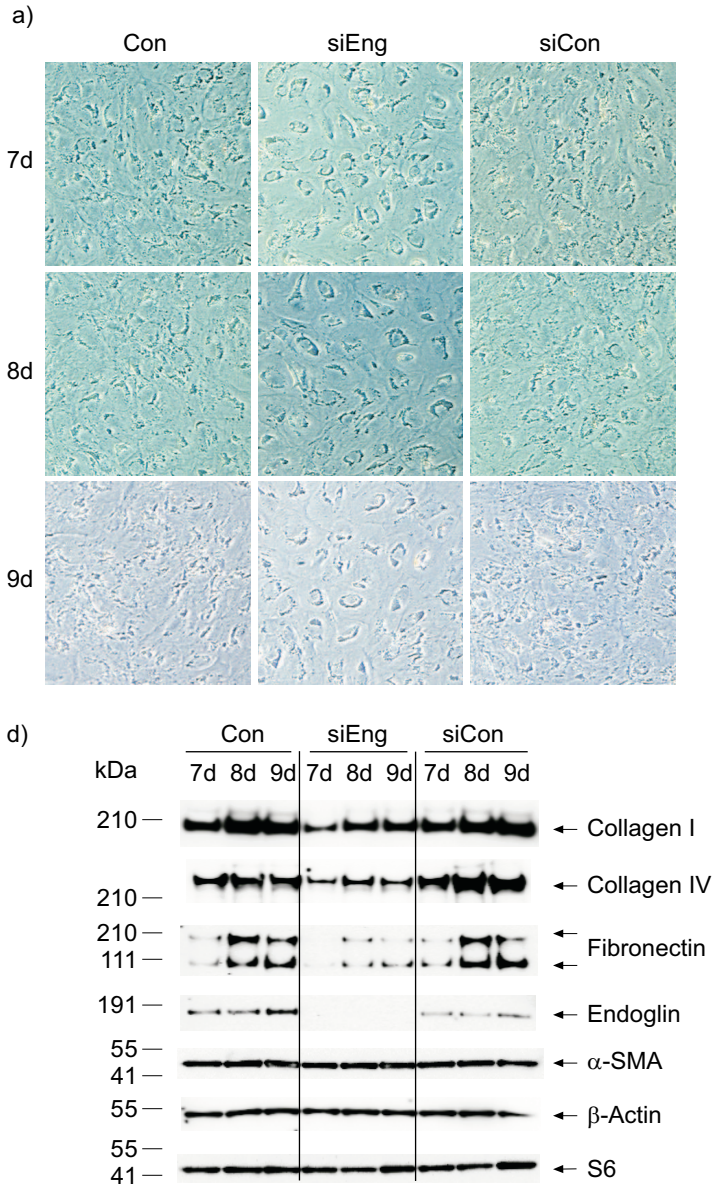


Figure 3.6: Morphology and ECM expression of HSC on the days 7, 8 and 9 of culture. HSC were transfected with siRNA on day 1. At indicated time points the morphology was analyzed by (a) bright field microscopy (200 x magnification) and protein lysates were analyzed by (b) Western blotting. For Western blot analysis 20 μg or 5 μg protein were loaded onto a 4-12% Bis-Tris gel in order to analyze the expression of endoglin and α-SMA, respectively. Additionally, 10 μg protein were loaded onto a 3-8% Tris-Acetate gel in order to analyze the expression of ECM components. Untransfected HSC (Con) and HSC transfected with scrambled siRNA (siCon) were used as negative controls. S6 and β-Actin were used as loading controls. Protein standard size markers are indicated in the left margin.
Microscopy revealed an inhibition of morphological transdifferentiation of HSC transfected with siEng. Western blot analysis revealed a reduced amount of ECM components such as collagen type I, type IV and fibronectin. Furthermore, silencing of endoglin was confirmed by Western blot analysis.

nificantly reduced compared to untransfected HSC (Con) and HSC transfected with siCon. Reduction in collagen type IV and fibronectin expression became visible on day 7. α-SMA, as a marker of HSC activation and trandifferentiation remained unaffected in HSC transfected with siEng compared to untransfected HSC (Con) and HSC transfected with siCon.

Therefore, the overall tendency to transdifferentiate was reduced as indicated by two observations: 1. The inhibition of morphological transdifferentiation and 2. the reduced amount of ECM components.

Transfection of HSC on day 3, 4 and 5 of culture

Transfection of HSC with siEng on day 1 of culturing led to an inhibiton of transdifferentiation. This raises the question, if silencing of endoglin at later time points produce comparable effects? This is questionable, because at later time points the morphological transdifferentiation and collagen type I expression are already ongoing. Therefore, endoglin was silenced and analyzed at later time points of the transdifferentiation process.

In order to analyze these parameters, HSC were transfected with siRNA on day 3 (Fig. 3.7 a, d), day 4 (Fig. 3.7 b, e) and day 5 (Fig. 3.7 c, f). Bright field microscopy (Fig. 3.7 a, b, c) and Western blot analysis (Fig. 3.7 d, e, f) were performed on day 7, day 8 and day 9. Bright field microscopy revealed an inhibition in morphological transdifferentiation of HSC, which were transfected with siEng either on day 3 or on day 4. However, these differences were less in HSC transfected on day 4 compared to HSC transfected on day 3. Images of HSC transfected with siEng on day 5 were almost identical to the images of the corresponding controls. Western blot analysis revealed a very efficient down-regulation of endoglin in HSC transfected either on day 3 (Fig. 3.7 d), day 4 (Fig. 3.7 e) or day 5 (Fig. 3.7 f). As one representative of ECM components the quantity of collagen type I in HSC on day 7, day 8 and day 9 was analyzed by Western blotting. Transfection of HSC on day 3, on day 4 and on day 5 caused a reduction of collagen type I at each time point analyzed. However, changes in collagen type I abundance were less in HSC transfected on day 5, thus reconfirming the results observed in bright field microscopy.

3.2.2 Cytoskeleton organization

As the lack of endoglin caused alterations of the cellular morphology during transdifferentiation, the organization of the cytoskeleton of HSC was analyzed next.

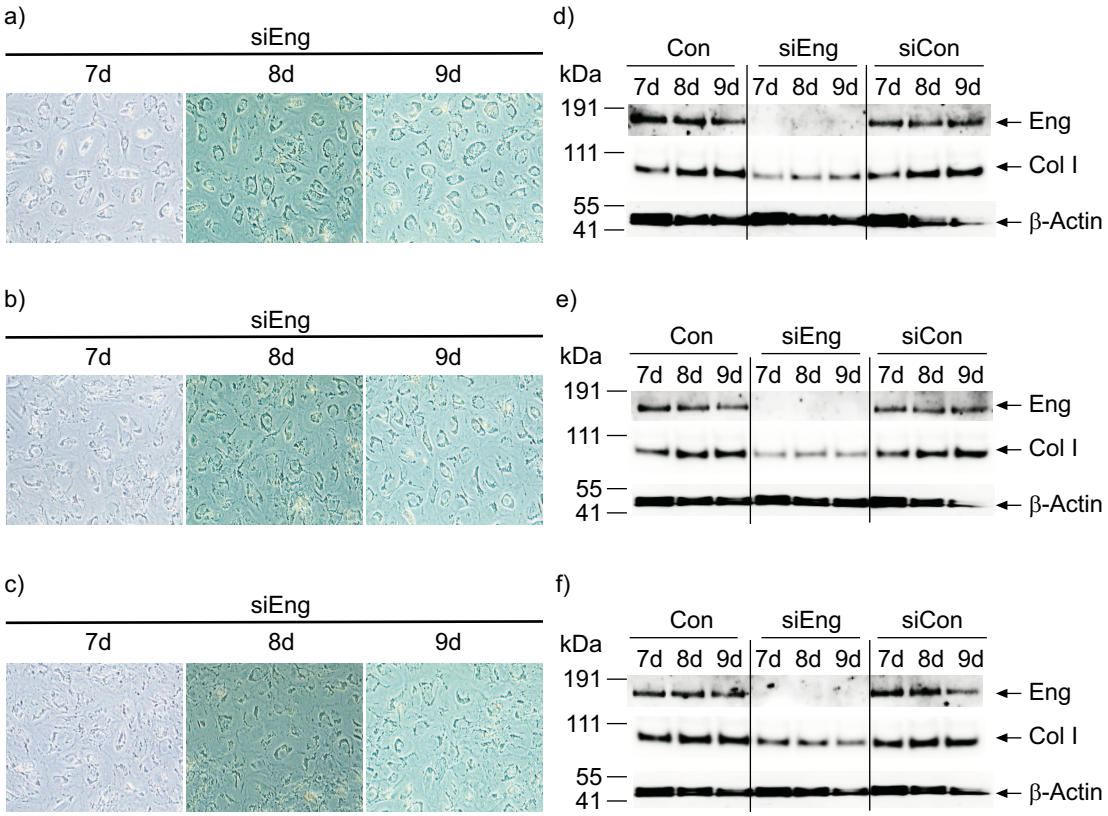


Figure 3.7: Endoglin silencing on day 3, day 4 and day 5 of culture. Bright field microscopy (a, b, c) and Western blot analysis (d, e, f) of HSC transfected with siRNA on day 3, on day 4 and on day 5. HSC were isolated, seeded on 6-well plates and transfected with siRNA either on day 3 (a, c), on day 4 (b, e) or on day 5 (c, f). Images were taken (200 x magnification) and protein lysates of HSC harvested on day 7, on day 8 and on day 9 were analyzed. 10 μg protein were loaded onto a 3-8% Tris-Acetate gel and analyzed using a specific antibody directed against collagen type I. To demonstrate endoglin down-regulation 20 μg of protein were loaded onto a 4-12% Bis-Tris gel and analyzed using a specific antibody directed against endoglin. β-Actin was used as a loading control. Protein standard size markers are indicated in the left margin. Untransfected HSC (Con) and HSC transfected with scrambled siRNA (siCon) were used as negative controls. Abbreviations: Col I, collagen type I; Eng, endoglin
Morphological transdifferentiation was significantly inhibited when HSC were transfected with siEng either on day 3 or on day 4. In contrast, transfection of HSC with siEng on day 5 resulted in less significant changes in morphological transdifferentiation. Furthermore, the amount of collagen type I is slightly reduced in HSC transfected with siEng at each time point analyzed.

HSC were isolated, seeded either on tissue culture dishes (Fig. 3.8 a, b, f, g and Fig. 3.9) or on glass slides (Fig. 3.8 c, d and e) and transfected with siRNA on day 1. To investigate the organization of the cytoskeleton F-actin was stained with phalloidin that directly binds to actin fibres. In addition the LIM domain protein CRP2 was overexpressed. It has been shown that CRP2 binds to the actin fibres and may be an indirect interaction partner for endoglin. Therefore, HSC were partially infected on day 6 with either an adenovirus overexpressing CRP2 or with an adenovirus overexpressing the CRP2-GFP fusion protein. On day 8 cells were fixed with 4% of PFA. Bright field microscopy was performed (Fig. 3.8 a) and images of the autofluorescence of HSC were taken under UV-light (Fig. 3.8 b). F-actin of uninfected HSC (Fig. 3.8 c) and of HSC infected with an adenovirus overexpressing the untagged version of CRP2 (Fig. 3.8 e) were stained with phalloidin. Images of HSC infected with the adenovirus CRP2-GFP were taken under UV-light (Fig. 3.8 d). Nuclei were counterstained with DAPI.

Images obtained by bright field microscopy and by autofluorescence reconfirmed the inhibition of morphological transdifferentiation. HSC transfected with siEng did not lose their circular arranged lipid droplets (Fig. 3.8 a and b). Furthermore, HSC transfected with siEng showed differences in the phalloidin staining pattern compared to untransfected HSC (Con) and HSC transfected with scrambled siRNA (siCon) (Fig. 3.8 c). HSC transfected with siEng revealed a lack of parallel actin-fibers and a more pronounced radial staining at the edge of the cells. Control cells showed a staining pattern with parallel bundles of F-actin all over the cell. In order to analyze the alterations observed in phalloidin stained HSC in more detail HSC were infected with an adenovirus overexpressing a GFP-tagged version of CRP2. HSC transfected with siEng revealed a different CRP2-GFP staining pattern compared to HSC transfected with siCon and untransfected HSC (Con). In HSC transfected with siEng a discontinuous staining pattern with marked spots at the ends of short fiber structures and a faint stain at the edge of the cell (Fig. 3.8 d) were observed. To rule out the possibility that these effects were due to the GFP-tag, HSC were first infected with a virus overexpressing an untagged version of CRP2 and afterwards HSC were stained using phalloidin. Phalloidin staining revealed differences in the organization of the cellular actin skeleton between HSC transfected with siEng and the corresponding controls (Fig. 3.8 e). HSC transfected with siEng showed a discontinuous staining pattern with accumulation of F-actin at different positions within the cell.

The staining pattern of untransfected HSC (Con) and HSC transfected with scrambled siRNA (siCon) were comparable within all staining procedures (phalloidin, CRP2-

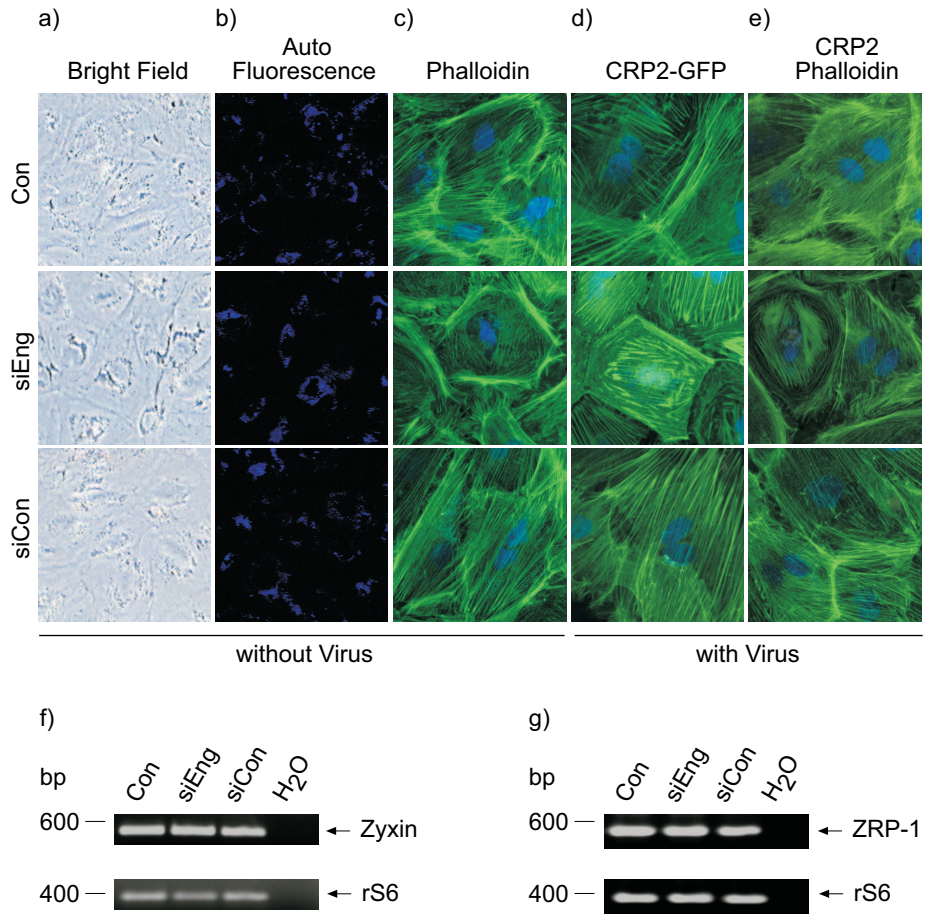


Figure 3.8: Organization of the cytoskeleton and mRNA expression of proteins associated with endoglin. HSC were transfected with siRNA on day 1 (a-e) and partially infected on day 6 with an adenovirus overexpressing either CRP2-GFP (d) or CRP2 (e). On day 8 cells were fixed in 4% PFA, stained and images were taken (400 x magnification). Cells overexpressing CRP2 were stained with phalloidin. Nuclei were counterstained with DAPI. Untransfected HSC (Con) and HSC transfected with scrambled siRNA (siCon) were used as negative controls. The morphology and autofluorescence of HSC were analyzed (a, b). The formation of the cytoskeleton was analyzed (c, d, e) using phalloidin and CRP2-GFP. Comparative RT-PCR was performed in order to demonstrate the expression of Zyxin (523 bp) and ZRP-1 (520 bp) in HSC (F). For comparative RT-PCR mRNA was isolated from HSC harvested on day 8 and reverse transcribed to cDNA. S6 was used as a loading control. Molecular weight markers are indicated in the left margin.
The appearance of circular arranged lipid droplets supports the finding that transdifferentiation is inhibited. Additionally, endoglin silencing resulted in a re-arrangement of the cytoskeleton and to a relocalization of CRP2.

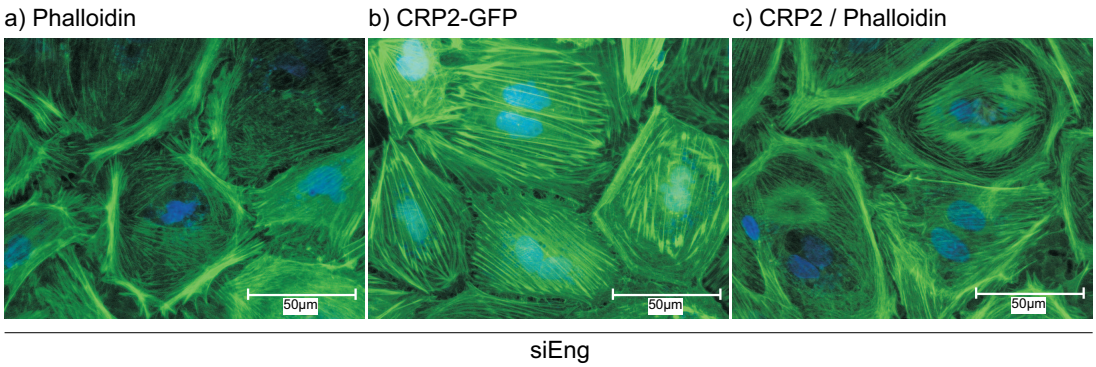


Figure 3.9: Silencing of endoglin results in a re-arrangement of the cytoskeleton. For better visualization enlarged images (400 x magnification) of HSC lacking endoglin are presented once again (additional to Fig. 3.8 c, d, e). (a) Image of phalloidin stained HSC. (b) Image of the CRP2-GFP fluorescence pattern of HSC. (c) Image of phalloidin stained HSC, which were overexpressing CRP2.

GFP, CRP2 phalloidin). All control cells showed a staining pattern with parallel bundles of F-actin all over the cell. In contrast, silencing of endoglin led to different staining pattern with respect to all three staining procedures (phalloidin, CRP2-GFP, CRP2 phalloidin). For a better visualization, images are enlarged presented in Fig. 3.9. These images exclusively show the staining pattern of HSC transfected with siEng. Therefore, the actin cytoskeleton and the CRP2 localization are changed in the absence of endoglin.

Zyxin has been shown to regulate migration of endothelial cells by influencing the organization of the cytoskeleton. Furthermore, it was shown that this effect was mediated by an interaction of Zyxin with endoglin [51]. ZRP-1 (zyxin related protein-1) shows high similarities to Zyxin [124] and it has been shown that endoglin regulates the organization of the cytoskeleton by binding to ZRP-1 [52]. Since at least Zyxin directly binds CRP2, the localization of CRP2 and the organization of the cytoskeleton might be governed by an indirect interaction of CRP2 and endoglin, which in turn might be mediated by Zyxin and/or ZRP-1. Therefore, Zyxin as well as ZRP-1 might be the missing links between the observed alterations of the cytoskeleton and endoglin down-regulation. In order to substantiate the hypothesis that Zyxin and ZRP-1 are an important component for the organization of the cytoskeleton, mRNA expression of Zyxin and ZRP-1 in HSC was confirmed by RT-PCR. Furthermore, RT-PCR revealed an endoglin independent expression of Zyxin and ZRP-1 in cultured HSC (Fig. 3.8 f and g).

3.2.3 Migration

It is assumed that HSC *in vivo* have the potential to migrate towards the inflammatory regions in order to participate in the wound healing process. Comparable to HSC *in vivo*, HSC *in vitro* have the potential to migrate on tissue culture plates towards a spot with a low number of HSC. To analyze the impact of endoglin silencing on HSC migration, a wound healing assay was performed. HSC were isolated and plated onto tissue culture plates. On day 1 HSC were transfected with siRNA. On day 2 a 100 μl tip was used to make a scratch as shown in Fig. 3.10. Subsequent floating cells were removed by washing twice with DMEM containing 10% FCS. In order to follow the movement of the cells, images were taken using bright field microscopy. In figure 3.10 representative images of day 2, day 8 and day 14 are presented. Untransfected HSC (Con) and HSC transfected with scrambled siRNA (siCon) were used as negative controls. This assay revealed no significant differences in migration of HSC transfected with siEng compared to the corresponding controls.

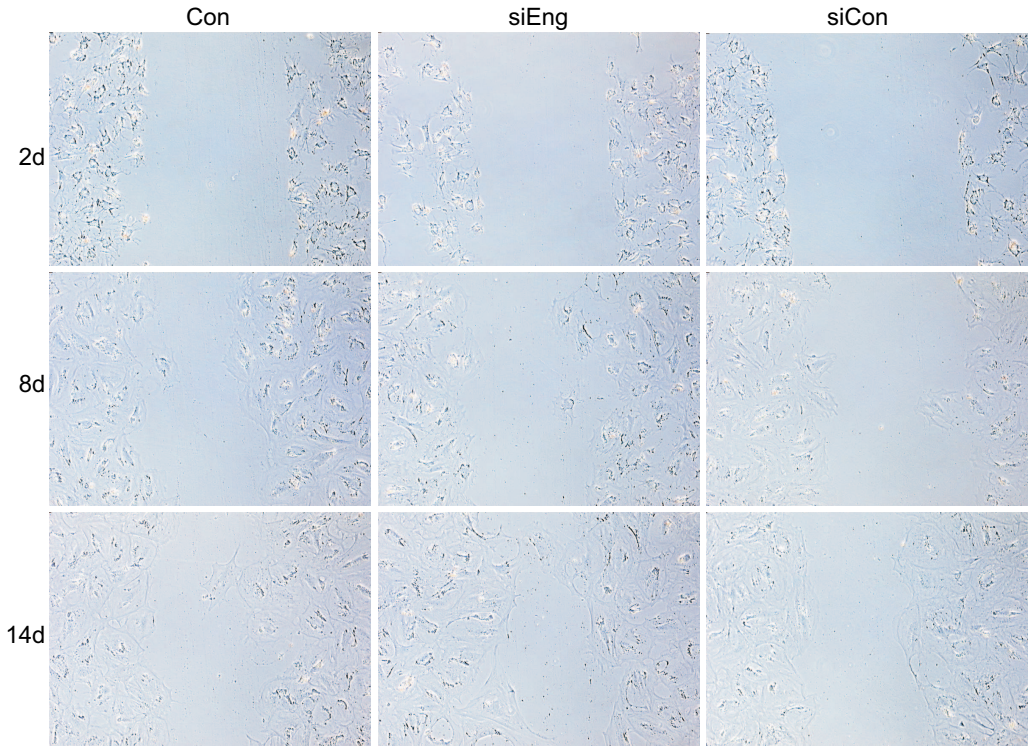


Figure 3.10: Migration of HSC. On day 1 HSC were transfected with siRNA. One day later a 100 μl tip was used to make a scratch. Bright field microscopy was used to analyze the migration of HSC. Representative bright field images of day 1, day 7 and day 13 are shown.
Migration of HSC was evident, but no differences in the migration pattern of HSC transfected with siEng, siCon or untransfected HSC were observed.

3.2.4 Proliferation

Another feature of HSC during transdifferentiation is an increase in cell proliferation. One method to determine cell proliferation is the measurement of ^{3}H-thymidine incorporation. This method has been the traditional method for detection of cell proliferation for a long time and is known as very sensitive. However, the handling and disposal of radioisotopes as well as the incorporation of ^{3}H-thymidine as a result of DNA repair are the main disadvantages. This is worth of mention, because HSC exhibit an increased cell repair. An alternative to ^{3}H-thymidine proliferation assay is the BrdU proliferation assay. In these methods bromodeoxyuridine (BrdU) is incorporated into newly synthesized DNA strands of proliferating cells. This assay is free of radioisotopes and excludes incorporation through cell repair processes, but compared to ^{3}H-thymidine the BrdU assay is not as sensitive. However, to analyze the impact of endoglin silencing on cell proliferation both proliferation assays - ^{3}H-thymidine and BrdU - were performed. HSC were isolated and transfected with siRNA on day 1. Depending on the assay HSC were either exposed to ^{3}H-thymidine on day 3 for a time period of 24 h or exposed to BrdU on day 4 for a time period of 48 h. Untransfected HSC (Con) and HSC transfected with scrambled siRNA (siCon) were used as negative controls. The BrdU assay (Fig:. 3.11 a) revealed an inhibition of cell proliferation for HSC transfected with siEng. The inhibition of proliferation is approx. 30% compared to untransfected HSC (Con) and HSC transfected with siCon. Proliferation of untransfected HSC (Con) and HSC transfected with scrambled siRNA (siCon) was equal. Comparable to BrdU the ^{3}H-thymidine assay (Fig:. 3.11 b) revealed an inhibition of proliferation for HSC transfected with siEng. The inhibition of proliferation for HSC transfected with siEng is approx. 50% compared to untransfected HSC (Con) and approx. 30% compared to HSC transfected with siCon.

Statistical analysis was performed with an unpaired Student's t-test for both incorporation assays. The BrdU assay revealed $p = 0.00043$ for HSC transfected with siEng compared to untransfected HSC (Con) and $p = 0.003$ for HSC transfected with siEng compared to HSC transfected with siCon. The ^{3}H-thymidine assay revealed $p = 0.00002$ for HSC transfected with siEng compared to untransfected HSC (Con) and $p = 0.0002$ for HSC transfected with siEng compared to HSC transfected with siCon. Therefore, both assays revealed highly significant differences (≤ 0.01) in cell proliferation between HSC transfected with siEng and the respective controls.

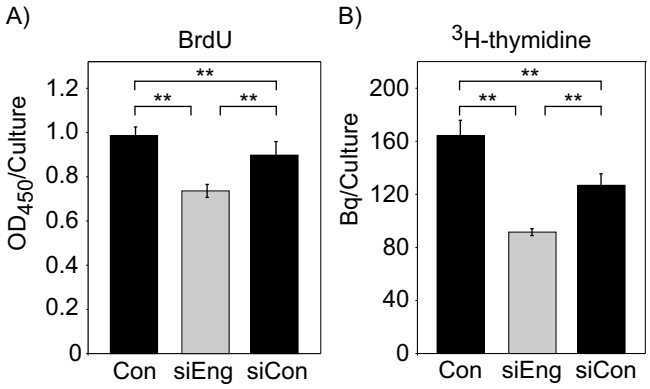


Figure 3.11: BrdU and ^{3}H-thymidine proliferation assays. HSC were transfected with siRNA on day 1. (a) On day 4 HSC were treated with BrdU and incorporation of BrdU was determined 48 h later by measuring the OD_{450} per well. (b) On day 3 HSC were treated with ^{3}H-thymidine and incorporated radioactivity was measured 24 h later. Statistical analysis was performed for both incorporation assays with an unpaired Student's t-test. Significant differences (≤ 0.01) are indicated by asterisks.
In both proliferation assays HSC transfected with siEng proliferate less than the respective controls.

3.2.5 Whole genome microarray

To further analyze the molecular background of the disturbed transdifferentiation in HSC lacking endoglin an Agilent whole-genome microarray was performed. This array comprises the expression of more than 41000 rat genes. Sample preparation, RNA isolation and final data analysis were accomplished as part of this thesis. Quality check, RNA amplification, hybridization and raw data analysis were processed by Miltenyi Biotec GmbH.

RNA isolation and quality check

A total number of 8 animals were sacrificed and subsequent 8 independent HSC isolations, transfections and sample preparations were performed. As described in materials and methods, HSC were transfected with siRNA on day 1. Total RNA was isolated on day 8, cDNA was synthesized using 1 μg of total RNA and silencing of endoglin was analyzed by comparative RT-PCR (Fig. 3.12 a). RT-PCR revealed a significant reduction of endoglin mRNA in all RNA samples obtained from HSC transfected with siEng. A specific transcript for the ribosomal S6 protein was used as loading control. Out of the initial 8 groups 4 groups were used for microarray analysis and were analyzed at Miltenyi. Putative RNA degradation was analyzed by Miltenyi using a Bioanalyzer. The results were visualized in a gel image (Fig. 3.12 b) and in an electropherogram (Fig.

3.12 c). The RIN (RNA Integrity Number) was calculated and revealed a RIN of 10 for all samples. A RIN number of 10 indicates perfect, not degraded RNA. Therefore, all samples were suitable for microarray analysis. One group (out of four groups) was independently processed (single). The corresponding samples (Con, siEng, siCon) of the remaining three groups were pooled and further processed as one group (pool). Each group consisted of untransfected HSC (Con), HSC transfected with siEng (siEng) and HSC transfected with siCon (siCon).

Four sets of hybridization were performed. Hybridization no. 1 (single) and no. 3 (pool) were performed to identify genes, which were differentially expressed caused by the transfection procedure. Within hybridization no. 1 and within hybridization no. 3 the expression profiles of untransfected HSC (Con) and HSC transfected with siCon were compared. Hybridization no. 2 (single) and no. 4 (pool) were performed to identify genes, which are differentially expressed caused by endoglin down-regulation. Within hybridization no. 2 and within hybridization no. 4 the expression profiles of HSC transfected with siEng and HSC transfected with siCon were compared. Details of the hybridization scheme are described in detail in chapter 2.21.2.

Results of the whole genome microarray

The data output received from Miltenyi included the complete raw data sets as well as one list for each hybridization containing the differentially expressed genes. Genes are defined as differentially expressed when they show a fold change ≥ 2 and p-value ≤ 0.01. The complete raw data sets were deposited in the Gene Expression Omnibus (GEO) repository. The accession numbers are GSM256740 for hybridization no. 1, GSM-256756 for hybridization no. 2, GSM256757 for hybridization no. 3 and GSM256758 for hybridization no. 4. In contrast to the raw data, the lists of differentially expressed genes were processed as follows. Genes, which were differentially expressed caused by the transfection procedure (Gene lists 1 and 3), were removed from gene lists 2 and 4. To further select genes differentially expressed caused by endoglin down-regulation, the intersection of gene lists 2 and 4 was formed. In this way genes, which were not listed in both hybridizations, were skipped. The remaining genes form a group of selected candidate genes and are listed in Appendix A. 44 genes listed in Appendix A are up regulated and 64 genes are down regulated. Genes listed in Appendix A were further analyzed regarding their function. Genes, which might be linked to the observed cellular alterations, were manually chosen and are presented in figure 3.13. Some of these genes have been linked to TGFβ-1 and/or BMP-7 signaling (e.g. Ltbp2, Noggin,

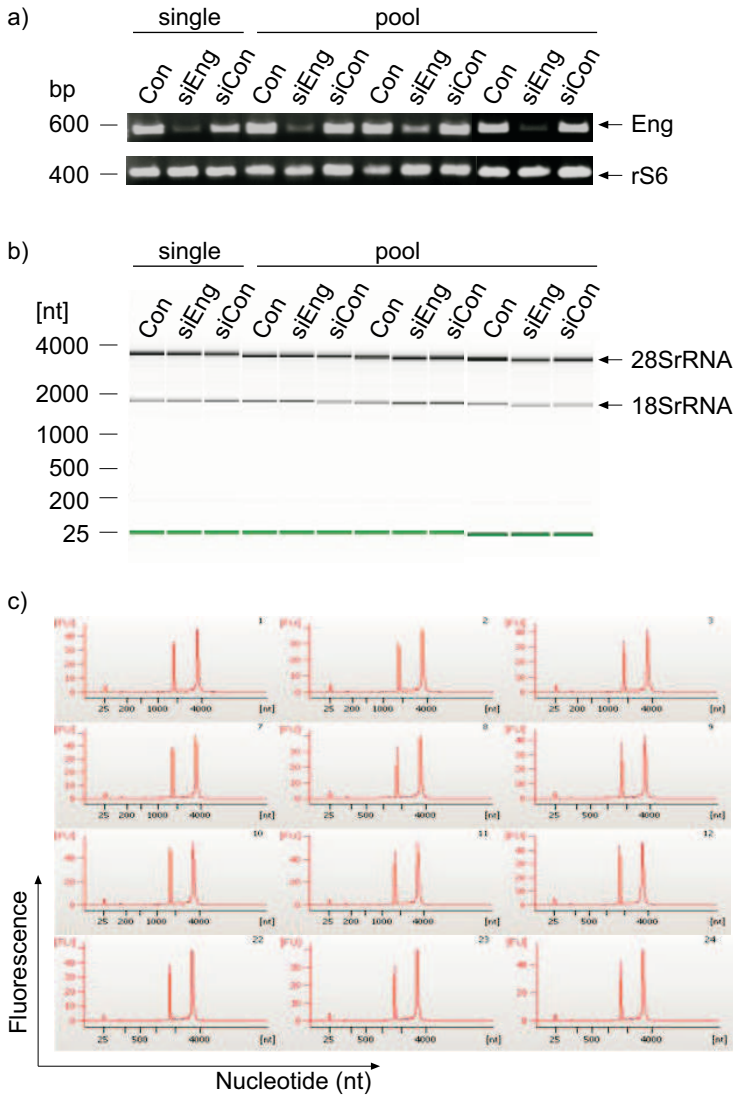


Figure 3.12: RNA quality check. HSC were transfected with siRNA on day 1 and total RNA was isolated on day 8. 1 μg of total RNA was reverse transcribed into cDNA in order to perform comparative RT-PCR. (a) Endoglin silencing was analyzed by RT-PCR. S6 was used as a loading control. Total RNA degradation was analyzed by Miltenyi and visualized in (b) a gel image and in (c) an electropherogram. (b) The gel image showed exclusively the 18S and the 28S RNA band and an internal standard (green band). RNA standard size marker is indicated in the left margin. (c) The electropherogram showed only two prominent peaks, the 18S RNA and 28S RNA.
Endoglin mRNA was significantly reduced in RNA samples obtained from HSC transfected with siEng. No degradation was detected. All samples obtained a RIN of 10, thus, being suitable for microarray analysis.

ALK1), matrix assembly and turnover (e.g. α_2M, MMP10, Cthrc1) and differentiation of endothelial cells (e.g. Edg7). The eye-catcher of this array was α_2-macroglobulin. In HSC lacking endoglin α_2-macroglobulin showed a fold change of about 14 in its expression ("single" microarray). In comparison endoglin showed a fold change of only 8 in the same hybridization.

Northern blot analysis for endoglin, α_2-macroglobulin, collagen type I and fibronectin was performed in order to reconfirm the results of the microarray analysis. GAPDH was used as a loading control (Fig. 3.13 b). 5 μg of total RNA was loaded onto the gel. Northern blot analysis reconfirmed the results obtained by microarray analysis. This includes the efficient down-regulation of endoglin as an internal control and the efficient down-regulation of α_2-macroglobulin. Furthermore, Northern blot analysis revealed no differences in mRNA expression of collagen type I and fibronectin.

Abbreviations and gene symbols used in Fig. 3.13 are α_2M, α_2-macroglobulin; Wisp1, WNT1-inducible signaling pathway protein; Eng, endoglin; Ptgis, Prostaglandin I2 synthase; Vil, villin; Cthrc1, collagen triple-helix repeat-containing protein 1; PapIn, Plakophilin-related armadillo repeat protein-interacting PDGZ protein; Mfap4, microfibril-associated protein 4; Rgs5, regulator of G protein signaling 5; Ltbp2, latent transforming growth factor-β-binding protein 2; Acvrl1, activin A receptor type II-like1; Sfrp1, secreted frizzled-related protein 1; Laminin α-4 chain, laminin alpha 4 chain; Mfap5, microfibrillar associated protein 5; Rgn, regucalcin; NCAML1, Rattus norvegicus L1 cell adhesion molecule; Tm4sf1, tumor-associated antigen L6; K1CJ, Keratin, type I cytoskeletal 10; Nog, noggin; Kdr, tyrosine kinase growth factor receptor; MMP10, matrixmetalloproteinase 10, Cxcl2, chemokine (CXC motif) ligand 2; Edg7, endothelial differentiation gene 7; Nppc, natriuretic peptide precursor C.

Gene classification

Most of the differentially expressed genes, which are listed in Appendix A, are already well characterized. They are associated with different cellular features and processes. To determine the cellular feature, to which these genes belong to, a pathway analysis was performed by Miltenyi. Eight groups were distinguished, i.e. structural, stress, signaling mechanism, signaling, organismal, metabolism, cellular process, cellular behavior. These groups were further divided into subgroups. Genes listed in Appendix A and their corresponding proteins, respectively were allocated to one of these groups. Unless no information about the gene or protein was available. Double allocations were possible. Finally, a classification scheme as shown in figure 3.14 was received.

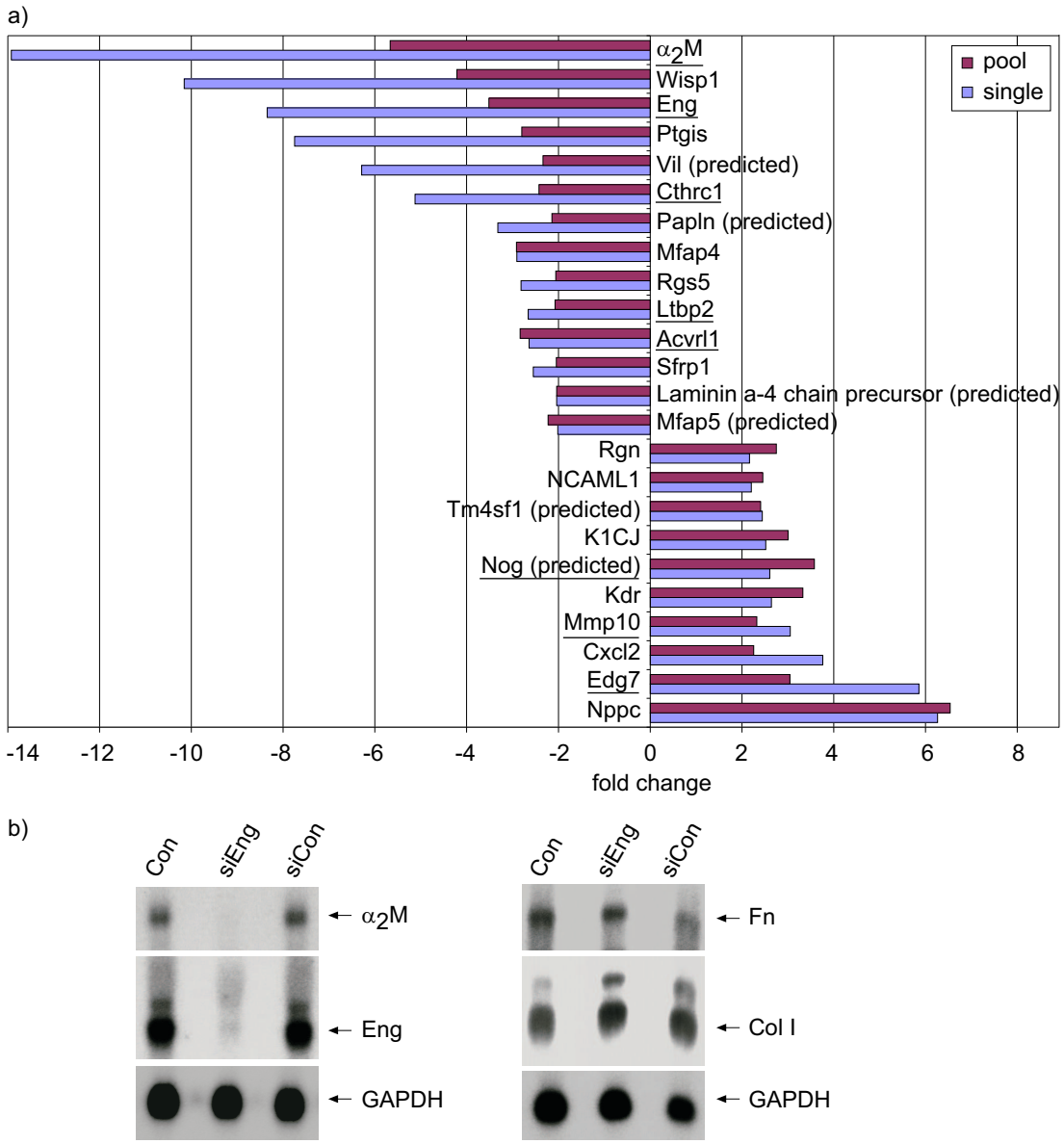


Figure 3.13: A list of selected microarray genes and their verification by Northern blot analysis. (a) A selection of 24 differentially expressed genes are listed in the diagram. These genes were chosen because their expression was strongly modified or their corresponding proteins might be jointly responsible for the cellular alterations, which were observed in HSC transfected with siEng. Endoglin, as an internal control is 8.3 fold down regulated in hybridization no. 2 (single sample) and 3.5 fold down regulated in hybrdidization no. 4 (pool). The x-axis indicates the fold change in gene expression. (b) Northern blot analysis was performed to verify the result of the microarray for endoglin, α_2-macroglobulin, collagen type I (Col I) and fibronectin (Fn). mRNA for Northern blot analysis was isolated from HSC, which were harvested on day 8. 5 μg of total RNA were loaded onto a formaldehyde agarose gel. *GAPDH* was used as a loading control. Abbreviations and gene symbols are described in the body text.
Northern blot analysis reconfirmed the results of the microarray for endoglin, α_2-macroglobulin, collagen type I and fibronectin.

In this scheme more than 110 differentially expressed genes and their corresponding proteins are associated with receptor signaling, followed by around 90 differentially expressed genes and their corresponding proteins, which are associated with development. Around 60 genes and their corresponding proteins are associated with cellular import and export. Furthermore, around 60 genes and their corresponding proteins are associated with cell differentiation. Except for these four subgroups (receptor signaling, development, cellular import and export, differentiation) the number of genes in the remaining subgroups were not above average.

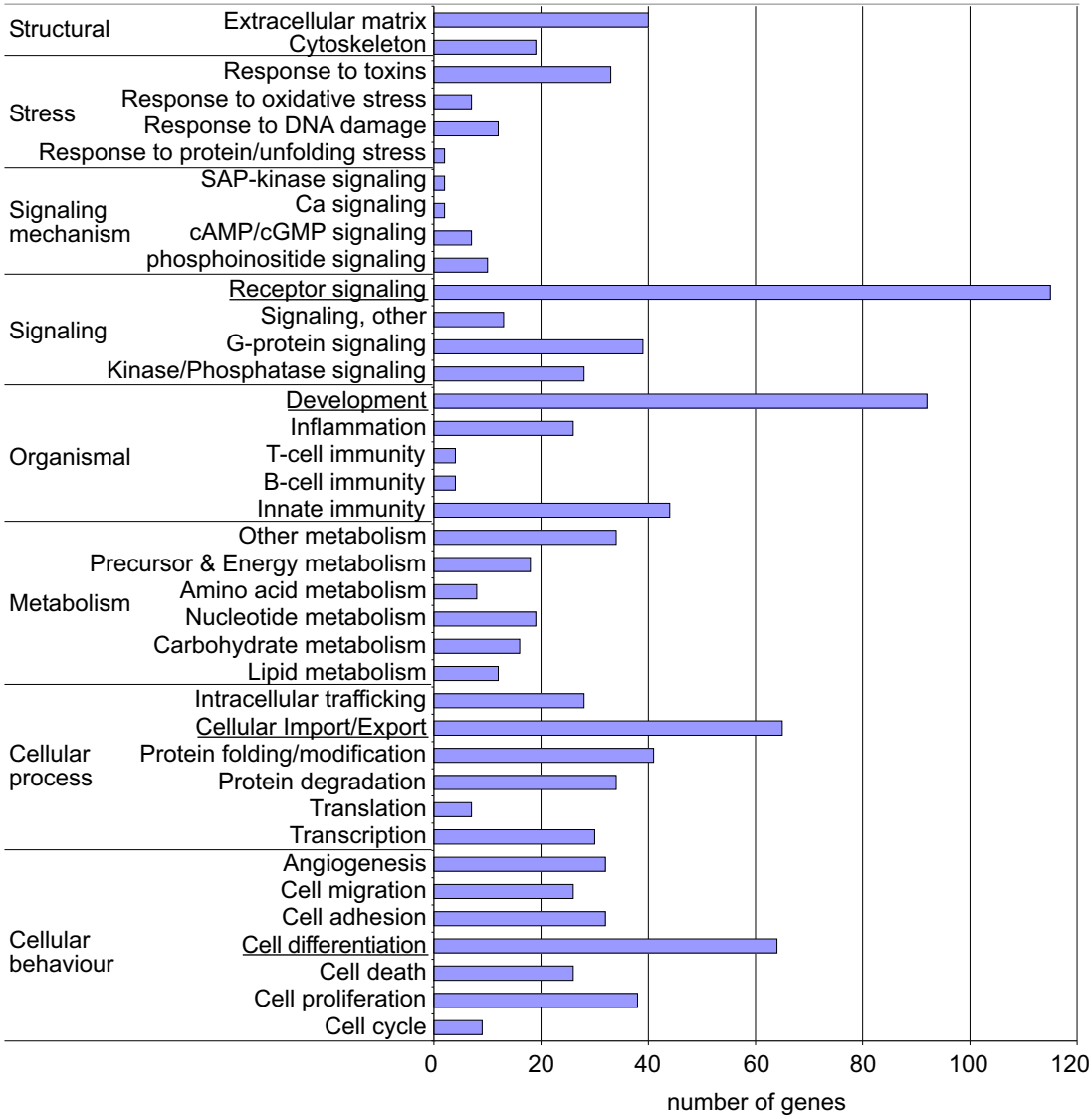


Figure 3.14: Classification of the differentially expressed genes (siEng *vs.* siCon) and their corresponding proteins into subgroups of cellular features. 8 groups and in total 38 subgroups are distinguished. X-axis: number of genes belonging to the indicated subgroup (Y-axis).
Most of the differentially expressed genes and their corresponding proteins were allocated to receptor signaling, followed by development and cellular import/export as well as cell differentiation. The number of genes in the remaining subgroups were not above average.

3.2.6 Summary: Characterization of endoglin deficient HSC

Before completing this section, results are summarized in figure 3.15.

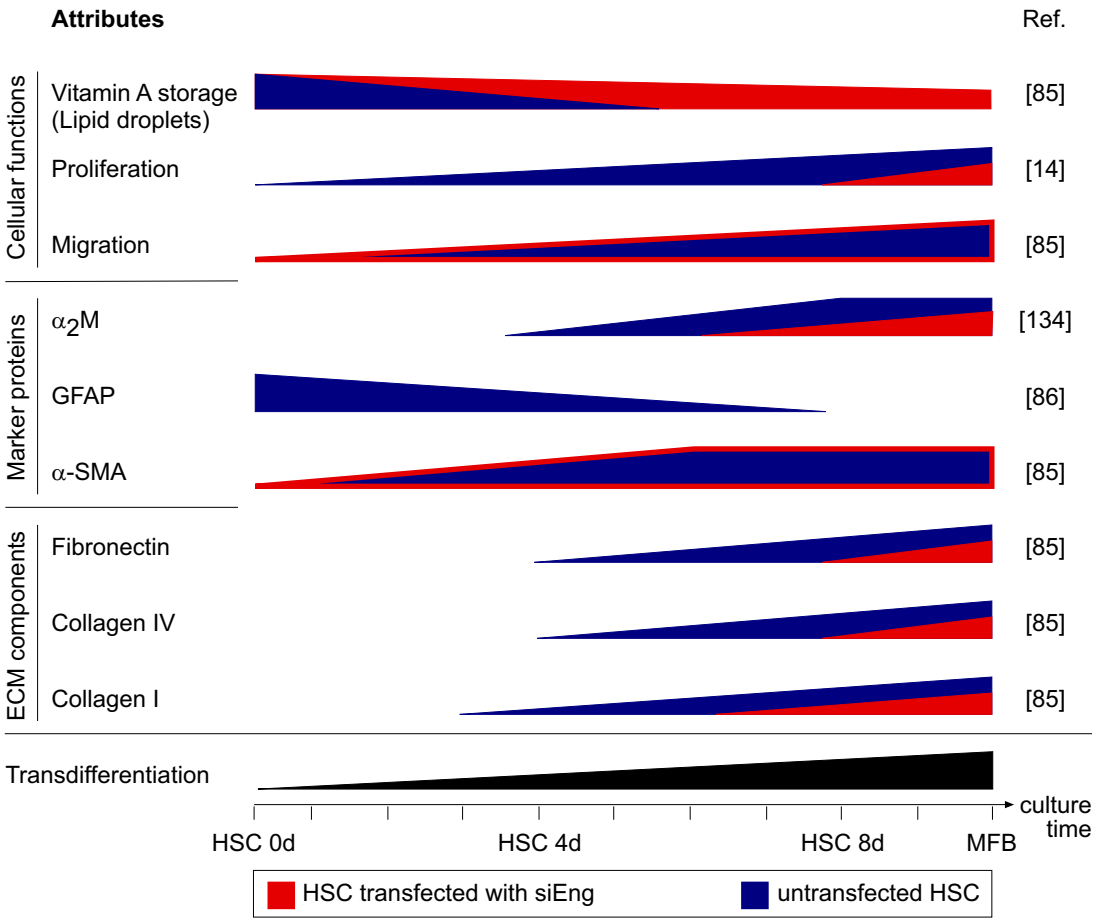


Figure 3.15: Transdifferentiation of control HSC *vs.* HSC transfected with siEng. Changes of different cell features, which were caused by endoglin silencing, are described in this image. Blue arrows describe the changes in control cells and red arrows describe the changes in HSC transfected with siEng on day 1. X-axis: day of culture; Y-axis: attributes, which are modified during transdifferentiation.

3.3 α_2-Macroglobulin

In consequence of endoglin silencing α_2-macroglobulin expression was mostly affected as revealed in the cDNA microarray. This result was reconfirmed by Northern blot analysis. α_2-Macroglobulin is known as a marker of transdifferentiation and as an inhibitor of matrix metalloproteinases. Therefore, it is likely that α_2-macroglobulin might act down stream of endoglin thus being involved in the observed cellular alterations.

3.3.1 α_2-Macroglobulin down-regulation through endoglin silencing

As an inhibitor of metalloproteinases α_2-macroglobulin is involved in degradation of ECM components. Therefore, down-regulation of α_2-macroglobulin might result in an increased MMP activity and this in turn might result in an increased degradation of ECM components, such as collagen type I, IV and fibronectin. This hypothesis might explain the results obtained by Western blot analysis (Fig. 3.5, 3.6 and Fig. 3.7). Due to these facts α_2-macroglobulin was investigated in more detail. First of all down-regulation of α_2-macroglobulin in HSC lacking endoglin was additionally analyzed by Western blotting. The antibody, which was used to detect α_2-macroglobulin, was raised against human α_2-macroglobulin. HSC were either transfected with siRNA on day 1 (Fig. 3.16 a) and cell lysates were analyzed on days 4, 5, 6, 7, 8 and 9 or transfected on day 3 (Fig. 3.16 b), on day 4 (Fig. 3.16 c) and on day 5 (Fig. 3.16 d) and cell lysates were analyzed on days 7, 8 and 9. HSP70 and PonceauS were used as loading controls. In cell lysates of HSC transfected on day 1 the amount of α_2-macroglobulin was significantly reduced at all time points analyzed. The corresponding controls revealed an increase in α_2-macroglobulin expression starting on day 4. Transfection of HSC with siEng at later time points did also result in a significant decrease of α_2-macroglobulin. Furthermore, a time delay in α_2-macroglobulin down-regulation as a consequence of endoglin down-regulation became obvious in figure 3.16 d. Cell lysates analyzed in figure 3.16 d were obtained from HSC transfected with siRNA on day 5. Transfection of HSC on day 5 led to a maximal endoglin knock down on day 7. At this time point α_2-macroglobulin is still detectable, but on day 8 α_2-macroglobulin is significantly decreased. Therefore, down-regulation of endoglin is followed by α_2-macroglobulin down-regulation with a time delay of 24 h.

Using Western blot analysis it could be demonstrated that α_2-macroglobulin is less abundant in HSC lacking endoglin. However, the observed reduction is not as strong as expected. One explanation might be the extracellular localization of α_2-macroglobulin.

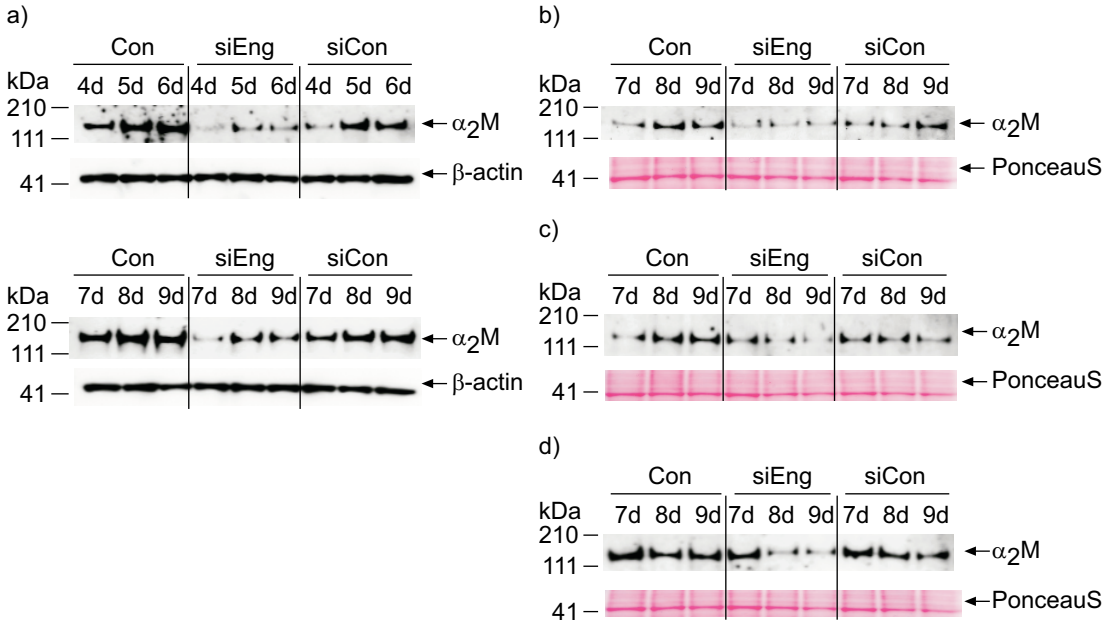


Figure 3.16: Western blot analysis of α_2-macroglobulin in HSC transfected with either scrambled siRNA or with siRNA targeting endoglin. HSC were transfected with siRNA on day 1 (a), on day 3 (b), on day 4 (c) or on day 5 (d). HSC were analyzed by Western blotting using cell lysates of HSC harvested at the indicated time points. 20 μg of protein were loaded onto a 3-8% Tris-Acetate gel and α_2-macroglobulin was detected with an antibody specific for α_2-macroglobulin. HSP70 and PonceauS were used as loading controls. Untransfected HSC (Con) and HSC transfected with scrambled siRNA (siCon) were used as negative controls. Protein standard size markers are indicated in the left margin.
α_2-macroglobulin was down regulated in HSC transfected with siEng at all time points analyzed. Only exception, HSC transfected on day 7.

Therefore, the amount of α_2-macroglobulin in the culture medium of cultured HSC was verified by Western blot analysis. However, specific detection of rat α_2-macroglobulin in the conditioned cell supernatant was not possible. FCS as a supplement of the cell culture medium contains a high amount of calf α_2-macroglobulin. The antibody, which was used to detect rat α_2-macroglobulin, did cross reacts with calf α_2-macroglobulin. Thus, it was not possible to distinguish between rat α_2-macroglobulin and calf α_2-macroglobulin.

3.3.2 Gelatinase and collagenase assay

As already mentioned α_2-macroglobulin is known as an inhibitor of matrix metalloproteinases. To proof whether α_2-macroglobulin down-regulation leads to an increase in matrix metalloproteinase activity, a gelatinase assay was performed. To test the functionality of this assay, especially under cell culture conditions, a control assay was performed as shown in figure 3.17 a. HSC were cultured in 96-well plates and DMEM containing 10% FCS. One day after initial plating, cells were transfected with siRNA. On day 4 the gelatinase assay was initiated and the fluorescence was measured at the indicated time points. *Clostridium* collagenase was applied in different concentrations (0.005 U/ml, 0.025 U/ml, 0.05 U/ml) to a mixture of fluorescein-labeled DQ gelatin conjugate and reaction medium. This medium was either 1 x reaction buffer (a component of the EnzChek Gelatinase/Collagenase Assay Kit), H_2O or DMEM containing either 10% FCS or containing 0.1% BSA, penicillin, streptomycin and L-glutamine. Fluorescence was measured in a fluorescence microplate reader equipped with standard fluorescein filters. It turned out that all reaction mediums are suitable. However, the test revealed a reduced fluorescence when reaction buffer was replaced with DMEM containing 10% FCS or 0.1% BSA. Based on this result gelatinase activity and collagenase I activity of untransfected HSC (Con) and HSC transfected with siEng and siCon were determined. For these experiments fluorescein-labeled DQ gelatin conjugate (Fig. 3.17 b) or fluorescein-labeled DQ collagen type I conjugate (Fig. 3.17 c) were added either to conditioned medium (DMEM 10% FCS), to HSC cultivated in 10% FCS or cultivated in DMEM 0.1% BSA or cultivated in reaction buffer. As a positive control Costridium collagenase was additionally added to one sample. Fluorescence was measured at the beginning of the experiment, after 24 h incubation and after 48 h incubation. Incubation of HSC was performed at 37°C in a CO_2 incubator with a concentration of 5% CO_2 and 100% relative humidity. Even though fluorescence increased marginally during incubation, no differences between HSC transfected with siEng and controls were observed.

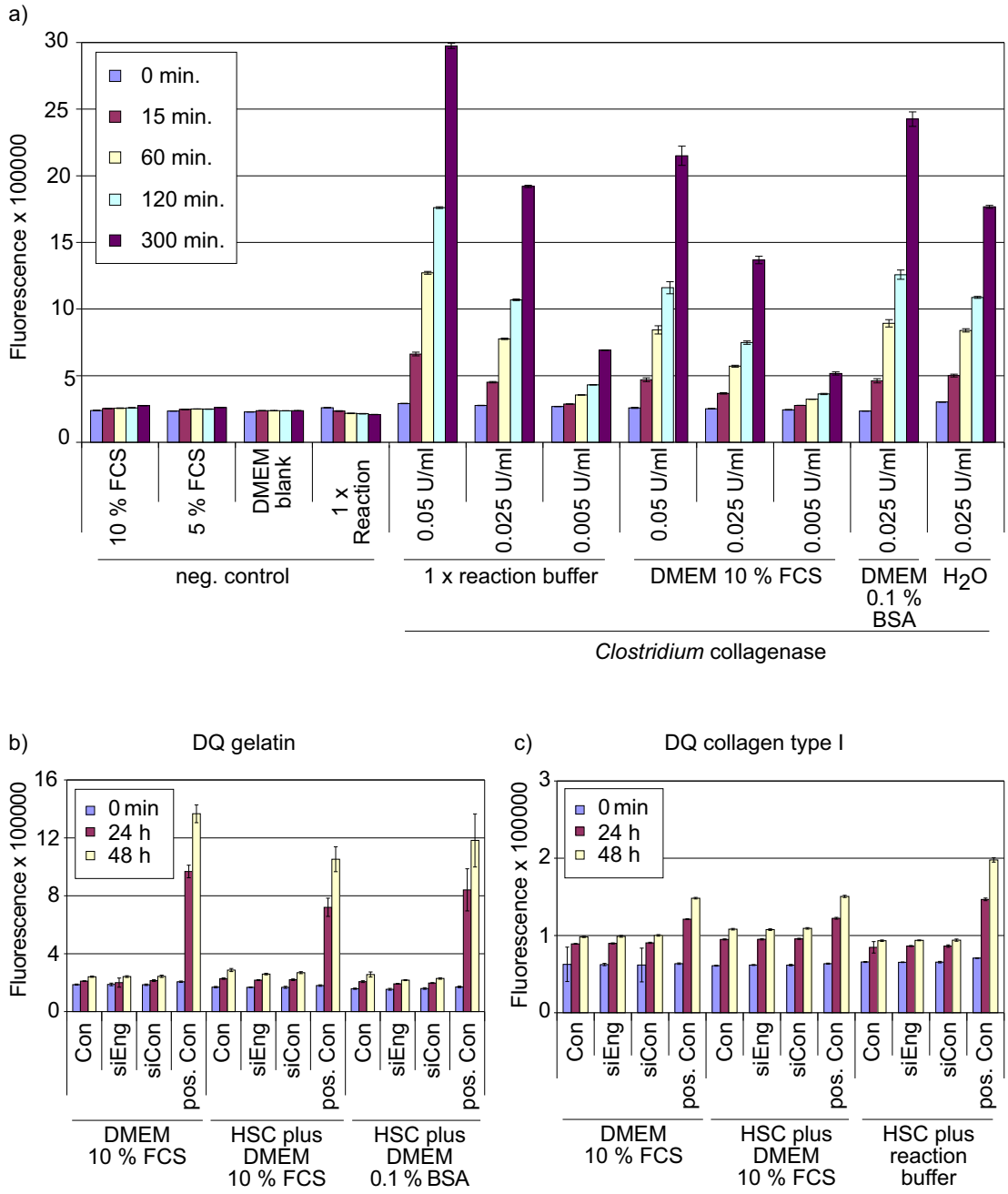


Figure 3.17: Determination of the proteinase activity using the EnzChek gelatinase and collagenase assay kit. HSC were cultured in 96-well plates and DMEM containing 10% FCS. One day after initial plating, cells were transfected with siRNA. On day 4 the gelatinase/collagenase assay was initiated and fluorescence was measured at 530 nm at the indicated time points. (a) The functionality of this assay was initially tested using different buffers and different concentrations of *Clostridium* collagenase (0.05 U/ml, 0.025 U/ml, 0.005 U/ml). (b) Gelatinase activity of untransfected HSC (Con) and of HSC transfected with siEng or siCon was measured. (c) Collagenase I activity of untransfected HSC (Con) and of HSC transfected with siEng or siCon was measured. *Clostridium* collagenase was used as positive control.
No differences were detected between untransfected HSC (Con) and HSC transfected with siEng or siCon.

The positive control containing *Clostridium* collagenase showed a significant increase in fluorescence. Therefore, it is likely that this assay is not suitable for this kind of experiment. Otherwise it might be that collagenase I and gelatinase activity is not changed in HSC transfected with siEng compared to the corresponding controls.

3.3.3 siRNA targeting α_2-macroglobulin

Due to the fact that the inhibition of MMP activity is only one putative function of α_2-macroglobulin more experiments were performed. To analyze if α_2-macroglobulin acts down stream of endoglin, α_2-macroglobulin was silenced. For this purpose siRNA directly targeting α_2-macroglobulin mRNA was used. Similar to the evaluation of siEng functionality the time and concentration dependent silencing effects of siα_2M were tested.

HSC were transfected with siRNA on day 3. siRNA was applied as a mixture of two different siRNAs targeting α_2-macroglobulin mRNA. The final concentration of siRNA in the transfection mixture was 5 nM or 10 nM. Bright field microscopy (200 x magnification) of HSC was performed on days 8 and 9 (Fig. 3.18 a) and showed an inhibition of morphological transdifferentiation in HSC transfected with siα_2M. The character of inhibition is comparable to the inhibition obtained by transfection of HSC with siEng. HSC transfected with either siEng or siα_2M did not lose their circular arranged lipid droplets. Furthermore, the development of cell-cell contacts seemed to be decreased. Next the quantity of collagen type I and type IV was analyzed by Western blotting using protein lysates of HSC, which were harvested on day 8 (Fig. 3.18 b). Western blot analysis showed equal amounts of collagen type I and type IV. However, down-regulation of α_2-macroglobulin was confirmed using an antibody specifically raised against rat α_2-macroglobulin. Therefore, it is likely that silencing of α_2-macroglobulin inhibits morphological transdifferentiation, but has no impact on the quantity of collagen type I and type IV.

Functional characterization of α_2-macroglobulin just started with these experiments. To further support the hypothesis that α_2-macroglobulin acts down stream of endoglin more experiments need to be done. However, inhibition of morphological transdifferentiation is already the first hint.

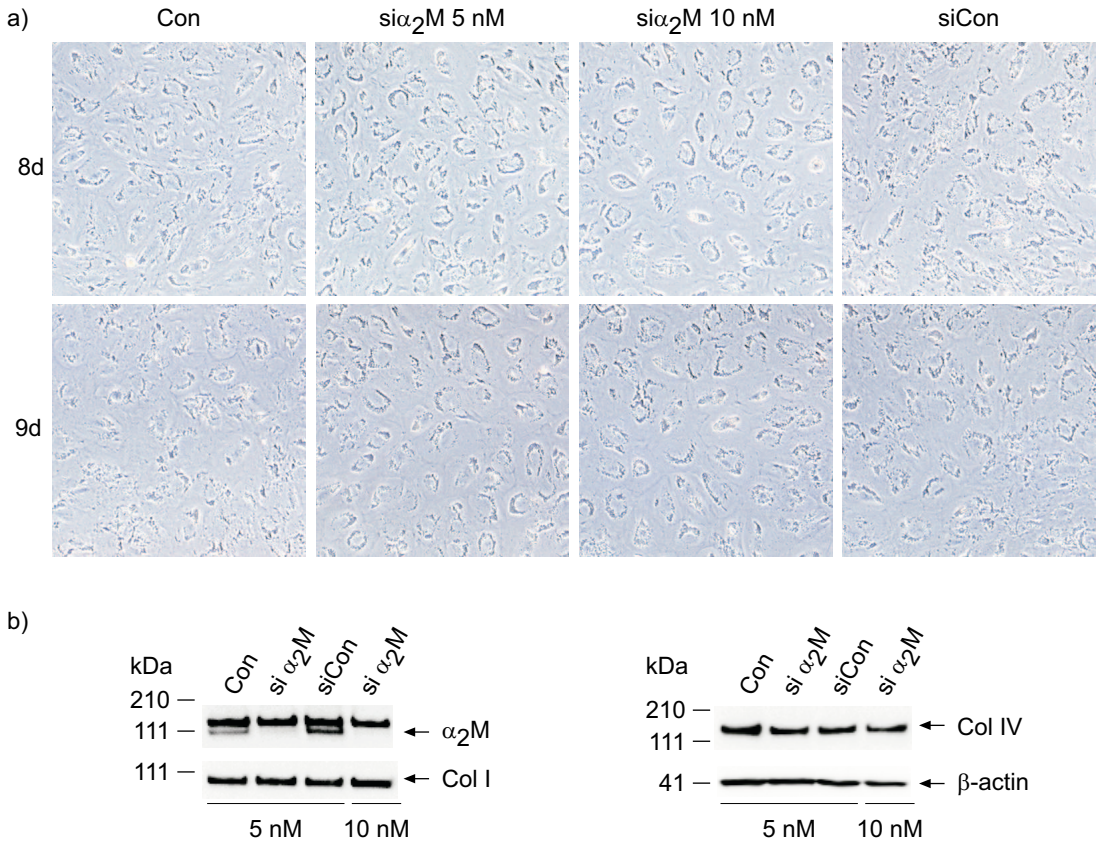


Figure 3.18: Effect of α_2-macroglobulin down-regulation on morphology and ECM expression in HSC. HSC were transfected with siRNA on day 3. Two concentrations of siRNA targeting α_2-macroglobulin were used (5 nM, 10 nM). (a) Images were taken on day 8 and on day 9. (b) HSC were analyzed by Western blotting using cell lysate of HSC harvested on day 8. 20 μg of protein were loaded onto a 3-8% Tris-Acetate gel. α_2-macroglobulin expression, as well as collagen type I and type IV expression were determined using specific antibodies. Untransfected HSC (Con) and HSC transfected with scrambled siRNA (siCon) were used as negative controls. Protein standard size markers are indicated in the left margin. β-Actin was used as a loading control.
Silencing of α_2-macroglobulin using siRNA directly targeting α_2-macroglobulin was confirmed. Silencing of α_2-macroglobulin resulted in an inhibition of morphological transdifferentiation. In contrast the amount of collagen type I and type IV remained unaffected.

3.4 Stimulation Assays

Endoglin binds and modulates cellular responses of a broad range of TGF-β superfamily members. To analyze the impact of endoglin directly on the TGF-β and the BMP pathways stimulation assays were performed. Beside Western blot analysis the $(CAGA)_{12}$MLP-luciferase construct and the $(BRE)_2$-luciferase construct were used as a read out system for these cytokines. The main idea of these reporter gene constructs is an individual promoter region followed by a DNA sequence, which encodes the firefly luciferase. Phosphorylated Smad3 specifically binds to the CAGA promoter region and phosphorylated Smad1 specifically binds to the BRE promoter region. As a consequence to binding the expression of luciferase is induced. Due to the fact that primary HSC are very difficult to transfect, but easy to infect a $(CAGA)_{12}$MLP-luciferase virus and a $(BRE)_2$-luciferase virus were generated.

3.4.1 TGF-β1 and BMP-7 stimulation experiments

The $(CAGA)_{12}$MLP-luciferase virus and the $(BRE)_2$-luciferase virus were generated, amplified and purified as described in material and methods. Prior to amplification the functionality of these viruses were tested in stimulation experiments using HSC (data not shown). After amplification and purification the optimal virus concentration to infect HSC and to perform stimulation experiments was tested (Fig. 3.19 a and b). In the afternoon (approx. 4 p.m.) of day 2 HSC were infected with different concentrations of either $(CAGA)_{12}$MLP-luciferase virus or $(BRE)_2$-luciferase virus. The next morning (approx. 10 a.m.)the medium was renewed using DMEM 10% FCS and again replaced for starvation with DMEM 0.5% FCS in the late afternoon (approx. 4 p.m.). After approximately 16 h of starvation HSC were stimulated with either 1 ng/ml TGF-β1 or 50 ng/ml BMP-7. After stimulation for a time period of 8 h HSC were harvested and luciferase activity was measured. The test revealed an optimal concentration of $2 \cdot 10^8$ Pfu/ml for $(CAGA)_{12}$MLP-luciferase virus and an optimal concentration of $\geq 3 \cdot 10^8$ Pfu/ml for $(BRE)_2$-luciferase virus. Furthermore, the specificity of $(CAGA)_{12}$MLP-luciferase for TGF-β and the specificity of $(BRE)_2$-luciferase for BMP-7 was reconfirmed.

Subsequently, the impact of endoglin on the TGF-β (Fig. 3.20 a and c) and the BMP-7 pathways (Fig. 3.20 b) was analyzed. HSC were transfected with siRNA on day 1. For reporter gene assay HSC were additionally infected on day 2 with either the $(CAGA)_{12}$MLP-luciferase virus or the $(BRE)_2$-luciferase virus (a, b) and further processed as described for the initial test. On day 4 luciferase activity was measured and

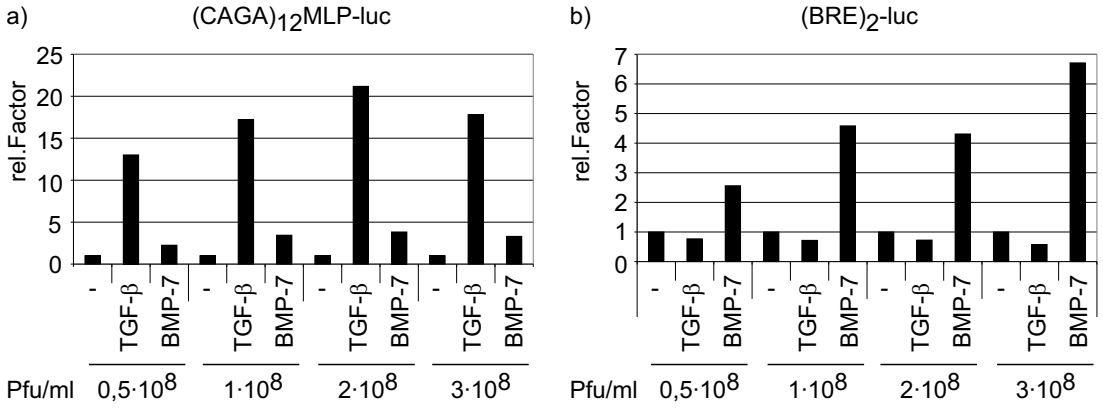


Figure 3.19: Initial test of the $(CAGA)_{12}$MLP-luciferase virus and the $(BRE)_2$-luciferase virus in HSC. HSC were transfected with siRNA on day 1 and infected with either the $(CAGA)_{12}$MLP-luciferase virus or the $(BRE)_2$-luciferase virus on day 2. Prior to stimulation HSC were starved and subsequent stimulated for 8 h with either 1 ng/ml TGF-β1 or 50 ng/ml BMP-7. Luciferase activity was measured and LCPS per μg protein were calculated.
The test revealed that both constructs are functional. Furthermore, $(CAGA)_{12}$MLP-luciferase is specific for TGF-β1 and $(BRE)_2$-luciferase is specific for BMP-7.

the protein concentration of the cell lysates was determined. LCPS (light counts per second) per μg protein were calculated and plotted in the graph (y-axis). Infected, but not stimulated HSC were used as negative controls. HSC transfected with siEng and stimulated with TGF-β1 showed an increased $(CAGA)_{12}$MLP-luciferase activity (Fig. 3.20 a). Stimulation with BMP-7 resulted in a marginal change of the $(CAGA)_{12}$MLP-luciferase activity. Luciferase activity of unstimulated HSC (negative controls) was almost equal among HSC transfected with siEng and the corresponding controls. In contrast luciferase activity of the negative controls of the $(BRE)_2$-luciferase assay (Fig. 3.20 b) resulted in different activities when compared to each other. HSC transfected with siEng and infected with $(BRE)_2$-luciferase virus forces a strong increase of the basal activity (Fig. 3.20 b). This means, that transfection of HSC with siEng induced an increase in the basal activity of the BMP-7 pathway. Untransfected HSC (Con) revealed the same stimulation pattern, when infected with the $(BRE)_2$-luciferase virus, as HSC transfected with siCon.

$(CAGA)_{12}$MLP-luciferase is activated through binding of phosphorylated Smad3. Therefore, phosphorylation of Smad3 was additionally verified by Western blot analysis (Fig. 3.20 b). HSC were transfected with siRNA on day 2. On day 3 the medium was renewed with DMEM 10% FCS and again replaced for starvation with DMEM 0.5% FCS in the late afternoon (approx. 4 p.m.). On day 4 HSC were stimulated for a time period of 1 h with either 1 ng/ml TGF-β1 or 50 ng/ml BMP-7. HSC were harvested,

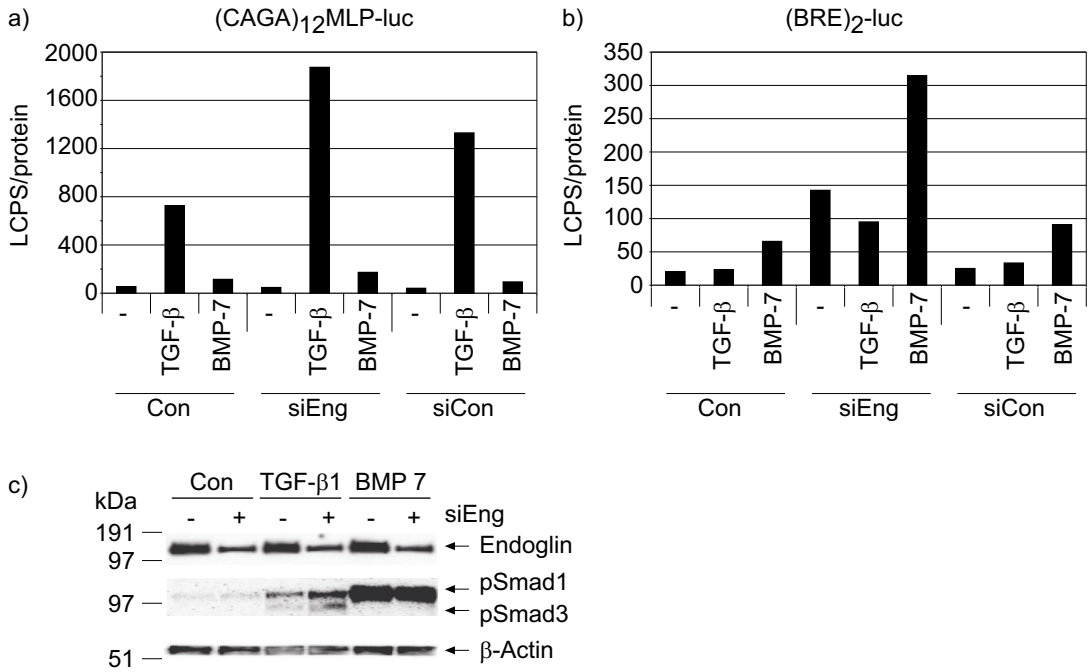


Figure 3.20: The effect of endoglin on Smad activation. Smad3 and Smad1 activation was analyzed by (a, b) reporter gene assay and (c) by Western blot analysis. HSC were transfected with siRNA on day 1. For reporter gene assay HSC were additionally infected on day 2 with either the $(CAGA)_{12}$MLP-luciferase virus or the $(BRE)_2$-luciferase virus (a, b). Prior to stimulation HSC were starved for 16 h and subsequent stimulated for 8 h with either 1 ng/ml TGF-β1 or 50 ng/ml BMP-7. Luciferase activity was measured (a, b) and LCPS per μg protein were calculated. (c) HSC were harvested using Ripa complete supplemented with the phophatase inhibitor cocktail II. For Western blot analysis 20 μg protein were loaded onto a 4-12% Bis-Tris gel. Antibodies specific for endoglin and phosphorylated Smad1/3 were used. β-Actin was used as a loading control.
TGF-β1 stimulation resulted in an increase in Smad3 phosphorylation in HSC lacking endoglin.

protein concentration was determined and 20 μg of cell lysate were loaded onto the gel. Endoglin expression and phosphorylation of Smad1 and Smad3 were detected using specific antibodies. Without any stimulation Smad1 and Smad3 were not phosphorylated. Upon stimulation with TGF-β1 a marginal increase in pSmad1 and pSmad3 was detected. However, HSC transfected with siEng showed a marginal increase in phosphorylation of Smad3 compared to the corresponding controls. Stimulation with BMP-7 resulted in phosphorylation of Smad1. Differences in the phosphorylation pattern of Smad1 between untransfected HSC (Con) and HSC transfected with siEng could not be detected.

Chapter 4

Discussion

For a coherent discussion it makes sense to form three sections. The first section discusses the RNAi approach, as the fundament of this thesis. The second section discusses the effect of endoglin silencing on hepatic stellate cells, especially under the aspect of transdifferentiation. In the third section the results of the initial stimulation experiments are discussed. Finally, the results of the second and third partition will be compared and discussed.

4.1 Down-regulation of endoglin

To examine the function of endoglin in HSC two kinds of RNAi approaches were established. In order to perform *in vivo* experiments, an adenoviral construct encoding shRNA targeting mouse endoglin was generated, amplified, purified and finally pretested in COS-7 and HSC. For *in vitro* experiments siRNA oligonucleotides were obtained from Qiagen and used to silence endoglin in HSC.

Generation of a functional shRNA virus is more demanding than the use of siRNA oligonucleotides, because the production of an adenovirus is a challenge of its own. First of all a homologous recombination of the shuttle vector and the viral backbone must be achieved. This step was simplified by using the BLOCK-iT Adenoviral RNAi Expression System, which provides the opportunity to perform the homologous recombination *in vitro*. Transfection of eucaryotic cells with large plasmids for homologous recombination is not very efficient. Furthermore, during homologous recombination and during amplification the insert might be lost by re-arrangements. This results in an increased number of wild type virus and an decreased number of the intended virus. Homologous recombination and amplification have been performed in between the

siRNA experiments using COS-7 and HSC. This amplification might explain why the adenovirus 12.1 is able to silence endoglin in COS-7, but loses its functionality in HSC. Another reason might be that endoglin is endogenously expressed in HSC while it is heterologously expressed in COS-7. Therefore, the non-coding sequence of both mRNA transcripts are different in size and sequence. This forces changes in the three dimensional structure and in the stability of the mRNA and alters the accessibility of the siRNA/RISC complex to the coding sequences. (siRNAs used in this study target a sequence within the coding sequence of endoglin)

In order to perform the *in vitro* experiments, siRNA oligonucleotides were taken into account. Transfection of HSC using siRNA oligonucleotides and HiPerFect - as transfection reagent - was initially in doubt, because primary HSC are normally very difficult to transfect. However, first experiments with fluorescence-labelled siRNA yielded a transfection efficiency of almost 100%. This high transfection efficiency of siRNA oligonucleotides compared to the very low transfection efficiency of a plasmid might be due to the size of the transfection complex, which is formed by DNA and transfection reagent. These complexes are smaller in case of the very short siRNA oligonucleotides. Furthermore, for a successful plasmid transfection the plasmid must finally reach the nucleus. In contrast siRNA function is mediated through the Dicer complex, which is localized within the cytoplasm. Last but not least it was possible to show that down-regulation of endoglin is due to mRNA degradation and not due to the disturbance of the transcriptional process. This was proven by Northern blot analysis as well as by semi-quantitative PCR. Anyway, the transfection efficiency, the knock down efficiency and the sustained character, which were confirmed in all experiments, provide a stable basis to characterize HSC lacking endoglin.

To confirm the specificity of the RNAi phenotype, it is important to exclude non-specific down-regulation of another gene as the inducer of the observed phenotype. Therefore, other siRNA targeting endoglin were tested regarding their efficiency to down regulate endoglin. This is an appropriate control, because two different siRNA are statistically not able to silence the same nonspecific mRNA. However, these siRNA were not efficient enough to silence endoglin to the same extant as siEng that was used during this study. Therefore, the confirmation of the specificity of the RNAi phenotype is still under investigation. Another alternative to confirm the specificity of the siRNA is to reintroduce the targeted gene. In order to reintroduce endoglin in HSC a virus overexpressing endoglin is necessary. Due to the fact that the generation of this virus is very time consuming this experiment is currently ongoing.

The activation of an interferon (IFN) response, which is caused by the introduction of dsRNA, could be excluded. An interferon response might lead to nonspecific translational inhibition, cell cycle arrest, a shutdown of the global protein expression or, potentially, to apoptosis shortly after transfection [104] [105]. However, modifications obtained for HSC transfected with siRNA targeting endoglin did not occur shortly after transfection, instead of this modifications became manifested on day 5 of culture. Furthermore, transfection of HSC with scrambled siRNA (siCon) did not lead to apoptosis or other obvious changes, e.g. morphological changes, compared to untransfected HSC. Therefore, modifications obtained on day 5 in HSC transfected with siEng were not due to an interferon response. Anyway, to further support that an interferon response can be excluded the activation of IFNs, e.g. type-I interferons, should be determined.

Furthermore, the kinetic of endoglin suppression is in accordance with previous studies, which show endoglin as a relatively stable glycoprotein with a half-life of approximately 17 h [112]. In this study endoglin silencing reached a suppression of 50-70% after 24 h and a suppression of 95-98% after 48 h post siRNA transfection. This result is comparable with the half life of 17 h obtained in other studies.

Even though the very efficient and sustained character of the knock down approach is the basis of the following experiments, it also raises a very important question. What kind of mechanism is responsible for silencing effect for at least 16 days? In order to exclude apoptosis a TUNEL test was performed. This assay revealed that HSC transfected with siEng were not apoptotic. This was supported by the observation that HSC were adherent at each time point analyzed. In contrast, floating cells were not detected at any time point analyzed. Therefore, down-regulation of endoglin is a persistent process in viable HSC. This suggests the existence of an autocrine feedback loop, in which endoglin triggers its own expression. However, to date there are no data published, which discuss such a feedback loop. Therefore, it might be that this siRNA might change the DNA methylation pattern within the coding region and, thus, within the promotor region of endoglin. Such a methylation process, which is induced by siRNA, within the coding region is not reported yet. However, there is at least one publication showing that synthetic siRNA, which targets CpG islands, is able to induce DNA methylation in mammalian cells. This in turn results in an repressed gene expression at the transcriptional level [109].

4.2 The impact of endoglin down-regulation on HSC transdifferentiation

As already mentioned it was possible to silence endoglin expression *in vitro* very efficiently for more than 17 days using siRNA oligonucleotides. This sustained and efficient knock down allowed us to analyze HSC transdifferentiation in the absence of endoglin. To mimic the *in vivo* transdifferentiation of HSC to MFB, an established *in vitro* transdifferentiation model was used. This model is based on the cultivation of primary HSC on uncoated tissue culture dishes in the presence of a high serum content (10% FCS) [113]. Under this experimental setting the suppression of endoglin resulted in multiple significant changes, such as a diminished loss of vitamin A as well as changes in cellular morphology. Both changes stand for an inhibition of transdifferentiation. This inhibition of transdifferentiation could also be induced when HSC were transfected with siEng at later time points, but before day 5 of initial culture. This indicates that an arrest of transdifferentiation and a partial reversion of cellular activation is possible in already fully activated HSC. Activation of HSC starts as a result of isolation and seeding. Consistently, such a phenotypic reversion of activated HSC was recently demonstrated in precision cut liver slices [114], indicating that HSC once activated have the potential to redifferentiate into a quiescent phenotype at least *in vivo*.

Morphological changes, which were observed during transdifferentiation of HSC, are due to a reprogramming of HSC. This reprogramming is characterized by the acquisition of contractile and migratory properties [115] and is accompanied by an increased expression of α-SMA [116]. Although significant differences in cellular morphology were observed, the expression of α-SMA was not altered in cells, in which endoglin expression was silenced. On the one hand this finding is consistent with previous studies, in which α-SMA expression was not modified when Smad7 and Smad3 were inactivated [117] [118]. Smad7 and Smad3 are important key components that affect the outcome of transdifferentiation. In contrast, a significant reduction of α-SMA expression in HSC was observed when the activity of profibrogenic cytokines, i.e. PDGF-B or TGF-β1, was abrogated [119] [120]. On the other hand the experimental setting permits the earliest maximal down-regulation of endoglin on day 3. At this time α-SMA expression is already initiated. Therefore, it might be too late to influence α-SMA expression. This is consistent with other studies, which were performed with stem cells. In stem cells endoglin deficiency inhibits α-SMA expression only before myogenic determination takes place. If endoglin is down-regulated after myogenic determination,

i.e. when α-SMA is expressed, there was no impact on α-SMA expression [121]. This is comparable to the results obtained in this thesis.

Although there were no changes in α-SMA expression in endoglin knock down cells compared to control cells, the organization of the actin cytoskeleton was greatly altered as initially demonstrated with phalloidin. To describe these alterations, which occurred in the absence of endoglin, in more detail CRP2-GFP was overexpressed. CRP2 is a LIM-domain protein and a specific marker for HSC with high affinity for the actin cytoskeleton [122]. CRP2-GFP was primarily localized along cytoskeletal fibers in control cells. However, it was re-localized to short fibres and their termini in the absence of endoglin. Additionally, an untagged version of CRP2 was overexpressed and F-actin was again stained with phalloidin. (Due to the strong fluorescence and the limitation of the filters a double stain of phalloidin and CRP2-GFP could not be performed.) On the one hand the staining pattern of this last experimental setting showed aspects of the phalloidin staining pattern and of CRP2-GFP staining pattern. On the other hand this last experimental setting revealed partially new alterations. Hence it is obvious that 1) the lack of endoglin forces changes in the organization of the cytoskeleton, 2) endoglin and CRP2 might interact, because 3) the localization of CRP2 differs when endoglin is silenced and 4) overexpression of CRP2 while endoglin is reduced results in a re-arrangement of the cytoskeleton. Therefore, it is likely that phalloidin directly binds F-actin while CRP2 binds to F-actin through another protein, which also interacts with endoglin, e.g. Zyxin. Zyxin is another member of the LIM-domain protein family and was previously found to interact with CRP2 [123]. It is further known that Zyxin binds to the C-terminus of endoglin [51]. Moreover, the interaction of Zyxin and endoglin in endothelial cells was found to be accompanied by a depletion of Zyxin at focal adhesion sites associated with inhibition of cell migration [51]. Therefore, Zyxin might be the missing link between endoglin, CRP2 and F-actin. If this link between CRP2 and endoglin is modified, CRP2 might be relocalized. This in turn may alter the organization of the cytoskeleton. On the other hand CRP2 is also a LIM-domain protein. Therefore, it might also be possible that CRP2 directly interacts with endoglin. Another putative candidate to link CRP2, endoglin and F-actin is ZRP-1 (Zyxin related protein1). ZRP-1 is highly homologous to Zyxin [124] and binds endoglin [52]. Furthermore, endoglin regulates cytoskeletal organization through binding to ZRP-1 [52] in endothelial cells. However, the diversity of cytoskeleton alterations can not be explained yet. More information especially about the interaction of endoglin with CRP2 and Zyxin and other components are necessary. Anyway, based on these results it is likely that endoglin and

Zyxin have essential functions in controlling HSC migration and contractility during transdifferentiation.

In order to investigate the function of endoglin in controlling HSC migration, a wound healing migration assay was performed. Surprisingly, no differences between migration of HSC lacking endoglin and the corresponding controls have been observed. This negative result is either caused by the low density of cells on the spot of HSC migration or the experimental setting in general is not appropriate. During this thesis it became obvious that inhibition of transdifferentiation and especially inhibition of morphological transdifferentiation, which is caused by endoglin down-regulation, depends on cell density. The lower the cell density the less the inhibitory effect, which is imposed by the absence of endoglin. A scratch and the following migration inevitably leads to a low number of cells around the scratch itself. Therefore, a migration assay will be performed, in which the potential of HSC to migrate through a thin layer of collagen I or fibronectin towards a defined stimulus is determined. On the other hand an inversion assay will be performed in which migration is facilitated by collagen degradation/increased MMP activity. This might be an appropriate experiment, because in previous studies it was demonstrated that endoglin enhances the invasive character of tumor cells [125].

Another classical feature of HSC during transdifferentiation is an increase in their proliferation rate. Due to the fact that the advantages and disadvantages of the ^{3}H-thymidine and the BrdU proliferation assays are still under discussion both assays were performed. In both assays HSC transfected with siEng were less proliferative than the corresponding controls. This modification might be caused by Alk1 and Alk5, because it was demonstrated in endothelial cells that cellular migration and proliferation is regulated by a balanced system of two TGF-β receptors, i.e. ALK5 and ALK1 [10]. Here ALK1 mediates migration/proliferation and requires the activation of ALK5 [9]. To date, the function of endoglin as a critical modulator of ALK1 responses is controversially discussed [23] [47] [126]. On the one hand it was shown that ALK1 promotes profibrogenic actions via induction of Id1 in HSC [127]. On the other hand it was shown that endoglin promotes antifibrogenic actions by directly antagonizing ALK5/Smad signaling [9]. In this thesis endoglin deficiency was found to be associated with reduced cellular proliferation. A reduced proliferation would point towards a decrease in ALK1 activity as a profibrogenic component. In line with this the comparative microarray revealed a reduction in ALK1 expression, whereas ALK5 expression was unaffected in cells lacking endoglin. This result supports the putative role for ALK1

in cell proliferation and may present a link between endoglin and ALK1 expression as well as endoglin and ALK1 function. Again substantiating the idea that endoglin may control transdifferentiation by promoting the ALK1 pathway. It is currently under investigation, if the reduced proliferation is due to a decreased ALK1 expression or if it is an indirect effect of the transdifferentiation arrest.

Based on the presented data it can not be determined whether the observed alterations are a consequence of the inhibition of transdifferentiation or whether the observed alterations are directly caused by endoglin down-regulation and therefore jointly responsible for the inhibition of transdifferentiation. To directly determine these interrelations, a detailed analysis of the underlying mechanisms and components has to be performed in a time dependent manner.

Since it was possible to show a putative role for endoglin in proliferation and, thus, in the ALK1 pathway, there might also be a putative role for endoglin in the regulation of the ECM expression. An increase in the expression of ECM components is a further classical feature of HSC during transdifferentiation. In contrast to proliferation ECM synthesis is regulated by the TGF-β1/ALK5/Smad3 signaling pathway. The TGF-β1/ALK5/Smad3 signaling pathway is responsible for the transcriptional activation of ECM components including collagen type I and fibronectin [117] [128] [129]. It has been shown that overexpression of endoglin inhibits the ALK5/Smad3 pathway and, therefore, inhibits ECM protein expression [48] [20]. In contrast, experiments in this thesis, which were performed with siRNA in the presence of a high serum content (10% FCS), imply that this pathway might not be affected by endoglin. Western blot analysis revealed a significant decrease of collagen type I, collagen type IV and fibronectin accumulation in HSC lacking endoglin. A reduced amount of collagen type I was also detected in the supernatant of HSC treated with siRNA targeting endoglin (data not shown). In contrary Northern blot analysis as well as microarray analysis did not show a corresponding down-regulation on the level of mRNA. Thus, changes in the ECM abundance are not the result of alterations in gene activity, which are normally caused by alterations in the TGF-β1/ALK5/Smad3 signaling pathway. However, there are two potential explanations: a reduced translation or an increased degradation. A reduced translation can be investigated by metabolic labelling. An increased degradation might be due to an increased MMP activity or a decreased TIMP activity. Therefore, MMP activity as well as TIMP activity should be investigated.

Endoglin is connected with a variety of different signaling pathways. This was already shown in former studies [130] and became additionally evident from this study.

down-regulation of endoglin results in a wide range of cellular alterations, which can not be explained with alterations of a single pathway or of a single molecular mechanism. To yield more information of the molecular mechanism, which are responsible for the inhibition of transdifferentiation, a cDNA microarray was performed. Due to the difficulty to determine a time point, which optimally reflects the observed alterations, the microarray assay was performed on day 8. On day 8 differences in transdifferentiation are obvious and already manifested. With this microarray a huge number of genes were identified, which were differentially expressed when endoglin was silenced. Therefore, this microarray opens up new possibilities to explain the observations that were revealed in the previous experiments. However, the array revealed that the expression of MMP10 (stromelysin-2), a protein that is involved in matrix protein degradation, was significantly increased. An increase of MMP10 in turn might contribute to the degradation of ECM components. This supports the finding that the decrease of ECM is rather caused by protein degradation than by gene regulation. The microarray data also revealed changes in gene expression of components of the Wnt signaling pathway. Members of this protein family are differentially expressed and regulated during transdifferentiation [131] [132] and determine the potential of HSC to transdifferentiate [133]. However, the strongest down-regulated gene identified in this microarray was α_2-macroglobulin. α_2-Macroglobulin was previously found to be upregulated in cultured HSC during *in vitro* transdifferentiation [134] [135]. This further supports the finding that endoglin suppression inhibits HSC transdifferentiation. Nowadays α_2-macroglobulin is also discussed as a marker for liver fibrosis [136]. Therefore, α_2-macroglobulin might be beneficial to find a link between these *in vitro* experiments and the *in vivo* processes. Additionally, α_2-macroglobulin is also known as a cytokine transporter for IL-8, IL-1, TNF-α and TGF-β and regulates the supply of these cytokines [137]. To date it is unknown if and how the absence of α_2-macroglobulin in its role as a cytokine transporter influences the transdifferentiation process, but its involvement is most likely. Last but not least the gene classification supports the results, which were obtained in this thesis, in a global point of view. "Receptor signaling" reconfirms the well established function of endoglin as an important receptor for cell signaling. "Development" and "cell differentiation" are appropriate to cover all the observed cell alterations. However, cellular import and export are not investigated yet, but their investigations might reveal very interesting and informative results.

So far all the experiments were performed with siRNA targeting endoglin. However, based on the efficient down-regulation of α_2-macroglobulin, as a consequence

of endoglin silencing, α_2-macroglobulin was directly down regulated. Direct down-regulation was evoked using siRNA targeting α_2-macroglobulin. In this way it can be determined a) if α_2-macroglobulin functions as a down-stream component of endoglin and b) which alterations of the endoglin knock down phenotype is caused by the lack of α_2-macroglobulin. Even though these siα_2M experiments just started first results were already obtained. Bright field microscopy revealed an inhibition of morphological transdifferentiation. These alterations are akin to the observation made with siRNA targeting endoglin. In contrast ECM abundance seems to be unaffected in HSC transfected with siα_2M. Therefore, it seems that the lack of α_2-macroglobulin might be responsible for at least the morphological alterations observed in siEng experiments.

However, before further experiments can be performed, the specificity of the antibodies need to be confirmed. While the α_2-macroglobulin antibody, which is raised against human, is very weak and difficult to handle, the other α_2-macroglobulin antibody, which is raised against rat, revealed an unspecific band.

4.3 The role of endoglin in the TGF-β1 and BMP-7 pathways

As mentioned before an established in vitro transdifferentiation model was used to mimic the *in vivo* transdifferentiation of HSC to MFB. This model is based on the cultivation of primary HSC on uncoated tissue culture dishes in the presence of a high serum content (10% FCS) [113]. In this way it was possible to characterize the function of endoglin during the process of transdifferentiation. However, endoglin binds several ligands of the TGF-β superfamily and the growth medium contains a broad range of different ligands. Therefore, the agonist or the agonist spectrum causing the alterations in the absence of endoglin are unknown. To narrow this range stimulation experiments were performed using TGF-β and BMP-7, which are key cytokines in liver fibrosis.

Prior to stimulation experiments the $(CAGA)_{12}$MLP-luciferase virus and the $(BRE)_2$-luciferase virus were generated, amplified and tested regarding their functionality and specificity. $(CAGA)_{12}$MLP-luciferase is known to be specifically activated by phosphorylation of Smad3 [110]. Smad3 phosphorylation in turn is induced by TGF-β1 [138] [11]. $(BRE)_2$-luciferase in HSC is known to be specifically activated by phosphorylation of Smad1 [20]. Smad1 phosphorylation in turn is mainly induced by BMP-7 and only marginally induced by TGF-β1 [20]. Due to the fact that the conversion of particle to plaque forming units (Pfu) was roughly estimated, the optimal concentration

of virus was determined using different virus concentrations. The test revealed an optimal concentration of $2 \cdot 10^8$ Pfu/ml for $(CAGA)_{12}$MLP-luciferase virus and an optimal concentration of $\geq 3 \cdot 10^8$ Pfu/ml for $(BRE)_2$-luciferase virus. Summarized, it was demonstrated that both viral constructs are a) highly specific and b) very sensitive to the corresponding cytokine. After the functionality and the specificity of the $(CAGA)_{12}$MLP-luciferase virus $(BRE)_2$-luciferase virus had been tested the impact of endoglin on the TGF-β and the BMP-7 pathways was analyzed by reporter gene assay and by Western blot analysis.

Western blot analysis revealed an increased Smad3 phosphorylation in HSC stimulated with TGF-β1 (1 μg/ml; 1 h). This was supported by the reporter gene assay, which revealed an increased Smad3 activity in HSC stimulated with TGF-β1 (1 μg/ml; 6 h). However, phosphorylation of Smad3 in HSC transfected with siEng was stronger than in the corresponding controls. Furthermore, stimulation with BMP-7 results in a marginal increase in Smad3 phosphorylation and activity. But compared to the TGF-β1 stimulation the phosphorylation of Smad3 induced by BMP-7 stimulation is marginal increased in HSC lacking endoglin. These results imply an inhibitory function of endoglin towards the TβRII/ALK5/Smad3 pathway. This is consistent with former studies, which also show an inhibitory function of endoglin towards the TβRII/ALK5/Smad3 pathway [20].

Phosphorylation and activity of Smad1 are increased upon stimulation with BMP-7 in all samples analyzed. Stimulation with TGF-β1 leads to a marginal increase in Smad1 phosphorylation and activity. Except in the reporter gene assay, where TGF-β1 did not activate Luciferase expression. In this assay HSC lacking endoglin show a decrease of Smad1 activity when stimulated with TGF-β1. However, the most important observation revealed by the BRE-reporter gene assay is a stimulation independent increase of phosphorylated Smad1 in HSC lacking endoglin. This means that the basal level of Smad1 activity is increased in HSC transfected with siEng. This in turn points towards an inhibitory function of endoglin towards the BMP-ligand activated Smad1 pathway.

Finally, stimulation experiments and experiments performed in high serum content were compared. The results obtained in the presence of a high serum content (10% FCS) and the results obtained by stimulation experiments seem to be contrary. While stimulation experiments with TGF-β1 revealed an inhibitory function of endoglin towards the TβRII/ ALK5/Smad3 pathway, the inhibition of transdifferentiation process in high serum content points towards an activating function of endoglin. However, there was no link between endoglin and the TβRII/ALK5/Smad3 pathway in experiments, which

were performed in high serum content.

Due to the fact that integration of many signals form the final output signal, it might be difficult to transfer the result of a single stimulation experiment to a complex stimulation situation. Experiments performed in the presence of a high serum content are such a complex stimulation situation. Anyway, it is necessary to perform both kinds of experiments, because only the entire sum of the single components is able to explain the whole system.

Last but not least this thesis provides many stable and interesting results regarding endoglin and its function during HSC transdifferentiation. They are eager for further investigations.

Chapter 5

Conclusions

This research was innovative as it is the first to demonstrate that the reduction of endoglin expression in HSC causes dramatic changes in profibrogenic functions. These changes include an inhibition of the morphological transdifferentiation, a reduced proliferation and a decreased abundance of ECM components. Although TGF-β1 is one of the key regulators of these cellular processes, the present data do not necessarily implicate that these effects are caused by alterations in TGF-β signaling. On the other hand, an impact of endoglin on ALK1 signaling is obvious, because of the reduced ALK1 expression. This is further supported by the result of the reporter gene assay showing a different activation of Smad1 and Smad3 in HSC lacking endoglin. However, these manifold alterations observed in this study point out an involvement of many signaling pathways. First evidences are already given by the microarray, supporting an involvement of the WNT pathway. Therefore, it has to be further investigated to which extent alterations in ALK1 signaling and other signaling pathways (e.g. WNT, BMP) are responsible for the cellular changes observed in cells lacking endoglin. Additionally, the functional link between endoglin, CRP2, Zyxin and ZRP-1 needs to be further investigated in order to understand the alterations, which were observed in the organization of the cytoskeleton. Lastly, this study revealed α_2-macroglobulin as another interesting candidate, which might shape the phenotype of endoglin deficient HSC.

In summary: i) endoglin is essential for the transdifferentiation of HSC *in vitro*, ii) transdifferentiation of HSC to MFB *in vitro* is a process that can be at least partially reverted, iii) down-regulation of endoglin interferes with expression of ECM components, and iv) endoglin is involved in the organization of the cytoskeleton. Based on these findings, it is apparent that endoglin plays a pivotal role in transdifferentiation and most likely in hepatic fibrogenesis.

Appendix A

Selected candidate gene list

	Hybridization no. 4			Hybridization no. 2		
Name	Log (Ratio)	Fold Change	P-value	Log (Ratio)	Fold Change	P-value
DV725289	0.69447	4.9	1.07E-08	0.96442	9.2	4.73E-13
Nppc	0.81537	6.5	6.57E-12	0.79672	6.3	0.00004
Edg7	0.48352	3.0	0.00054	0.76781	5.9	0.00012
RGD1306907 predicted	0.65568	4.5	6.85E-09	0.74614	5.6	8.64E-11
Efcbp1	0.35148	2.2	2.00E-01	0.70138	5.0	1.03E-09
Cadps	0.74221	5.5	2.90E-10	0.66915	4.7	8.91E-09
Scn6a	0.58432	3.8	0.00739	0.66287	4.6	0.00298
Chst9 predicted	0.81576	6.5	5.70E-01	0.66052	4.6	1.16E-18
Olr144	0.77432	5.9	0.00004	0.63143	4.3	0.00591
Terc	0.47236	3.0	1.10E-04	0.61150	4.1	7.85E-01
Cxcl2	0.35366	2.3	0.00062	0.57537	3.8	1.52E-07
TC551367	0.51758	3.3	2.69E-06	0.54195	3.5	7.28E-07
Cxxc4	0.42324	2.6	8.82E-04	0.51847	3.3	0.00034
Akr1cl1 predicted	0.53510	3.4	1.15E-06	0.49809	3.1	9.09E-06
Kcnk2	0.45576	2.9	4.17E-04	0.49626	3.1	6.68E-02
AY390379	0.33356	2.2	1.20E-01	0.49443	3.1	9.79E-06
Mmp10	0.36588	2.3	3.30E-02	0.48445	3.1	1.86E-05
Card12 predicted	0.30559	2.0	0.00003	0.47481	3.0	4.17E-05
Omd	0.59851	4.0	4.37E-08	0.47466	3.0	2.99E-05
Ddit4l	0.32350	2.1	0.00001	0.46646	2.9	1.00E-01
TC549300	0.30380	2.0	0.00073	0.44852	2.8	0.00026
Kdr	0.52219	3.3	2.65E-06	0.42203	2.6	6.13E-04
LOC363665	0.55376	3.6	2.67E-12	0.41614	2.6	6.84E-01
Zc3h6 predicted	0.32911	2.1	0.00002	0.40892	2.6	0.00014
Cyp4b1	0.56706	3.7	2.78E-06	0.40744	2.6	1.94E-03
TC565338	0.47773	3.0	8.66E-01	0.40093	2.5	0.00042

CX570337	0.31343	2.1	3.83E-01	0.39302	2.5	3.67E-03
RGD1559861 predicted	0.32761	2.1	1.98E-01	0.39021	2.5	1.16E-02
Tm4sf1 predicted	0.38123	2.4	6.83E-03	0.38770	2.4	4.65E-03
Sncg	0.42609	2.7	6.86E-04	0.38358	2.4	6.41E-03
ENSRNOT00000021746	0.51314	3.3	1.45E-01	0.37854	2.4	1.72E-02
Slc25a27	0.30872	2.0	0.00004	0.36757	2.3	8.95E-02
Chrne	0.39920	2.5	6.80E-03	0.35050	2.2	0.00015
CF106921	121.117	16.3	7.35E-12	0.34768	2.2	7.32E-02
Cpne7 predicted	0.41668	2.6	1.63E-03	0.34536	2.2	6.81E-02
NCAML1	0.38978	2.5	0.00039	0.34301	2.2	0.00505
Kcnj5	0.32143	2.1	8.32E-01	0.33992	2.2	1.85E-01
RGD1310562 predicted	0.67388	4.7	1.19E-03	0.33789	2.2	1.43E-01
Rgn	0.43950	2.8	3.73E-14	0.33511	2.2	0.00748
LOC362068	0.39186	2.5	2.38E-01	0.31925	2.1	0.00002
Itpka	0.35136	2.2	5.91E-02	0.31790	2.1	7.24E-01
LOC309100	0.31020	2.0	7.36E-01	0.31114	2.0	5.12E-01
Gatm	0.31868	2.1	2.81E-01	0.30251	2.0	7.49E-01
Cox8h	0.45565	2.9	9.31E-05	0.30182	2.0	7.42E-01
NM001013165	-0.33079	-2.1	0.00002	-0.30226	-2.0	0.00005
Slc25a1	-0.32859	-2.1	1.58E-01	-0.30377	-2.0	6.73E-01
Mfap5 predicted	-0.34721	-2.2	5.22E-02	-0.30398	-2.0	6.60E-01
Kcnh1	-0.38353	-2.4	6.07E-03	-0.30660	-2.0	0.00002
LOC309816	-0.30956	-2.0	1.32E-04	-0.30961	-2.0	2.95E-05
Foxd4	-0.45426	-2.8	8.11E-14	-0.31043	-2.0	2.65E-05
Icsbp1 predicted	-0.32891	-2.1	3.54E-01	-0.31843	-2.1	3.69E-01
Slc7a7	-0.31290	-2.1	0.00108	-0.32212	-2.1	0.00214
LOC294909	-0.33512	-2.2	5.79E-01	-0.32517	-2.1	0.00001
AY539911	-0.32152	-2.1	2.36E-01	-0.32931	-2.1	1.49E-01
Rgs4	-0.41276	-2.6	4.44E-12	-0.32997	-2.1	1.87E-06
RGD1309319 predicted	-0.36561	-2.3	8.36E-02	-0.33977	-2.2	3.71E-01
Gp38	-0.34889	-2.2	2.01E-01	-0.34384	-2.2	8.87E-01
Me1	-0.30641	-2.0	5.67E-01	-0.35156	-2.2	3.98E-02
LOC302786	-0.34440	-2.2	6.38E-02	-0.36124	-2.3	2.33E-02
Plekhb1	-0.34566	-2.2	0.00004	-0.36148	-2.3	7.42E-01
LOC289672	-0.32445	-2.1	2.40E-01	-0.36545	-2.3	2.18E-02
Hspcb	-0.35765	-2.3	2.70E-03	-0.37442	-2.4	2.53E-09
Ppp1r14c	-0.36634	-2.3	1.45E-08	-0.38386	-2.4	5.61E-10
Lcn7	-0.32200	-2.1	2.29E-01	-0.38450	-2.4	5.65E-03
Kctd15 predicted	-0.41545	-2.6	0.00002	-0.38716	-2.4	1.14E-02
Apln	-0.40953	-2.6	7.76E-12	-0.38752	-2.4	3.10E-10
LOC500109	-0.34314	-2.2	2.42E-01	-0.39377	-2.5	5.70E-03
Garp predicted	-0.47514	-3.0	2.91E-04	-0.40411	-2.5	0.00019
Sfrp1	-0.31092	-2.0	4.37E-01	-0.40602	-2.5	1.58E-03
LOC316465	-0.45923	-2.9	2.24E-04	-0.40833	-2.6	3.13E-03

Gpr43	-0.35553	-2.3	7.83E-02	-0.41090	-2.6	3.65E-03
Arhgdig predicted	-0.47284	-3.0	5.19E-02	-0.41472	-2.6	2.73E-03
Acvrl1	-0.45277	-2.8	1.29E-04	-0.42138	-2.6	6.51E-04
NM001014166	-0.37572	-2.4	2.06E-09	-0.42306	-2.6	1.51E-08
Ltbp2	-0.31644	-2.1	3.17E-01	-0.42449	-2.7	7.53E-05
Hspcb	-0.42491	-2.7	5.23E-04	-0.43195	-2.7	3.45E-04
Cmklr1	-0.32808	-2.1	3.87E-01	-0.43352	-2.7	2.74E-03
LOC299524	-0.38532	-2.4	5.41E-03	-0.43692	-2.7	2.59E-04
S82649	-0.38045	-2.4	7.16E-03	-0.44214	-2.8	1.89E-04
Rgs5	-0.31305	-2.1	3.88E-01	-0.44968	-2.8	1.23E-04
Mfap4	-0.46464	-2.9	5.76E-05	-0.46318	-2.9	6.57E-05
Bves	-0.49166	-3.1	0.00904	-0.46439	-2.9	0.00003
Serpinf1	-0.33688	-2.2	9.52E-02	-0.46725	-2.9	4.46E-05
RGD1307901 predicted	-0.33489	-2.2	1.37E-01	-0.46792	-2.9	7.33E-09
RGD1310242 predicted	-0.41269	-2.6	3.61E-03	-0.47297	-3.0	2.45E-01
LOC691995	-0.30359	-2.0	6.77E-01	-0.48871	-3.1	1.34E-05
LOC291871	-0.43982	-2.8	2.18E-04	-0.49335	-3.1	1.03E-05
Gprc5b predicted	-0.30646	-2.0	0.00053	-0.51119	-3.2	5.10E-02
Nptx2	-0.42928	-2.7	4.08E-04	-0.51175	-3.2	3.73E-06
XM232181	-0.31298	-2.1	0.00584	-0.52019	-3.3	0.00006
Papln predicted	-0.33089	-2.1	1.43E-01	-0.52106	-3.3	2.32E-06
Cspg4	-0.47955	-3.0	2.19E-04	-0.52455	-3.3	1.97E-06
RGD1307396 predicted	-0.30807	-2.0	7.69E-01	-0.58432	-3.8	1.13E-06
Sfmbt2 predicted	-0.62968	-4.3	0.00069	-0.60905	-4.1	0.00695
Tgm2	-0.35177	-2.2	3.93E-02	-0.61434	-4.1	1.90E-08
Prss35 predicted	-0.42866	-2.7	2.68E-13	-0.61883	-4.2	9.47E-01
Jph2	-0.34055	-2.2	1.65E-01	-0.62434	-4.2	1.63E-08
AW143823	-0.37713	-2.4	1.65E-09	-0.64010	-4.4	5.73E-19
LOC687266	-0.46682	-2.9	4.05E-04	-0.64181	-4.4	5.89E-04
M22360	-0.73631	-5.4	3.55E-10	-0.66392	-4.6	8.92E-07
Cthrc1	-0.38436	-2.4	5.67E-03	-0.70974	-5.1	2.79E-10
Postn predicted	-0.44465	-2.8	2.50E-04	-0.74043	-5.5	1.06E-10
Vil predicted	-0.36882	-2.3	3.13E-02	-0.79844	-6.3	1.04E-01
Ptgis	-0.44721	-2.8	1.42E-04	-0.88923	-7.7	7.30E-13
Eng	-0.54588	-3.5	5.92E-07	-0.92163	-8.3	2.34E-13
M84368	-0.67011	-4.7	1.49E-09	-0.94041	-8.7	1.47E-13
Wisp1	-0.62448	-4.2	1.18E-08	-100.677	-10.2	3.06E-14
A2m	-0.75321	-5.7	5.09E-11	-114.377	-13.9	2.08E-15

Table A.1: Selected candidate gene list

This table lists selected genes, which are differentially expressed in both hybridizations (hybridization no. 2 and no. 4). The complete raw data sets were deposited in the Gene Expression Omnibus (GEO) repository under accession numbers GSM256740, GSM256756, GSM256757 and GSM256758.

Appendix B

Vector maps

Vector maps presented in this section are obtained and further modified from either www.Invitrogen.com or from www.Promega.com. Inserts, which were used for the shRNA constructs, are presented below.

Endoglin shRNA 12
5-CACCGCACCCTCAGTTGCAACTTAGCGAACTAAGTTGCAACTGAGGGTGC-3
3-GTGGGAGTCAACGTTGAATCGCTTGATTCAACGTTGACTCCCACGAAAA-5

Endoglin shRNA 34
5-CACCGAAAGTCAGGCCTGTGATGGTGCGAACACCATCACAGGCCTGAC-3
3-CTTTCAGTCCGGACACTACCACGCTTGTGGTAGTGTCCGGACTGAAA-5

Endoglin shRNA 56
5-CACCGAATAGATGTACCAGAGTGCAGCGAACTGCACTCTGGTACATCTA-3
3-CTTATCTACATGGTCTCACGTCGCTTGACGTGAGACCATGTAGATAAAA-5

LacZ shRNA
5-CACCGCTACACAAATCAGCGATTTCGAAAAATCGCTGATTTGTGTAG-3
3-CGATGTGTTTAGTCGCTAAAGCTTTTTAGCGACTAAACACATCAAA-5

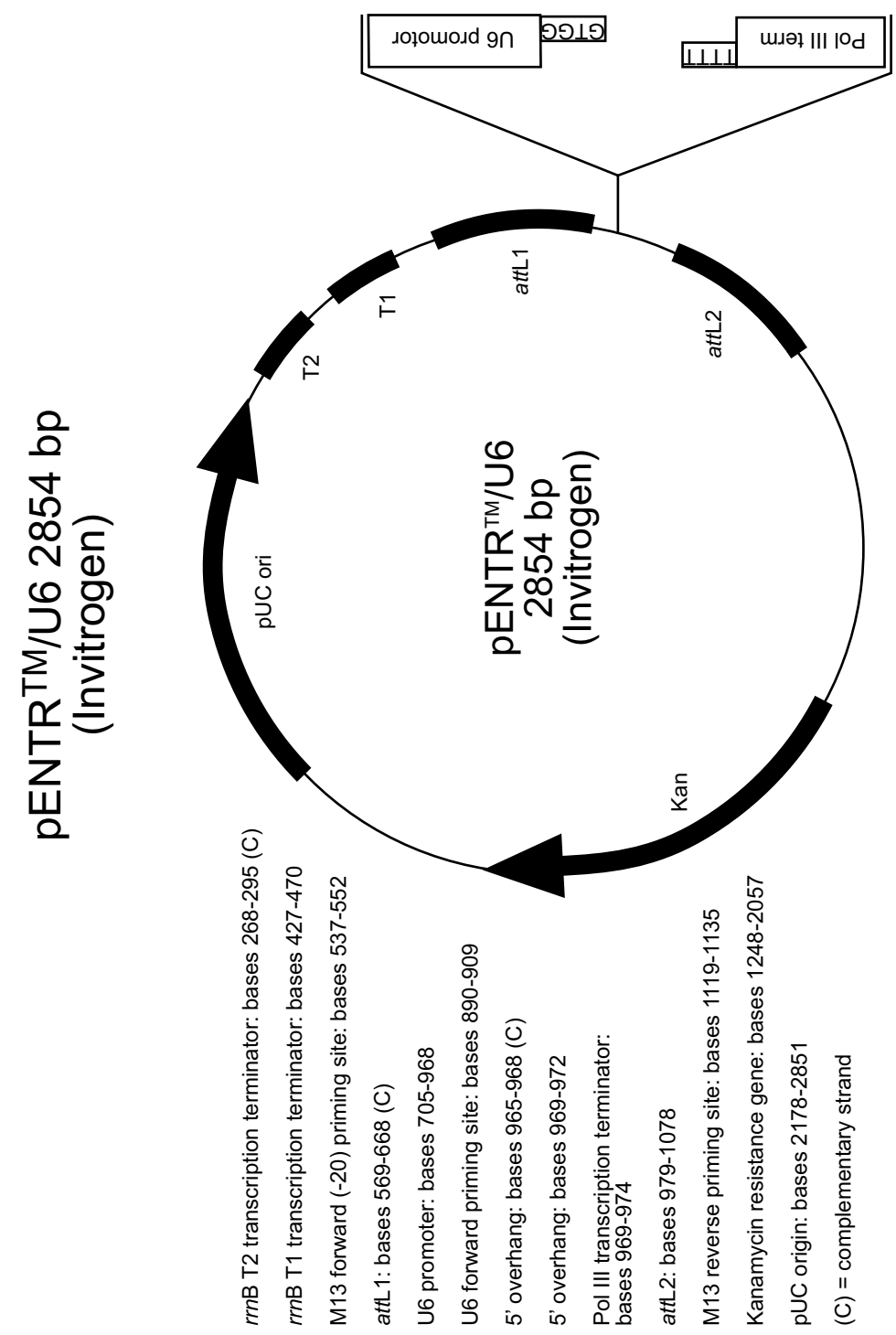


Figure B.1: Empty shuttle vector pENTR/U6

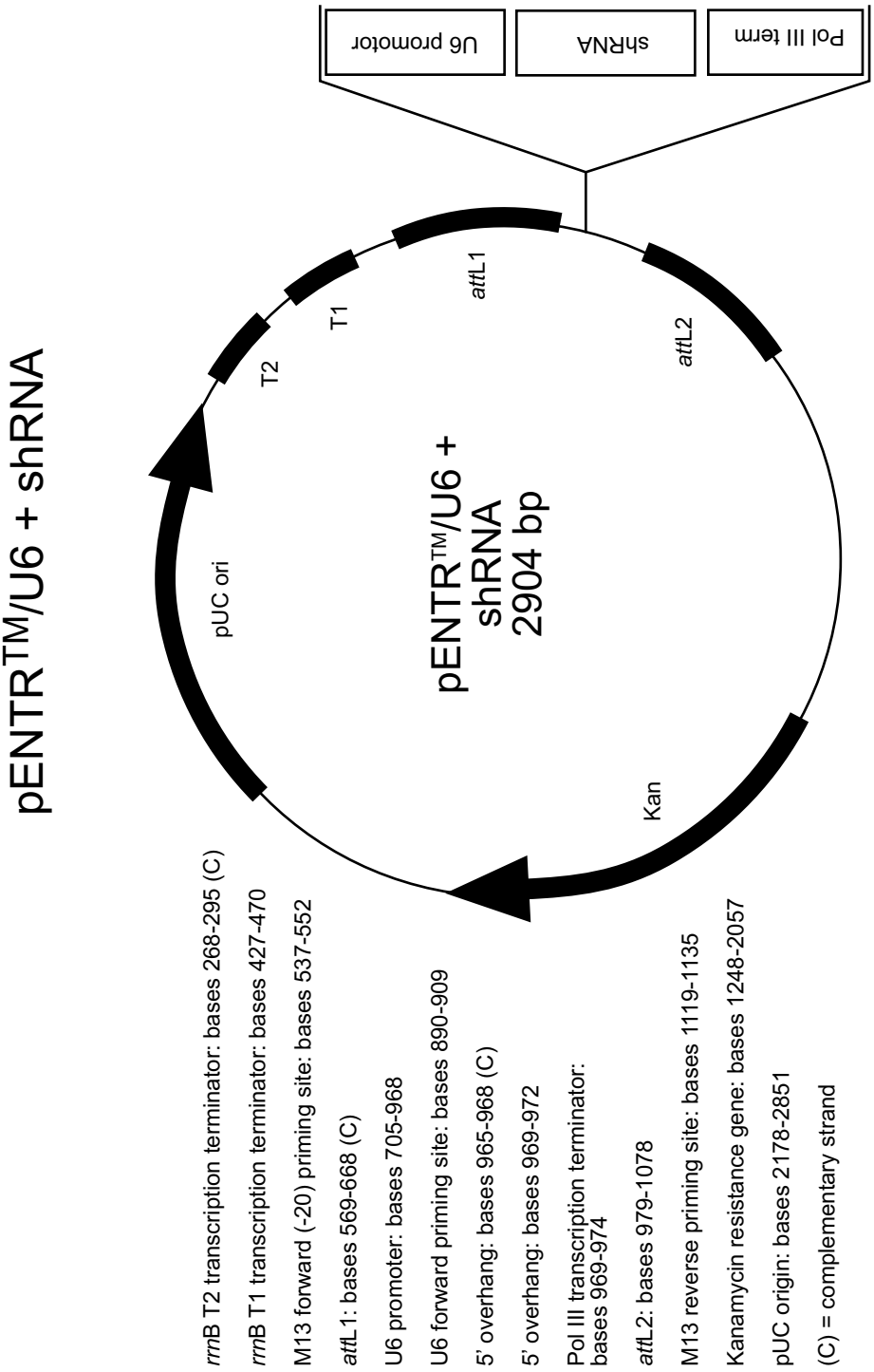


Figure B.2: Empty shuttle vector pENTR/U6 plus shRNA

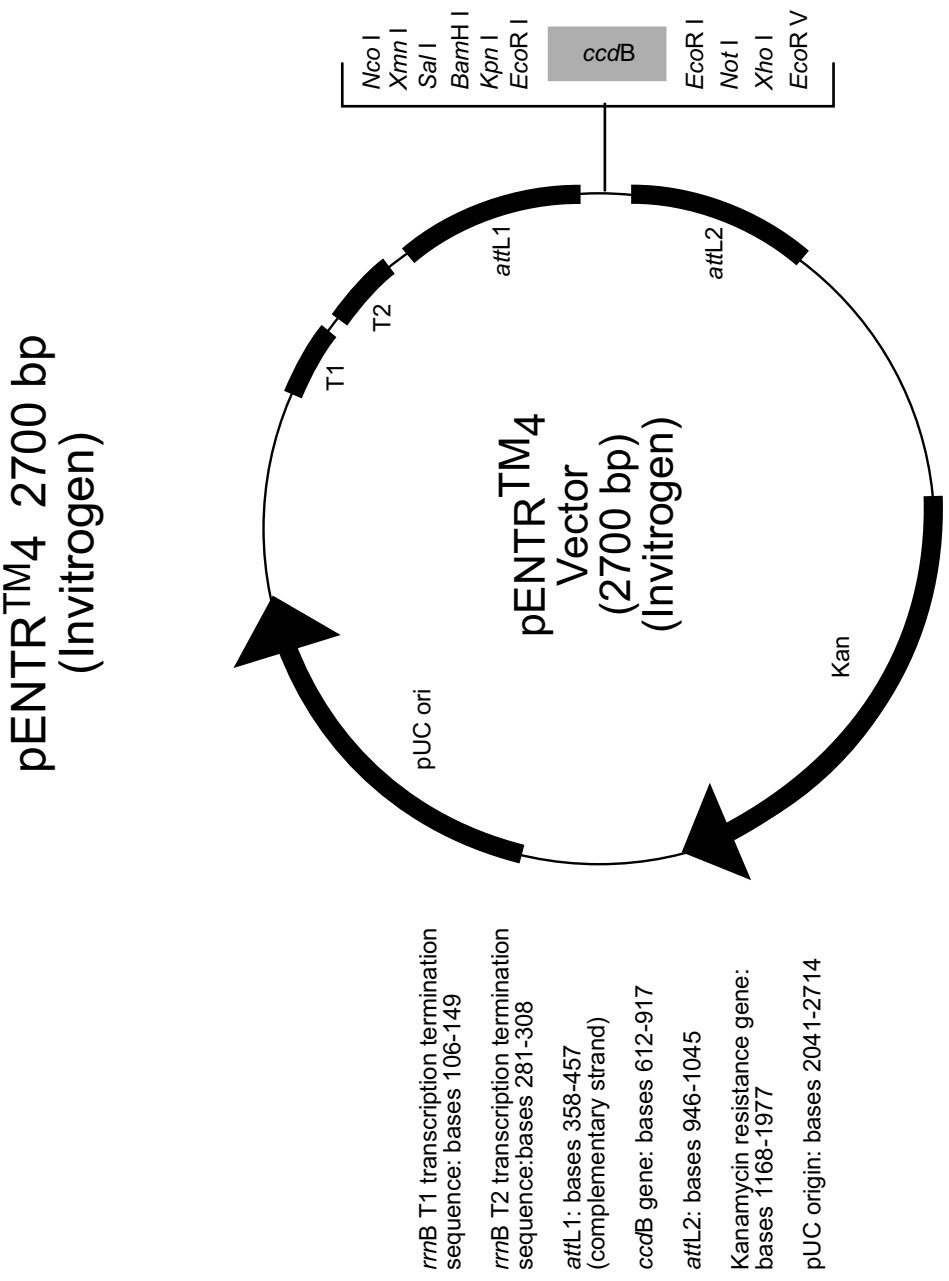


Figure B.3: Empty pENTR4 (Invitrogen)

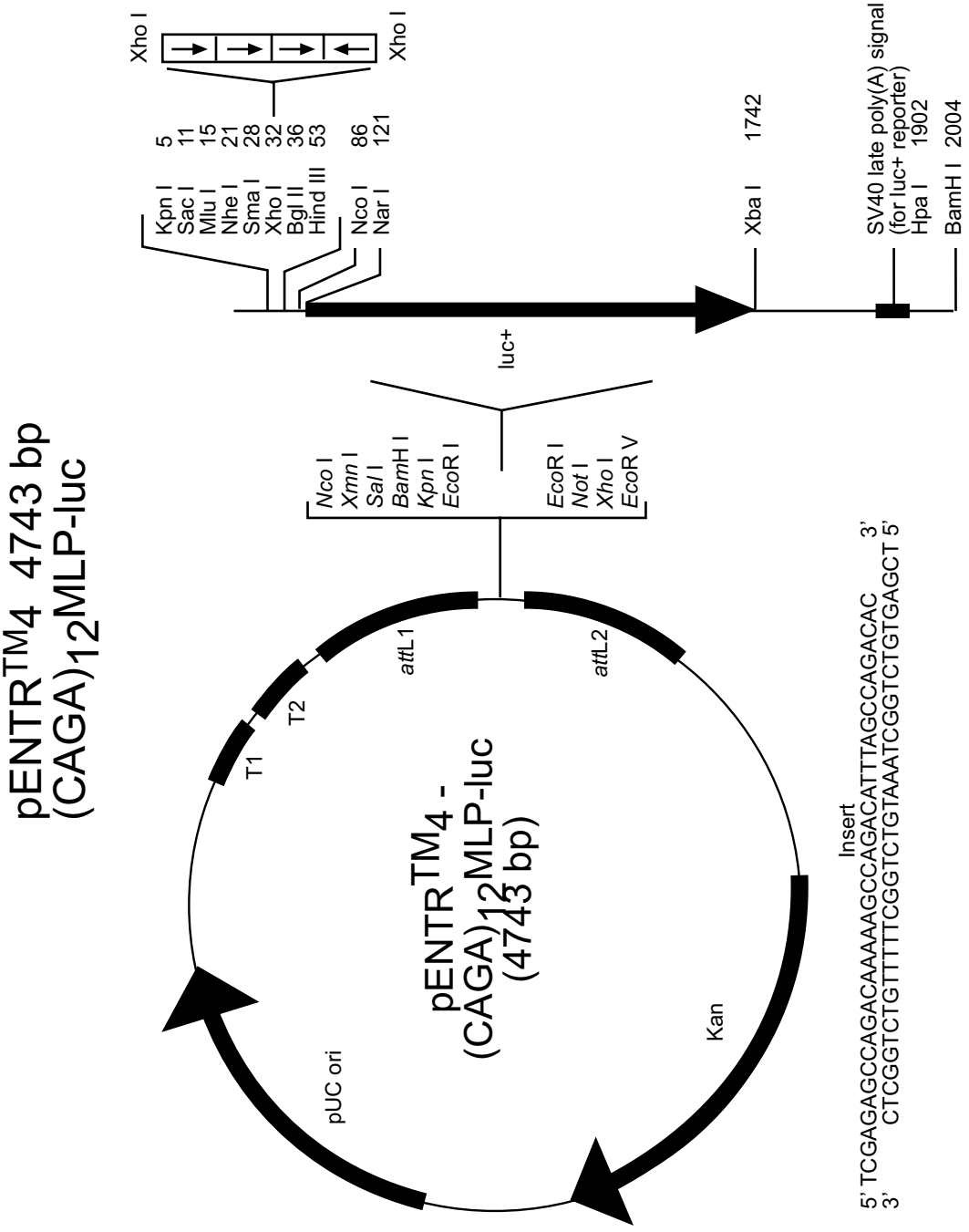


Figure B.4: pENTR4 plus $(CAGA)_{12}$MLP-luciferase

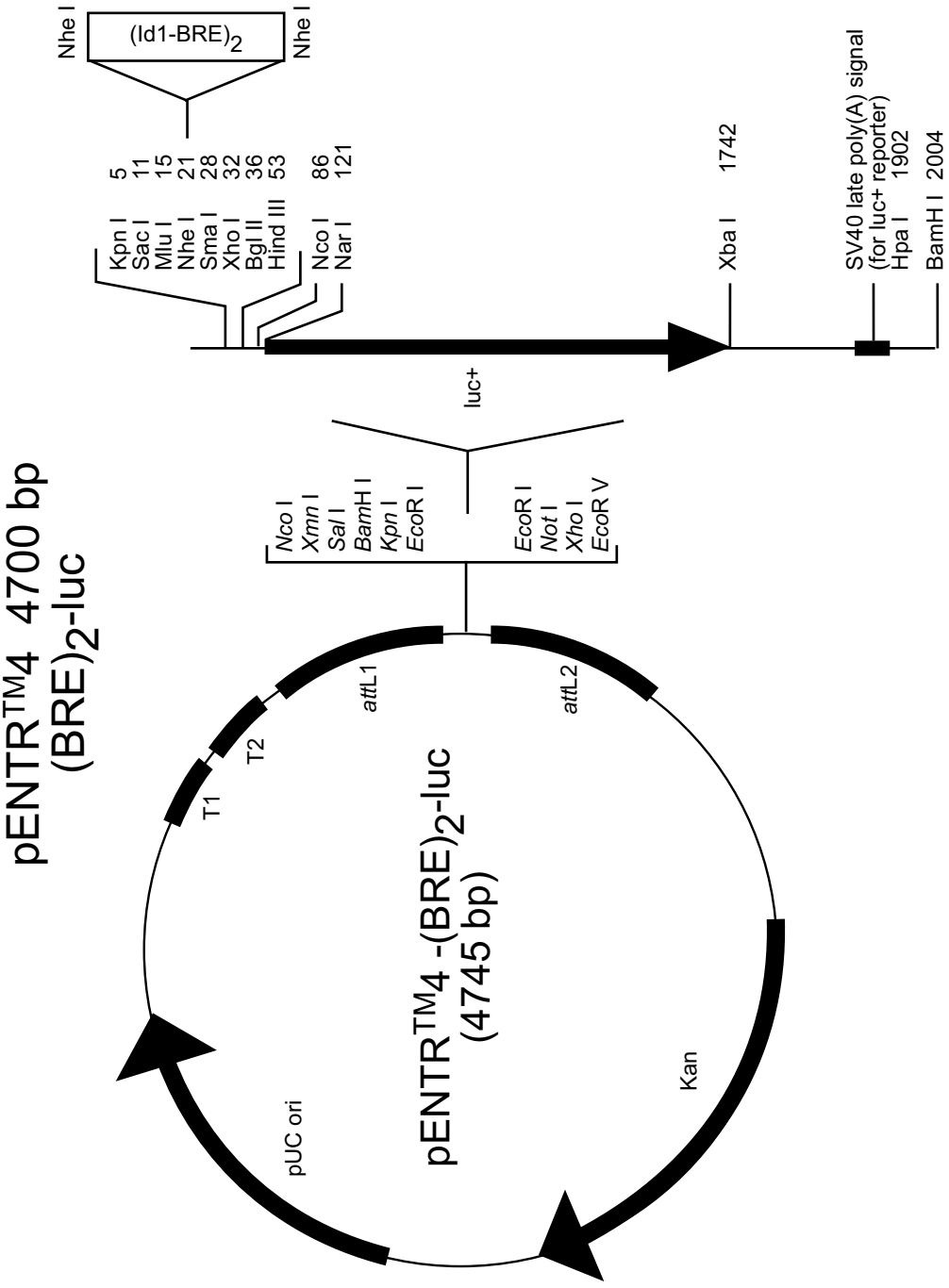


Figure B.5: pENTR4 plus $(BRE)_2$-luciferase

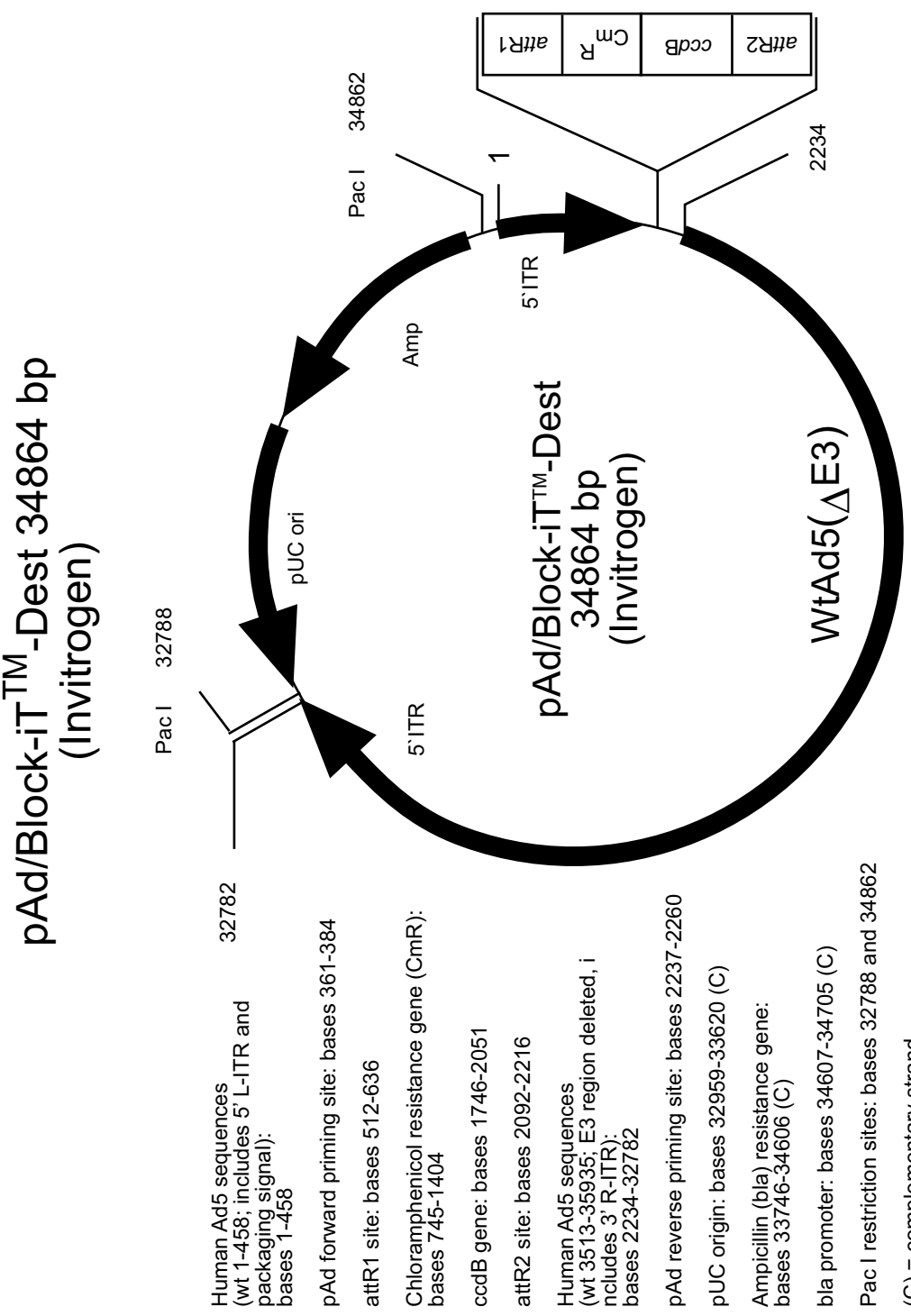


Figure B.6: Empty pAd/Block-*it*^{TM}-Dest 34864 bp Invitrogen

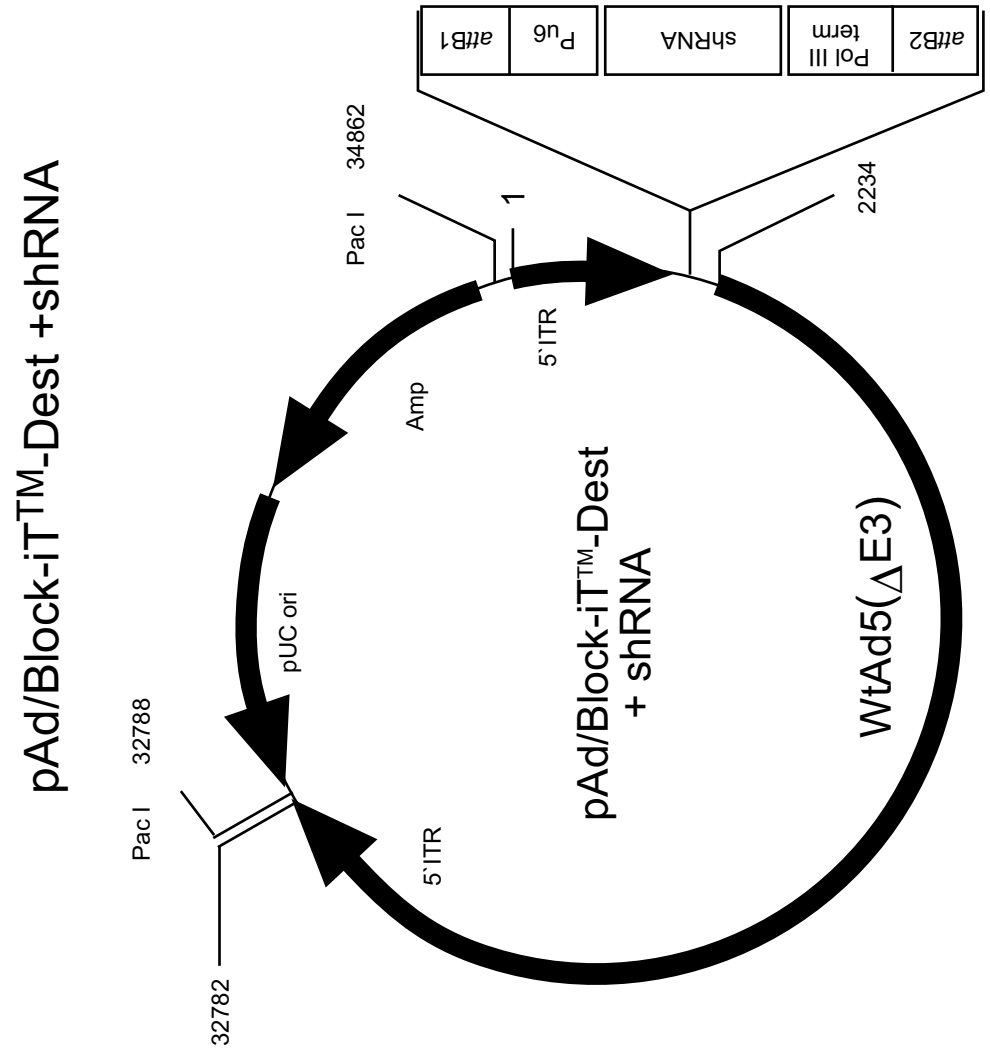


Figure B.7: pAd/Block-*it*^{TM}-Dest plus shRNA

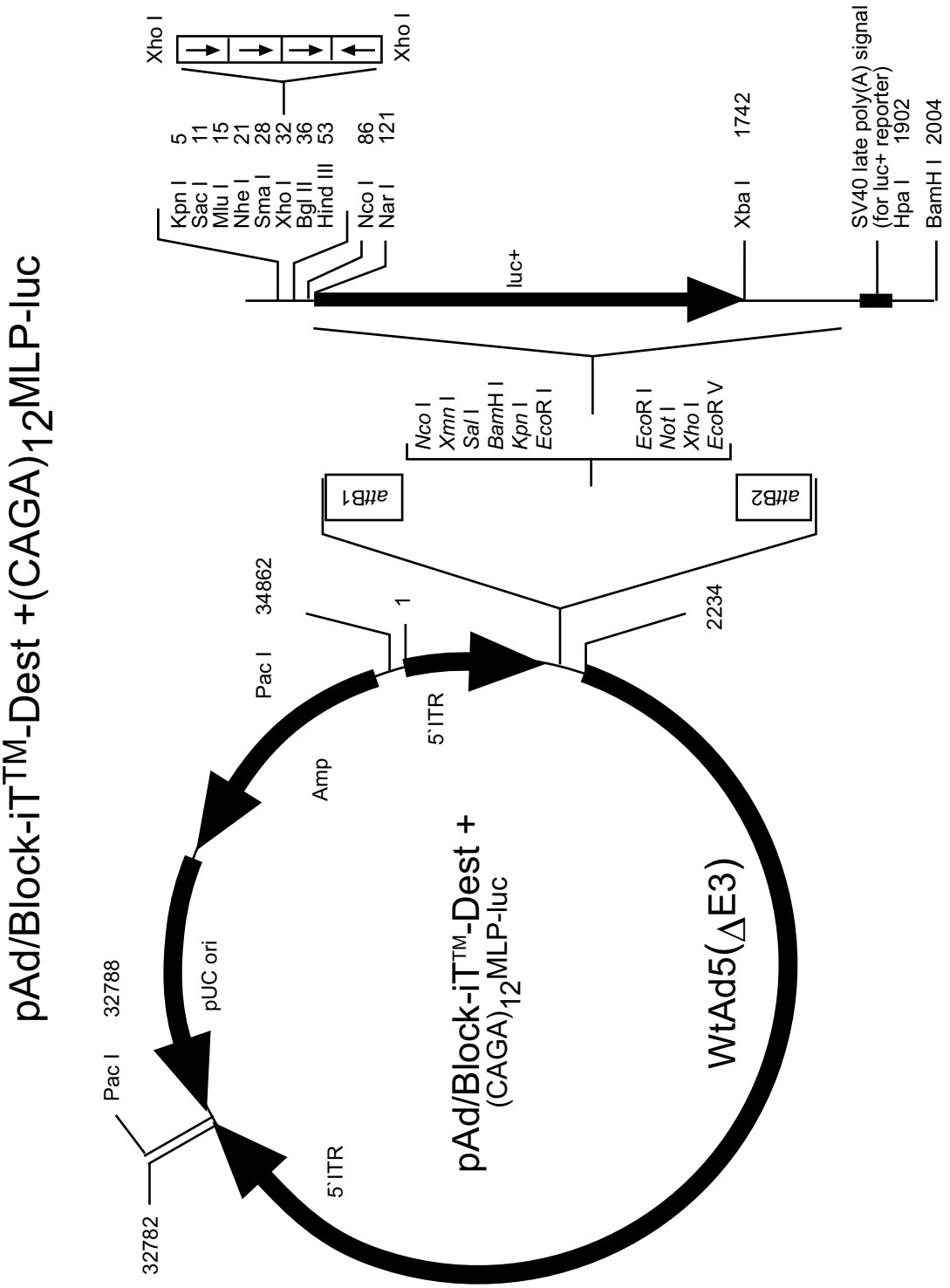


Figure B.8: pAd/Block-*it*^{TM}-Dest plus (CAGA)$_{12}$MLP-luciferase

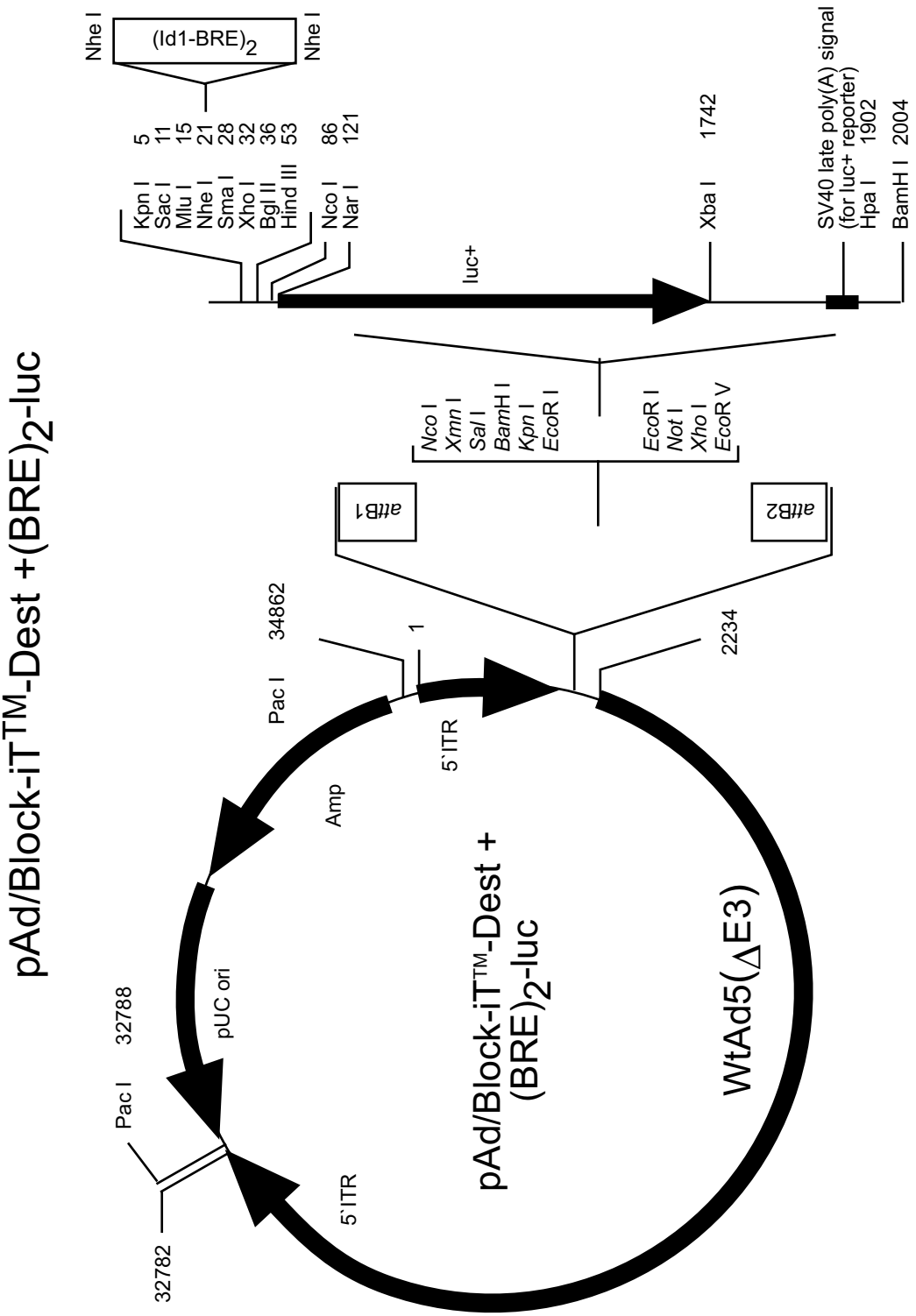


Figure B.9: pAd/Block-it^{TM}-Dest plus $(BRE)_2$-luciferase

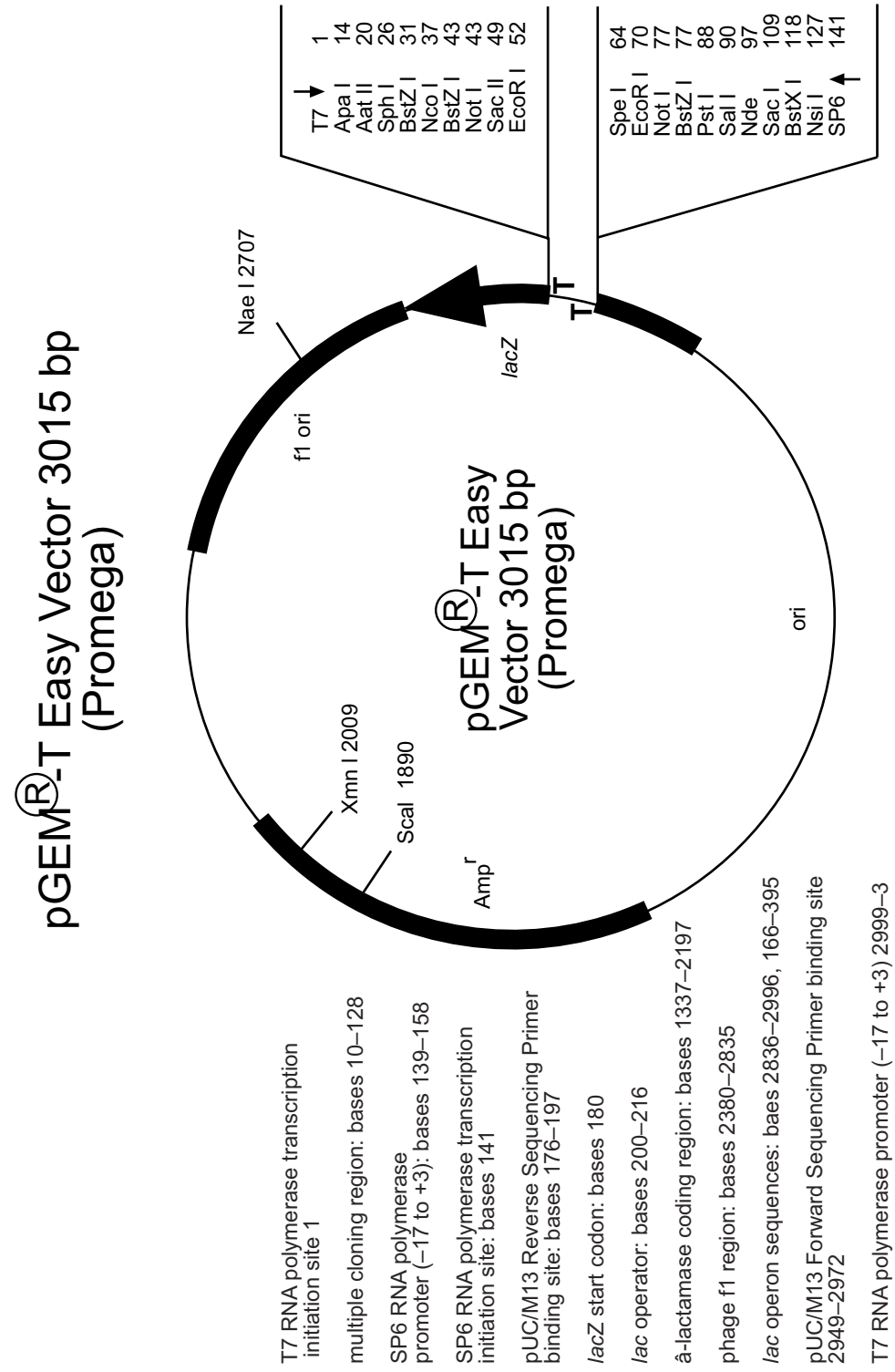


Figure B.10: Empty pGEMT Easy (Promega)

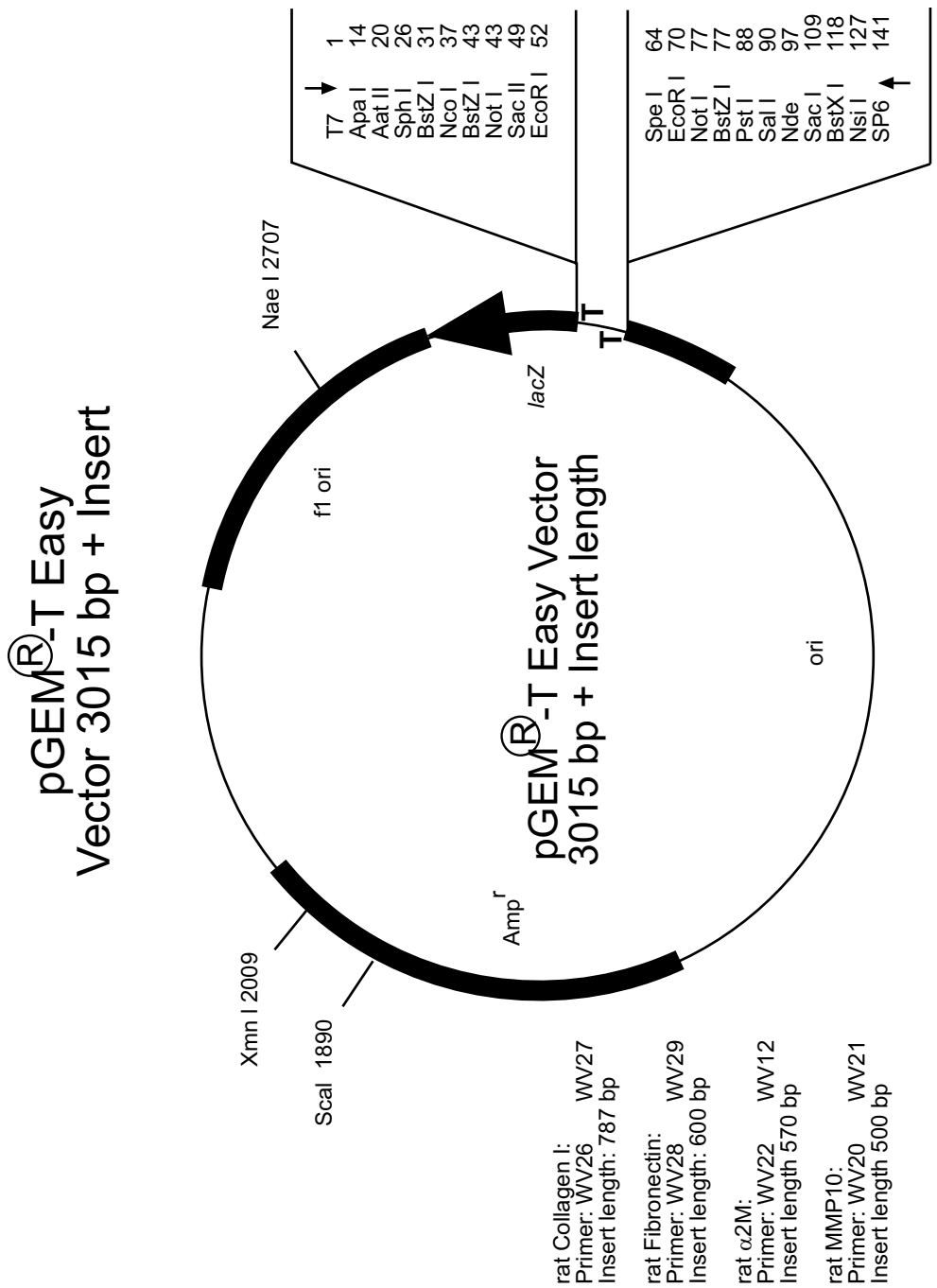


Figure B.11: pGEMT Easy plus insert

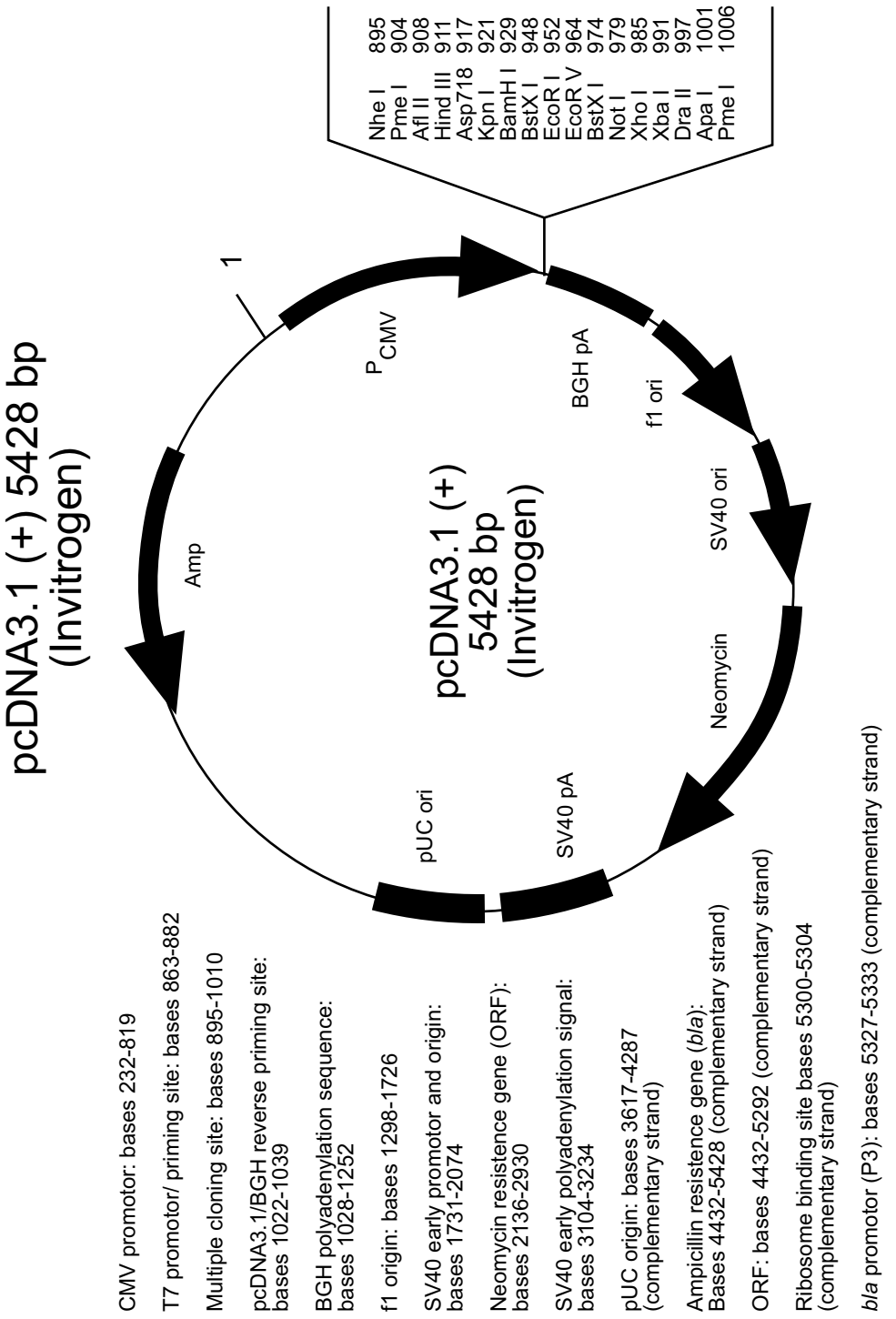


Figure B.12: Empty pcDNA 3.1(+) (Invitrogen)

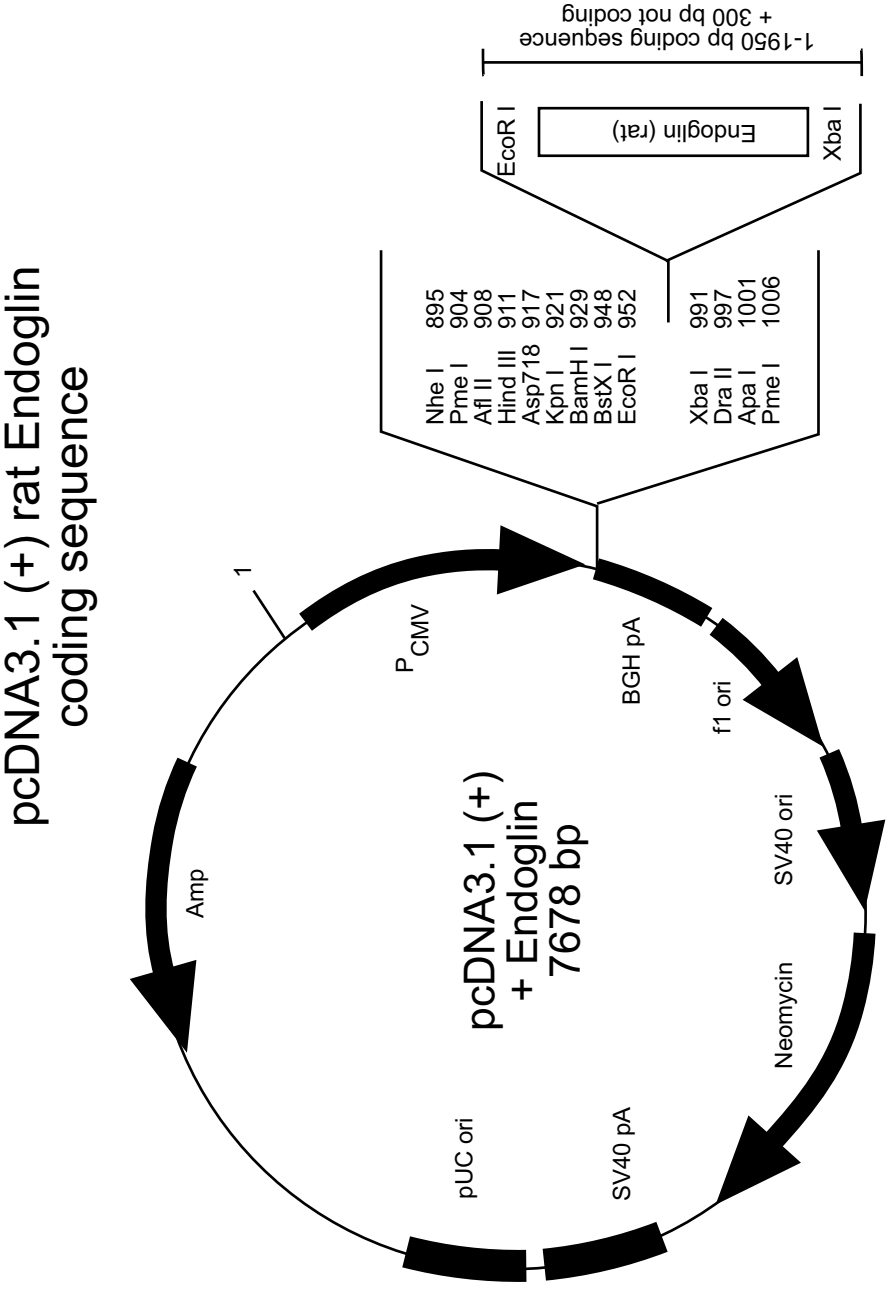


Figure B.13: pcDNA 3.1 (+) plus endoglin

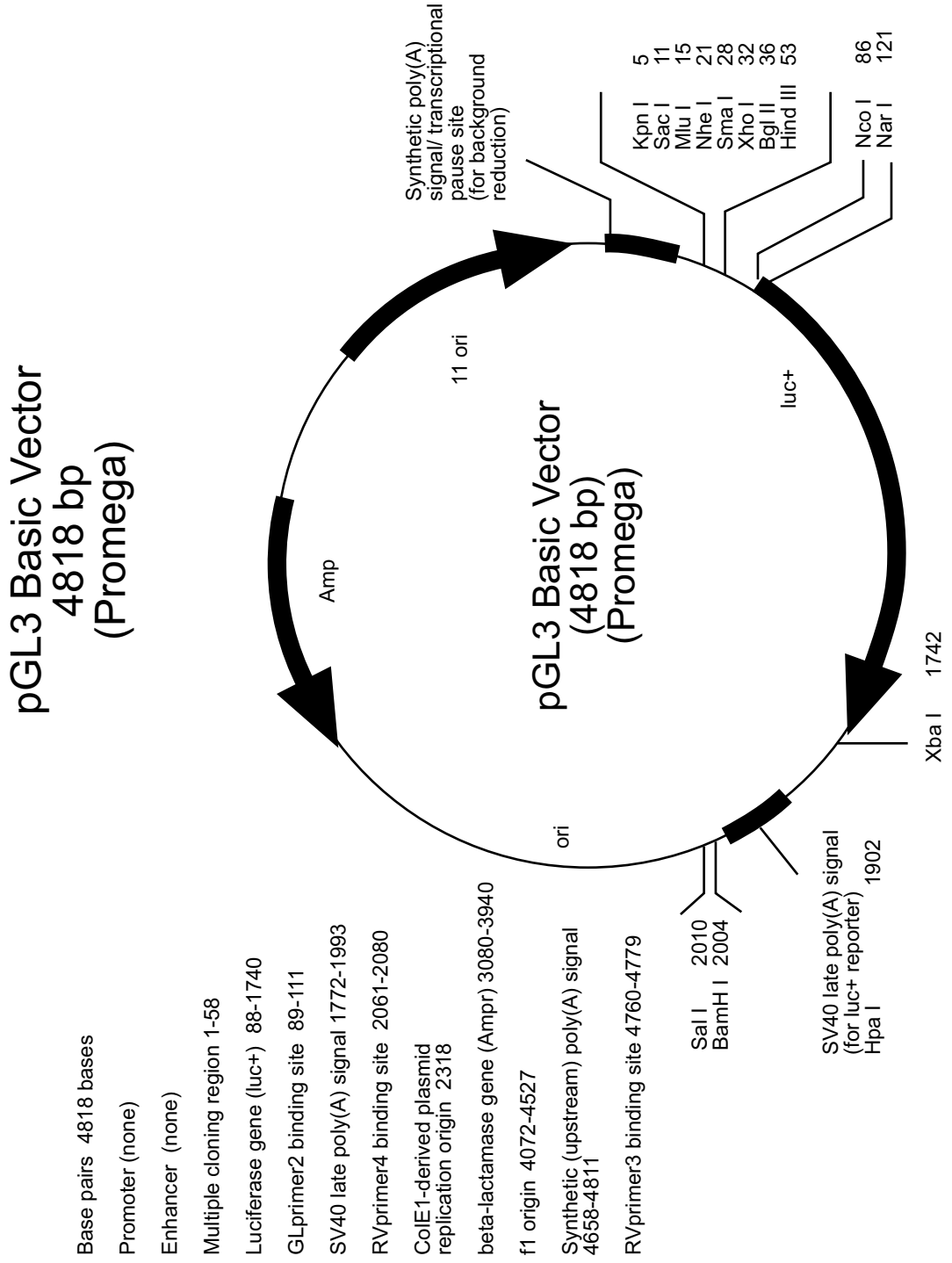


Figure B.14: Empty pGL3 basic vector

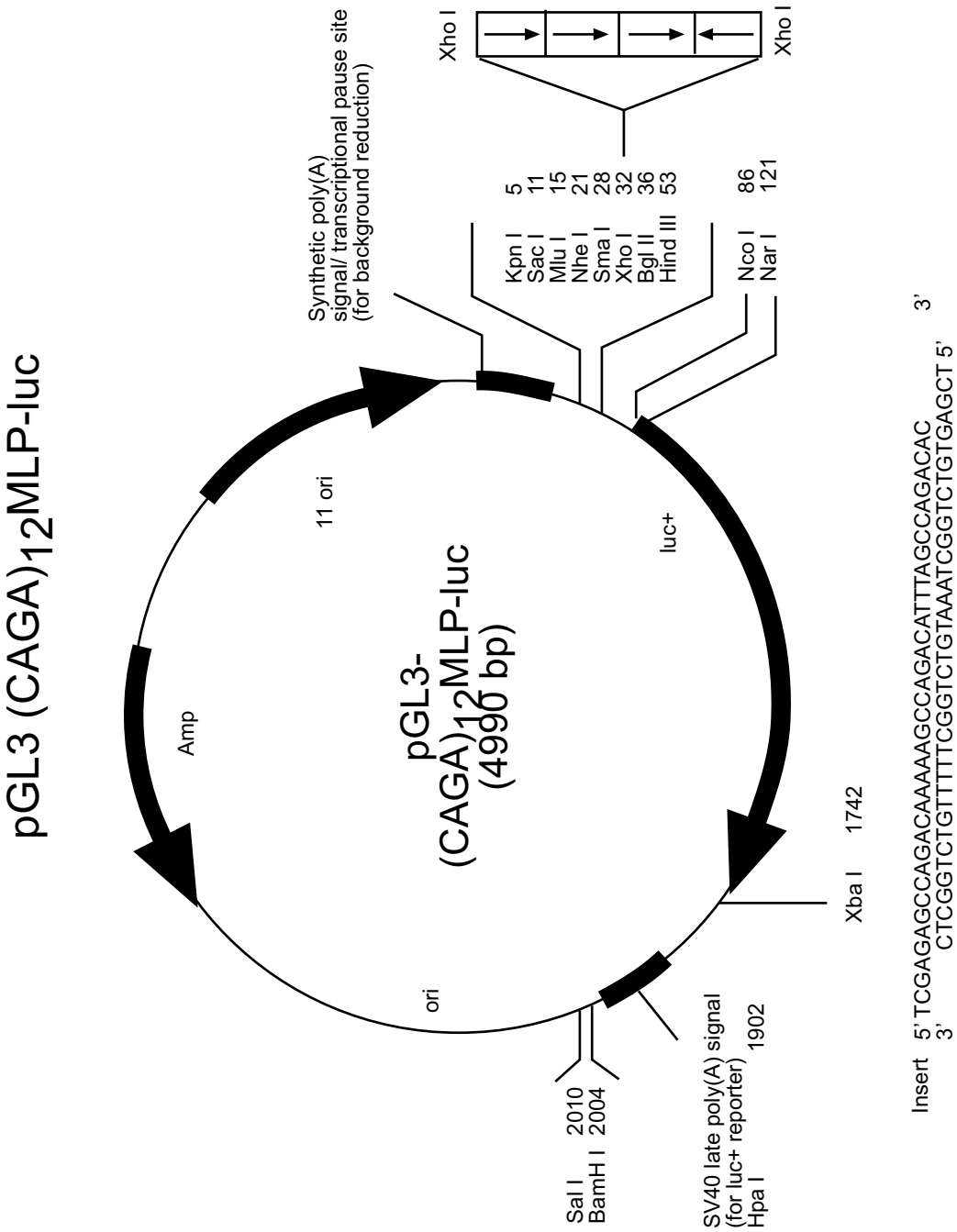


Figure B.15: pGL3 plus $(CAGA)_{12}$MLP-luciferase

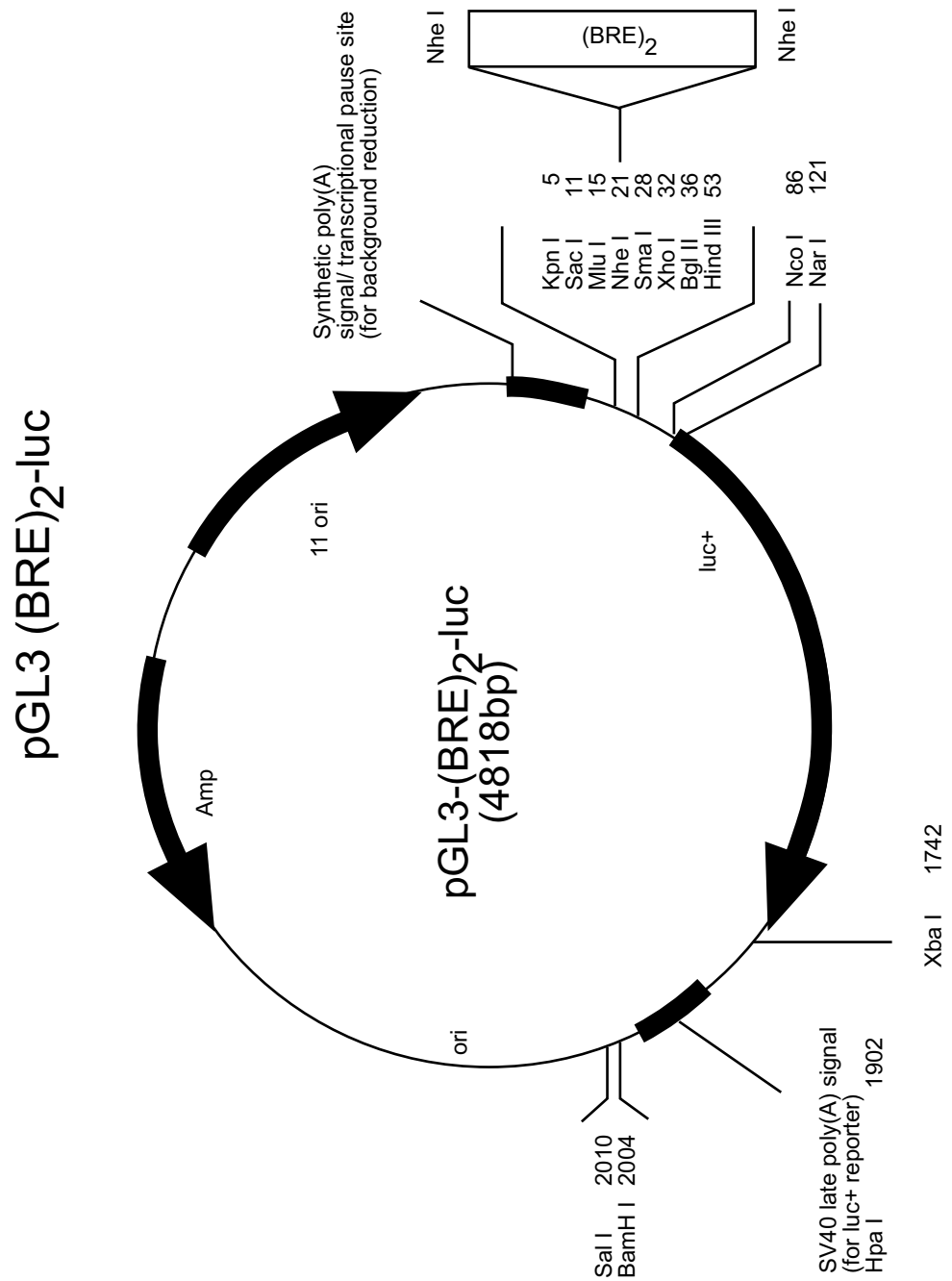


Figure B.16: pGL3 plus $(BRE)_2$-luciferase

Appendix C

Thanks

I would like to say thanks to Prof. Dr. med. Prof. h.c. (RCH) A.M. Gressner for giving me material support.

I would like to say thanks to Prof. Dr. rer. nat. R. Weiskirchen for every fair comment, discussion and warm words when thing(k)s were driving nuts. In the same way I would like to say thanks to Dr. rer. nat. Steffen K. Meurer. Dr. Meurer did support my work from the first until the last minute. He spent plenty of time by thinking about this thesis and by solving problems regarding this thesis. He is one of the most patient persons I ever met and it was a pleasure to work with him, to work for him and to be supervised by him. Thank you!

Furthermore, I would like to thank Senait Wieske -alias Miss Mengsteab- for giving me technical support, but especially for being such a good friend. I would like to say thanks to Mrs. Sibille Sauer-Lehnen for providing a huge amount of high quality HSC, as well as EMP and ATHY, which are the fundament of this thesis. Olaf Scherner, my favorite colleague, for being my external bibliography and for being always with me :) Eddy van de Leur for teaching me how to make an adenovirus, for helpful tips, tricks and nice discussions!

I would like to say thanks to Carmen for all the ATTATTCGGACCATTA..., Carina, Erawan, Falko, Jens, Lucia, Sabine and Ute for making this lab unique! Evgenia, Michael, Willy, Svenja, Swen and Nora for being such a good company and for making work much more E-N-J-O-Y-A-B-L-E! And all the others, who worked in this lab and who contributed to this thesis either way.

Last but not least I would like to say thanks to Özlem, Christian[2], Dennis, Isabelle and all the others who supported my work by being a never ending source of happiness and energy. Finally, I would like to say thanks to my whole family. Without their emotional, financial and professional support I would not be where I am now!

Appendix D

List of abbreviations

aa amino acid

α_2M α_2-macroglobulin

α-SMA α-smooth muscle actin

BMP-7 bone morphogenetic protein-7

bp base pair

BSA bovine serum albumin

°C degree Celsius

Col I collagen type I

Col IV collagen type IV

Da dalton

DNA deoxyribonucleic acid

DNase deoxyribonuclease

dsDNA double-stranded DNA

dsRNA double-stranded RNA

E. coli *Escherichia coli*

Eng endoglin

EtBr ethidium bromide

Fn fibronectin

g gram

g gravitational force

GFP green fluorescent protein

GFAP glial fibrillary acidic protein

h hour/ hours

HHT1 hereditary hemorrhagic telangiectasia type 1

HSC *hepatic stellate cells*

HSP70 heat shock protein 70

IgG immunoglobulin G

l liter

LCPS light counts per second

M mole per liter

min minutes

mM milli moles per liter

μ micro (x10^{-6})

mRNA messenger RNA

n nano (x10^{-9})

nt nucleotide

OD_{600} optical density at 600 nm

p pico (x10^{-12})

PCR polymerase chain reaction

PAGE polyacrylamide gel electrophoresis

Pfu Plaque forming unit

pH -log[H^+]

RNAi RNA interference

rpm revolutions per minute

SDS sodium dodecyl sulfate

shRNA short hairpin RNA

siRNA small interference RNA

ssDNA single stranded DNA

ssRNA single stranded RNA

TGF-β1 transforming growth factor beta 1

U unit of enzyme activity

v volume

V volt

w weight

Appendix E

Bibliography

[1] Dubois, C.M., Blanchette, F., Labrise, M.H., Leduc, R., Grondin, F., Seidah, N.G. Evidence that furin is an authentic transforming growth factor-beta1-converting enzyme. *Am. J. Pathol.*, **158**, 305-316, 2001.

[2] Moren, A., Olofsson, A., Stenman, G., Sahlin, P., Kanzaki, T., Claesson-Welsh, L., ten Dijke, P., Miyazono, K., Heldin, C.H. Identification and characterization of LTBP-2, a novel latent transforming growth factor-beta-binding protein. *J. Biol. Chem.*, **269**, 32469-32478, 1994.

[3] Taipale, J., Saarinen, J., Lohi, J., Saarinen, J., Kovanen, P.T., Keski-Oja, J. Human mast cell chymase and leukocyte elastase release latent transforming growth factor-beta 1 from the extracellular matrix of cultured human epithelial and endothelial cells. *J. Biol. Chem.*, **270**, 4689-4696, 1995.

[4] Taipale, J., Koli, K., Keski-Oja, J. Release of transforming growth factor-beta 1 from the pericellular matrix of cultured fibroblasts and fibrosarcoma cells by plasmin and thrombin. *J. Biol. Chem.*, **267**, 25378-25384, 1992.

[5] Wrana, J.L., Attisano, L., Carcamo, J., Zentella, A., Doody, J., Laiho, M., Wang, X.F., Massague, J. TGF beta signals through a heteromeric protein kinase receptor complex. *Cell*, **71**, 1003-1014, 1992.

[6] Wrana, J.L., Attisano, L., Wieser, R., Ventura, F., Massague, J. Mechanism of activation of the TGF-beta receptor. *Nature*, **370**, 341-347, 1994.

[7] Johnson, D.W., Berg, J.N., Baldwin, M.A., Gallione, C.J., Marondel, I., Yoon, S.J., Stenzel, T.T., Speer, M., Pericak-Vance, M.A., Diamond, A., Guttmacher, A.E., Jackson, C.E., Attisano, L., Kucherlapati, R., Porteous, M.E., Marchuk, D.A. Mutations

in the activin receptor-like kinase 1 gene in hereditary haemorrhagic telangiectasia type 2. *Nat. Genet.*, **13**, 189-195, 1996.

[8] Lux, A. Attisano, L. Marchuk, D.A. Assignment of transforming growth factor beta1 and beta3 and a third new ligand to the type I receptor ALK-1. *J. Biol. Chem.*, **274**, 9984-9992, 1999.

[9] Goumans, M.J., Valdimarsdottir, G., Itoh, S., Lebrin, F., Larsson, J., Mummery, C., Karlsson, S., ten Dijke, P. Activin receptor-like kinase (ALK)1 is an antagonistic mediator of lateral TGFbeta/ALK5 signaling. *Mol. Cell*, **12**, 817-828, 2003.

[10] Goumans, M.J., Valdimarsdottir, G., Itoh, S., Rosendahl, A., Sideras, P., ten Dijke, P. Balancing the activation state of the endothelium via two distinct TGF-beta type I receptors. *EMBO J.*, **21**, 1743-1753, 2002.

[11] Dooley, S., Delvoux, B., Lahme, B., Mangasser-Stephan, K., Gressner, A.M. Modulation of transforming growth factor beta response and signaling during transdifferentiation of rat hepatic stellate cells to myofibroblasts. *Hepatology.*, **31**, 1094-1106, 2000.

[12] Moustakas, A., Souchelnytskyi, S., Heldin, C.H. Smad regulation in TGF-beta signal transduction. *J. Cell Sci.*, **114**, 4359-4369, 2001.

[13] Bertolino, P., Deckers, M., Lebrin, F., ten Dijke, P. Transforming growth factor-beta signal transduction in angiogenesis and vascular disorders. *Chest*, **128**, 585S-590S, 2005.

[14] Parsons, C.J., Takashima, M., Rippe, R.A. Molecular mechanisms of hepatic fibrogenesis. *J. Gastroenterol Hepatol.*, **22**, S79-84, 2007.

[15] Velasco, S., Alvarez-Munoz, P., Pericacho, M., Dijke, P.T., Bernabeu, C., Lopez-Novoa, J.M., Rodriguez-Barbero, A. L- and S-endoglin differentially modulate TGFbeta1 signaling mediated by ALK1 and ALK5 in L_6E_9 myoblasts. *J. Cell Sci.*, **121**, 913-919, 2005.

[16] Tsukazaki, T., Chiang, T.A., Davison, A.F., Attisano, L., Wrana, J.L. SARA, a FYVE domain protein that recruits Smad2 to the TGFbeta receptor. *Cell*, **95**, 779-791, 1998.

[17] Wu, J.W., Fairman, R., Penry, J., Shi, Y. Formation of a stable heterodimer between Smad2 and Smad4. *J. Biol. Chem.*, **276**, 20688-94, 2001.

[18] Kavsak, P., Rasmussen, R.K., Causing, C.G., Bonni, S., Zhu, H., Thomsen, G.H., Wrana, J.L. Smad7 binds to Smurf2 to form an E3 ubiquitin ligase that targets the TGF beta receptor for degradation. *Mol. Cell*, **6**, 1365-1375, 2000.

[19] Hayashi, H., Abdollah, S., Qiu, Y., Cai, J., Xu, Y.Y., Grinnell, B.W., Richardson, M.A., Topper, J.N., Gimbrone, M.A. Jr., Wrana, J.L., Falb, D. The MAD-related protein Smad7 associates with the TGFbeta receptor and functions as an antagonist of TGFbeta signaling. *Cell*, **89**, 1165-1173, 1997.

[20] Scherner, O., Meurer, S.K., Tihaa, L., Gressner, A.M., Weiskirchen, R. Endoglin differentially modulates antagonistic transforming growth factor-beta1 and BMP-7 signaling. *J. Biol. Chem.*, **282**, 13934-13943, 2007.

[21] Miyazono, K., Maeda, S., Imamura, T. BMP receptor signaling: transcriptional targets, regulation of signals, and signaling cross-talk. *Cytokine Growth Factor Rev.*, **16**, 251-263, 2005.

[22] Bruno, E., Horrigan, S.K., Van Den Berg, D., Rozler, E., Fitting, P.R., Moss, S.T., Westbrook, C., Hoffman, R. The Smad5 gene is involved in the intracellular signaling pathways that mediate the inhibitory effects of transforming growth factor-beta on human hematopoiesis. *Blood*, **91**, 1917-1923, 1998.

[23] Lebrin, F., Goumans, M.J., Jonker, L., Carvalho, R.L.C., Valdimarsdottir, G., Thorikay, M., Mummery, C., Arthur, H. M., ten Dijke, P. Endoglin promotes enothelial cell proliferation and TGF-β /ALK1 signal transduction. *EMBO*, **23**, 4018-4028, 2004.

[24] Yue, J., Hartsough, M.T., Frey, R.S., Frielle, T., Mulder, K.M. Cloning and expression of a rat Smad1: regulation by TGFbeta and modulation by the Ras/MEK pathway. *J. Cell Physiol.*, **178**, 387-396, 1999.

[25] Wang, X.F., Lin, H.Y., Ng-Eaton, E., Downward, J., Lodish, H.F., Weinberg, R.A. Expression cloning and characterization of the TGF-beta type III receptor. *Cell*, **67**, 797-805, 1991.

[26] Lopez-Casillas, F., Wrana, J.L., Massague, J. Betaglycan presents ligand to the TGF beta signaling receptor. *Cell*, **73**, 1435-1444, 1993.

[27] Cheifetz, S., Bellon, T., Cales, C., Vera, S., Bernabeu, C., Massague, J., Letarte, M. Endoglin is a component of the transforming growth factor-beta receptor system in human endothelial cells. *J. Biol. Chem.*, **267**, 19027-19030, 1992.

[28] Li, D.Y., Sorensen, L.K., Brooke, B.S., Urness, L.D., Davis, E.C., Taylor, D.G., Boak, B.B., Wendel, D.P. Defective angiogenesis in mice lacking endoglin.. *Science*, **284**, 1534-1537, 1999.

[29] Arthur, H.M., Ure, J., Smith, A.J., Renforth, G., Wilson, D.I., Torsney, E., Charlton, R., Parums, D.V., Jowett, T., Marchuk, D.A., Burn, J., Diamond, A.G. Endoglin, an ancillary TGFbeta receptor, is required for extraembryonic angiogenesis and plays a key role in heart development. *Dev. Biol.*, **217**, 42-53, 2000.

[30] McAllister, K.A., Grogg, K.M., Johnson, D.W., Gallione, C.J., Baldwin, M.A., Jackson, C.E., Helmbold, E.A., Markel, D.S., McKinnon, W.C., Murrell, J., Endoglin, a TGF-beta binding protein of endothelial cells, is the gene for hereditary haemorrhagic telangiectasia type 1. *Nat. Genet.*, **8**, 345-351, 1994.

[31] Abdalla, S.A., Letarte, M., Hereditary haemorrhagic telangiectasia: current views on genetics and mechanisms of disease. *J. Med. Genet.*, **43**, 97-110, 2006.

[32] van den Driesche, S., Mummery, C.L., Westermann, C.J. Hereditary hemorrhagic telangiectasia: an update on transforming growth factor beta signaling in vasculogenesis and angiogenesis. *Cardiovasc Res.*, **58**, 20-31, 2003.

[33] Bellon, T., Corbi, A., Lastres, P., Cales, C., Cebrian, M., Vera, S., Cheifetz, S., Massague, J., Letarte, M., Bernabeu, C. Identification and expression of two forms of the human transforming growth factor-beta-binding protein endoglin with distinct cytoplasmic regions. *Eur J Immunol.*, **23**, 2340-2345, 1993.

[34] Gougos, A., Letarte, M. Primary structure of endoglin, an RGD-containing glycoprotein of human endothelial cells. *J. Biol. Chem.*, **265**, 8361-8364, 1990.

[35] Ge, A.Z., Butcher, E.C. Cloning and expression of a cDNA encoding mouse endoglin, an endothelial cell TGF-beta ligand. *Gene*, **138**, 201-206, 1994.

[36] Meurer, S.K., Tihaa, L., Lahme, B., Gressner, A.M., Weiskirchen, R. Identification of endoglin in rat hepatic stellate cells: new insights into transforming growth factor β receptor signaling. *J. Biol. Chem.*, **280**, 3078-3087, 2005.

[37] Koleva, R.I., Conley, B.A., Romero, D., Riley, K.S., Marto, J.A., Lux, A., Vary, C.P. Endoglin structure and function: Determinants of endoglin phosphorylation by transforming growth factor-beta receptors. *J. Biol. Chem.*, **281**, 25110-25123, 2006.

[38] Guerrero-Esteo, M., Sanchez-Elsner, T., Letamendia, A., Bernabeu, C. Extracellular and cytoplasmic domains of endoglin interact with the transforming growth factor-beta receptors I and II. *J. Biol. Chem.*, **277**, 29197-29209, 2002.

[39] Blanco, F.J., Santibanez, J.F., Guerrero-Esteo, M., Langa, C., Vary, C.P., Bernabeu, C.J. Interaction and functional interplay between endoglin and ALK-1, two components of the endothelial transforming growth factor-beta receptor complex. *J. Cell Physiol.*, **204**, 574-584, 2005.

[40] O'Connell, P.J., McKenzie, A., Fisicaro, N., Rockman, S.P., Pearse, M.J., d'Apice, A.J. Free in PMC Endoglin: a 180-kD endothelial cell and macrophage restricted differentiation molecule. *Clin Exp Immunol.*, **90**, 154-159, 1992.

[41] Gougos, A., Letarte, M. Identification of a human endothelial cell antigen with monoclonal antibody 44G4 produced against a pre-B leukemic cell line. *J. Immunol.*, **141**, 1925-1933, 1988.

[42] Adam, P.J., Clesham, G.J., Weissberg, P.L. Expression of endoglin mRNA and protein in human vascular smooth muscle cells. *Biochem. Biophys. Res. Commun.*, **247**, 33-37, 1998.

[43] Conley, B.A., Smith, J.D., Guerrero-Esteo, M., Bernabeu, C., Vary, C.P. Endoglin, a TGF-beta receptor-associated protein, is expressed by smooth muscle cells in human atherosclerotic plaques. *Atherosclerosis.*, **153**, 323-335, 2000.

[44] Robledo, M.M., Hidalgo, A., Lastres, P., Arroyo, A.G., Bernabeu, C., Sanchez-Madrid, F., Teixido, J. Characterization of TGF-beta 1-binding proteins in human bone marrow stromal cells. *Br. J. Haematol.*, **93**, 507-514, 1996.

[45] Scharpfenecker, M., van Dinther, M., Liu, Z., van Bezooijen, R.L., Zhao, Q., Pukac, L., Löwik, C.W., ten Dijke, P.J. BMP-9 signals via ALK1 and inhibits bFGF-induced endothelial cell proliferation and VEGF-stimulated angiogenesis. *Cell Sci.*, **120**, 964-972, 2007.

[46] Barbara, N.P., Wrana, J.L., Letarte, M. Endoglin is an accessory protein that interacts with the signaling receptor complex of multiple members of the transforming growth factor-beta superfamily. *J. Biol. Chem.*, **274**, 584-594, 1999.

[47] Jerkic, M., Rodriguez-Barbero, A., Prieto, M., Toporsian, M., Pericacho, M., Rivas-Elena, J.V., Obreo, J., Wang, A., Perez-Barriocanal, F., Arevalo, M., Bernabeu, C.,

Letarte, M., Lopez-Novoa, J.M. Reduced angiogenic responses in adult Endoglin heterozygous mice. *Cardiovasc. Res.*, **69**, 845-854, 2006.

[48] Guo, B., Slevin, M., Li, C., Parameshwar, S., Liu, D., Kumar, P., Bernabeu, C., Kumar, S. CD105 inhibits transforming growth factor-β Smad3 signaling. *Anticancer Res.*, **24**, 1337-1346, 2004.

[49] Guerrero-Esteo, M., Lastres, P., Letamendia, A., Perez-Alvarez, M.J., Langa, C., Lopez, L.A., Fabra, A., Garcia-Pardo, A., Vera, S., Letarte, M., Bernabeu, C. Endoglin overexpression modulates cellular morphology, migration, and adhesion of mouse fibroblasts. *Eur. J. Cell Biol.*, **78**, 614-623, 1999.

[50] Liu, Y., Jovanovic, B., Pins, M., Lee, C., Bergan, R.C. Overexpression of endoglin in human prostate cancer suppresses cell detachment, migration and invasion. *Oncogene*, **21**, 8272-8281, 2002.

[51] Conley, B.A., Koleva, R., Smith, J.D., Kacer, D., Zhang, D., Bernabeu, C., Vary, C.P. Endoglin controls cell migration and composition of focal adhesions: function of the cytosolic domain. *J. Biol. Chem.*, **279**, 27440-27449, 2004.

[52] Sanz-Rodriguez, F., Guerrero-Esteo, M., Botella, L.M., Banville, D., Vary, C.P., Bernabeu. C. Endoglin regulates cytoskeletal organization through binding to ZRP-1, a member of the Lim family of proteins. *J. Biol. Chem.*, **279**, 32858-32868, 2004.

[53] Yamashita, H., Ichijo, H., Grimsby, S., Moren, A., ten Dijke, P., Miyazono, K. Endoglin forms a heteromeric complex with the signaling receptors for transforming growth factor-beta. *J Biol Chem.*, **269**, 1995-2001, 1994.

[54] Wong, S.H., Hamel, L., Chevalier, S., Philip, A. Endoglin expression on human microvascular endothelial cells association with betaglycan and formation of higher order complexes with TGF-beta signaling receptors. *Eur. J. Biochem.*, **267**, 5550-5560, 2000.

[55] Parker, W.L., Goldring, M.B., Philip, A. Endoglin is expressed on human chondrocytes and forms a heteromeric complex with betaglycan in a ligand and type II TGFbeta receptor independent manner. *J. Bone Miner Res.*, **18**, 289-302, 2003.

[56] Santibanez, J.F., Blanco, F.J., Garrido-Martin, E.M., Sanz-Rodriguez, F., Del Pozo, M.A., Bernabeu, C. Caveolin-1 interacts and cooperates with the transforming growth factor-β type I receptor ALK1 in endothelial caveolae. *Cardiovasc Res.*, **77**, 791-799, 2008.

[57] Letamendia, A., Lastres, P., Botella, L.M., Raab, U., Langa, C., Velasco, B., Attisano, L., Bernabeu, C. Role of endoglin in cellular responses to transforming growth factor-beta. A comparative study with betaglycan. *J. Biol. Chem.*, **273**, 33011-33019, 1998.

[58] Rodriguez-Barbero, A., Obreo, J., Alvarez-Munoz, P., Pandiella, A., Bernabeu, C., Lopez-Novoa, J.M. Abstract Endoglin modulation of TGF-beta1-induced collagen synthesis is dependent on ERK1/2 MAPK activation. *Cell Physiol Biochem.*, **18**, 135-142, 2006.

[59] Lee, N. Y., Blobe, G. C. The interaction of endoglin with beta-arrestin2 regulates transforming growth factor-beta-mediated ERK activation and migration in endothelial cells. *J. Biol. Chem.*, **282**, 21507-21517, 2007.

[60] Chen, X., A microRNA as a translational repressor of APETALA2 in Arabidopsis flower development. *Science*, **303**, 2022-2025, 2004.

[61] Perez-Gomez, E., Villa-Morales, M., Santos, J., Fernandez-Piqueras, J., Gamallo, C., Dotor, J., Bernabeu, C., Quintanilla, M. A role for endoglin as a suppressor of malignancy during mouse skin carcinogenesis. *Cancer Res.*, **67**, 10268-10277, 2007.

[62] Nikiteas, N.I., Tzanakis, N., Theodoropoulos, G., Atsaves, V., Christoni, Z., Karakitsos, P., Lazaris, A.C., Papachristodoulou, A., Klonaris, C., Gazouli, M. Vascular endothelial growth factor and endoglin (CD-105) in gastric cancer. *Gastric Cancer.*, **10**, 12-17, 2007.

[63] El-Gohary, Y.M., Silverman, J.F., Olson, P.R., Liu, Y.L., Cohen, K., Miller, R., Saad, R.S. Endoglin (CD105) and vascular endothelial growth factor as prognostic markers in prostatic adenocarcinoma. *Am. J. Clin. Pathol.*, **127**, 572-579, 2007.

[64] Perez-Gomez, E., Eleno, N., Lopez-Novoa, J.M., Ramirez, J.R., Velasco, B., Letarte, M., Bernabeu, C., Quintanilla, M. Characterization of murine S-endoglin isoform and its effects on tumor development. *Oncogene.*, **24**, 4450-4461, 2005.

[65] Lastres, P., Martin-Perez, J., Langa, C., Bernabeu, C. Phosphorylation of the human-transforming-growth-factor-beta-binding protein endoglin. *Biochem. J.*, **301**, 765-768, 1994.

[66] Robinson, C.J., Johnson, D.D. Soluble endoglin as a second-trimester marker for preeclampsia. *Am. J. Obstet Gynecol.*, **197**, 174-175, 2007.

[67] Löffler, G., Petrides, P.E., Biochemie und Pathobiochemie. *Springer*, **6**, 1025-1029, 1998.

[68] Löffler, G., Petrides, P.E., Biochemie und Pathobiochemie. *Springer*, **6**, 1024-1024, 1998.

[69] Löffler, G., Petrides, P.E., Biochemie und Pathobiochemie. *Springer*, **6**, 1035-1036, 1998.

[70] Benyon, R.C., Iredale, J.P. Is liver fibrosis reversible? *Gut*, **46**, 443-446, 2000.

[71] Bataller, R., Brenner, D.A. Liver fibrosis. *J. Clin. Invest.*, **115**, 209-218, 2005.

[72] Popper, H., Uenfriend, S. Hepatic fibrosis. Correlation of biochemical and morphologic investigations. *Am. J. Med.*, **49**, 707-721, 1970.

[73] Anthony, P.P., Ishak, K.G., Nayak, N.C., Poulsen, H.E., Scheuer, P.J., Sobin, L.H. The morphology of cirrhosis. Recommendations on definition, nomenclature, classification by a working group sponsored by the World Health Organization. *J Clin Pathol.*, **31**, 395-414, 1978.

[74] Arthur, M.J. Reversibility of liver fibrosis and cirrhosis following treatment of hepatitis C. *Gastroenterology*, **122**, 1525-1528, 2002.

[75] Friedman, S.L. Molecular regulation of hepatic fibrosis, an integrated cellular response to tissue injury. *J. Biol. Chem.*, **275**, 2247-2250, 2000.

[76] Gabele, E., Brenner, D.A., Rippe, R.A. Liver fibrosis: signals leading to the amplification of the fibrogenic hepatic stellate cell. *Front Biosci.*, **8**, 69-77, 2003.

[77] Milani, S., Herbst, H., Schuppan, D., Kim, K.Y., Riecken, E.O., Stein, H. Procollagen expression by nonparenchymal rat liver cells in experimental bilary fibrosis. *Gastroenterology*, **98**, 175-184, 1990.

[78] Marra, F. Hepatic stellate cells and the regulation of liver inflammation. *J. Hepatol.*, **31**, 1120-1130, 1999.

[79] Arthur, M.J. Fibrogenesis II. Metalloproteinases and their inhibitors in liver fibrosis. *Am. J. Physiol. Gastrointest Liver Physiol.*, **279**, G245-249, 2000.

[80] Iredale JP, Murphy G, Hembry RM, Friedman SL, Arthur MJ. Human hepatic lipocytes synthesize tissue inhibitor of metalloproteinases-1. Implications for regulation of matrix degradation in liver. *J. Clin. Invest.* , **90**, 282-287, 1992.

[81] Canbay, A., Friedman, S., Gores, G.J. Apoptosis: the nexus of liver injury and fibrosis. *Hepatology*, **39**, 273-278, 2004.

[82] Maher, J.J. Interactions between hepatic stellate cells and the immune system. *Semin. Liver Dis.*, **21**, 417-426, 2001.

[83] Pinzani, M. Liver fibrosis. *Spinger Semin Immunuopathol.*, **21**, 475-490, 1999.

[84] Olaso, E., Friedman, S.L., Molecular regulation of hepatic fibrogenesis. *J. Hepatol.*, **29**, 836-847, 1998.

[85] Friedman, S.L., Hepatic stellate cells: protean multifunctional, and enigmatic cells of the liver. *Physiol. Rev.*, **88**, 125-172, 2008.

[86] Uyama, N., Zhao, L., Van Rossen, E., Hirako, Y., Reynaert, H., Adams, D.H., Xue, Z., Robson, R., Pekny, M., Geerts, A., Hepatic stellate cells express synemin, a protein bridging intermediate filaments to focal adhesion *Gut*, **55**, 1276-1289, 2006.

[87] Friedman, S.L. Liver fibrosis – from bench to bedside. *J. Hepatol.*, **38**, S38-53, 2003.

[88] Rockey, D. The cellular pathogenisis of portal hypertension: stellate cell contractility, endothelin and nitric oxide. *Hepatology*, **25**, 2-5, 1997.

[89] Rockey, D.C. Hepatic blood flow regulation by stellate cells in normal and injured liver. *Semin. Liver Dis.*, **21**, 337-349, 2001.

[90] Fire, A., Xu, S., Montgomery, M.K., Kostas, S.A., Driver, S.E., Mello, C.C., Potent and specific genetic interference by double-stranded RNA in Caenorhabditis elegans. *Nature*, **391**, 806-811, 1998.

[91] Plasterk, R.H. RNA silencing: the genomes immune system *Science*, **296**, 1263-1265, 2002.

[92] Bartel, D.P. MicroRNAs: genomics, biogenesis, mechanism, and function. *Cell*, **116**, 281-297, 2004.

[93] C.M. Croce and G.A. Calin, miRNAs, cancer, and stem cell division. *Cell*, **122**, 6-7, 2005.

[94] Martinez, J., Patkaniowska, A., Urlaub, H., Lührmann, R., Tuschl, T. Single-stranded antisense siRNAs guide target RNA cleavage in RNAi. *Cell*, **110**, 563-574, 2002.

[95] Bernstein, E., Caudy, A.A., Hammond, S.M., Hannon, G.J., Role for a bidentate ribonuclease in the initiation step of RNA interference. *Nature*, **409**, 363-366, 2001.

[96] Elbashir, S.M., Martinez, J., Patkaniowska, A., Lendeckel, W., Tuschl, T. Functional anatomy of siRNAs for mediating efficient RNAi in Drosophila melanogaster embryo lysate. *EMBO J.*, **20**, 6877-6888, 2001.

[97] Nykänen, A., Haley, B., Zamore, P.D. ATP requirements and small interfering RNA structure in the RNA interference pathway. *Cell*, **107**, 309-321, 2001.

[98] Parker, J.S., Barford, D. Argonaute: A scaffold for the function of short regulatory RNAs. *Trends Biochem. Sci.*, **31**, 622-630, 2006.

[99] Hammond, S.M., Bernstein, E., Beach, D., Hannon, G.J. An RNA-directed nuclease mediates post-transcriptional gene silencing in Drosophila cells. *Nature*, **404**, 293-296, 2000.

[100] Zamore, P.D., Tuschl, T., Sharp, P.A., Bartel, D.P. RNAi: double-stranded RNA directs the ATP-dependent cleavage of mRNA at 21 to 23 nucleotide intervals. *Cell*, **101**, 25-33, 2000.

[101] Aukerman, M.J., Sakai, H. Regulation of flowering time and floral organ identity by a MicroRNA and its APETALA2-like target genes. *Plant Cell*, **16**, 555, 2004.

[102] Chen, K., Mehta, J.L., Li, D., Joseph, L., Joseph, J. Transforming growth factor beta receptor endoglin is expressed in cardiac fibroblasts and modulates profibrogenic actions of angiotensin II. *Circ. Res.*, **95**, 1167-1173, 2004.

[103] Judge, A.D., Sood, V., Shaw, J.R., Fang, D., McClintock, K., MacLachlan, I. Sequence-dependent stimulation of the mammalian innate immune response by synthetic siRNA. *Nat. Biotechnol.*, **23**, 457-462, 2005.

[104] Tuschl, T., Zamore, P.D., Lehmann, R., Bartel, D.P., Sharp, P.A., Targeted mRNA degradation by double-stranded RNA *in vitro*. *Genes Dev.*, **13**, 3191-3197, 1999.

[105] Sledz, C.A., Holko, M., de Veer, M.J., Silverman, R.H., Williams, B.R. Activation of the interferon system by short-interfering RNAs. *Nat. Cell Biol.*, **5**, 771-772, 2003.

[106] Volpe, T.A., Kidner, C., Hall, I.M., Teng, G., Grewal, S.I., Martienssen, R.A. Regulation of heterochromatic silencing and histone H3 lysine-9 methylation by RNAi. *Science*, **297**, 1818-1819, 2002.

[107] Hall, I.M., Shankaranarayana, G.D., Noma, K., Ayoub, N., Cohen, A., Grewal, S.I. Establishment and maintenance of a heterochromatin domain. *Science*, **297**, 2232-2237, 2002.

[108] Verdel, A., Jia, S. Gerber, S., Sugiyama, T., Gygi, S., Grewal, S.I., Moazed, D. RNAi-mediated targeting of heterochromatin by the RITS complex. *Science*, **303**, 672-676, 2004.

[109] Kawasaki, H., Taira, K. Induction of DNA methylation and gene silencing by short interfering RNAs in human cells. *Nature*, **431**, 211-217, 2004.

[110] Dennler, S., Itoh, S., Vivien, D., ten Dijke, P., Huet S., Gauthier, J.M. Direct binding of Smad3 and Smad4 to critical TGF beta-inducible elements in the promoter of human plasminogen activator inhibitor-type 1 gene. *EMBO*, **17**, 3091-3100, 1998.

[111] Korchynskyi, O., ten Dijke, P. Identification and functional characterization of distinct critically important bone morphogenetic protein-specific response elements in the Id1 promoter. *J. Biol. Chem.*, **7**, 4883-4891, 2002.

[112] Paquet, M.E., Pece-Barbara, N., Vera, S., Cymerman, U., Karabegovic, A., Shovlin, C., Letarte, M. Analysis of several endoglin mutants reveals no endogenous mature or secreted protein capable of interfering with normal endoglin function. *Hum. Mol. Genet.*, **10**, 1347-1357, 2001.

[113] Weiskirchen, R., Gressner, A.M. Isolation and culture of hepatic stellate cells. *Methods Mol. Med.*, **117**, 99-113, 2005.

[114] Guyot, C., Combe, C., Balabaud, C., Bioulac-Sage, P., Desmoulire, A. Fibrogenic cell fate during fibrotic tissue remodelling observed in rat and human cultured liver slices. *J. Hepatol.*, **46**, 142-150, 2007.

[115] Mann, D.A., Smart, D.E. Transcriptional regulation of hepatic stellate cell activation. *Gut*, **50**, 891-896, 2002.

[116] Rockey, D.C., Housset, C.N., Friedman, S.L. Activation-dependent contractility of rat hepatic lipocytes in culture and in vivo. *J. Clin. Invest.*, **92**, 1795-1804, 1993.

[117] Schnabl, B., Kweon, Y.O., Frederick, J.P., Wang, X.F., Rippe, R.A., Brenner, D.A. The role of Smad3 in mediating mouse hepatic stellate cell activation. *Hepatology*, **34**, 89-100, 2001.

[118] Dooley, S., Hamzavi, J., Breitkopf, K., Wiercinska, E., Said, H.M., Lorenzen, J., Ten Dijke, P., Gressner, A.M. Smad7 prevents activation of hepatic stellate cells and liver fibrosis in rats. *Gastroenterology*, **125**, 178-191, 2003.

[119] Arias, M., Sauer-Lehnen, S., Treptau, J., Janoschek, N., Theuerkauf, I., Buettner, R., Gressner, A.M., Weiskirchen, R. Adenoviral expression of a transforming growth factor-beta1 antisense mRNA is effective in preventing liver fibrosis in bile-duct ligated rats. *BMC Gastroenterol.*, **3**, 29, 2003.

[120] Borkham-Kamphorst, E., Herrmann, J., Stoll, D., Treptau, J., Gressner, A.M., Weiskirchen, R. Dominant-negative soluble PDGF-beta receptor inhibits hepatic stellate cell activation and attenuates liver fibrosis. *Lab Invest.*, **84**, 766-777, 2004.

[121] Mancini, M.L., Verdi, J.M., Conley, B.A., Nicola, T., Spicer, D.B., Oxburgh, L.H., Vary, C.P. Endoglin is required for myogenic differentiation potential of neural crest stem cells. *Dev. Biol.*, **308**, 520-533, 2007.

[122] Weiskirchen, R., Moser, M., Weiskirchen, S., Erdel, M., Dahmen, S., Buettner, R., Gressner, A.M. LIM-domain protein cysteine- and glycine-rich protein 2 (CRP2) is a novel marker of hepatic stellate cells and binding partner of the protein inhibitor of activated STAT1. *Biochem. J.*, **359**, 485-496, 2001.

[123] Louis, H.A., Pino, J.D., Schmeichel, K.L., Pomis, P., Beckerle, M.C. Comparison of three members of the cysteine-rich protein family reveals functional conservation and divergent patterns of gene expression. *J. Biol. Chem.*, **272**, 27484-27491, 1997.

[124] Zumbrunn, J., Trueb, B. A zyxin-related protein whose synthesis is reduced in virally transformed fibroblasts. *Eur. J. Biochem.*, **241**, 657-663, 1996.

[125] Oxmann, D., Held-Feindt, J., Stark, A.M., Hattermann, K., Yoneda, T., Mentlein, R. Endoglin expression in metastatic breast cancer cells enhances their invasive phenotype. *Oncogene*, Epub ahead of print, 2008.

[126] Pece-Barbara, N., Vera, S., Kathirkamathamby, K., Liebner, S., Di Guglielmo, G.M., Dejana, E., Wrana, J.L., Letarte, M. Endoglin null endothelial cells proliferate faster and are more responsive to transforming growth factor beta1 with higher affinity receptors and an activated Alk1 pathway. *J. Biol. Chem.*, **280**, 27800-27808, 2005.

[127] Wiercinska, E., Wickert, L., Denecke, B., Said, H.M., Hamzavi, J., Gressner, A.M., Thorikay, M., ten Dijke, P., Mertens, P.R., Breitkopf, K., Dooley, S. Id1 is a critical mediator in TGF-beta-induced transdifferentiation of rat hepatic stellate cells. *Hepatology*, **43**, 1032-1041, 2006.

[128] Tsukada, S., Westwick, J.K., Ikejima, K., Sato, N., Rippe, R.A. SMAD and p38 MAPK signaling pathways independently regulate alpha1(I) collagen gene. *J. Biol. Chem.*, **280**, 10055-11064, 2005.

[129] Uemura, M., Swenson, E.S., Gaa, M.D., Giordano, F.J., Reiss, M., Wells, R.G. Smad2 and Smad3 play different roles in rat hepatic stellate cell function and alpha-smooth muscle actin organization. *Mol. Biol. Cell*, **16**, 4214-4224, 2005.

[130] Bernabeu, C., Conley, B.A., Vary, C.P. Novel biochemical pathways of endoglin in vascular cell physiology. *J. Cell Biochem.*, **102**, 1375-1388, 2007.

[131] Jiang, F., Parsons, C.J., Stefanovic, B. Gene expression profile of quiescent and activated rat hepatic stellate cells implicates Wnt signaling pathway in activation. *J. Hepatol.*, **45**, 401-409, 2006.

[132] Cheng, J.H., She, H., Han, Y.P., Wang, J., Xiong, S., Asahina, K., Tsukamoto, H. Wnt antagonism inhibits hepatic stellate cell activation and liver fibrosis. *Am. J. Physiol. Gastrointest. Liver Physiol.*, **294**, G39-G49, 2008.

[133] Kordes, C., Sawitza, I., Häussinger, D. Canonical Wnt signaling maintains the quiescent stage of hepatic stellate cells. *Biochem. Biophys. Res. Commun.*, **367**, 116-123, 2008.

[134] Kawser, C.A., Iredale, J.P., Winwood, P.J., Arthur, M.J. Rat hepatic stellate cell expression of alpha2-macroglobulin is a feature of cellular activation: implications for matrix remodelling in hepatic fibrosis. *Clin. Sci.*, **95**, 179-186, 1998.

[135] Andus, T., Ramadori, G., Heinrich, P.C., Knittel, T., Meyer zum Büschenfelde, K.H., Cultured Ito cells of rat liver express the alpha 2-macroglobulin gene *Eur. J. Biochem.*, **168**, 641-646, 1987.

[136] Gangadharan, B., Antrobus, R., Dwek, R.A., Zitzmann, N. Novel serum biomarker candidates for liver fibrosis in hepatitis C patients. *Clin. Chem.*, **53**, 1792-1799, 2007.

[137] LaMarre, J., Wollenberg, G.K., Gonias, S.L., Hayes, M.A. Cytokine binding and clearance properties of proteinase-activated alpha 2-macroglobulins. *Lab Invest.*, **65**, 3-14, 1991.

[138] Inagaki, Y., Nemoto, T., Nakao, A., Dijke, P., Kobayashi, K., Takehara, K., Greenwel, P. Interaction between GC box binding factors and Smad proteins modulates cell lineage-specific alpha 2(I) collagen gene transcription. *J Biol Chem.*, **276**, 16573-16579, 2001.

Eidesstattliche Erklärung

Ich versichere eidesstattlich, dass ich diesen Promotionsantrag erstmalig einreiche und keine früheren Versuche einer Promotion unternommen habe und dass ich die Dissertation selbstständig verfasst und alle in Anspruch genommenen Quellen und Hilfen in der Dissertation vollständig angegeben habe, - einschließlich Tabellen und Abbildungen - die anderen Werken im Wortlaut oder dem Sinn nach entnommen sind, in jedem Fall als Entlehnung kenntlich gemacht habe; dass diese Dissertation noch keiner anderen Fakultät zur Prüfung vorgelegen hat; dass sie abgesehen von unten angegebenen Teilpublikationen noch nicht veröffentlicht worden ist, sowie dass ich eine solche Veröffentlichung vor Abschluß des Promotionsverfahrens nicht vornehmen werde. Die Bestimmungen der geltendenden Promotionsordnung sind mir bekannt.

Aachen, den 4.4.2008 Wanda Nicolette Vreden

Appendix F

Curriculum Vitae

Name, Vorname:	Vreden, Wanda Nicolette	
Geburtsdatum/-ort:	06.12.1979 Duisburg	
Eltern:	Angelika Anna Maria Vreden-Birrenbach, Arzthelferin Norbert Vreden, Staatlich geprüfter Lebensmittelchemiker	
Nationalität:	deutsch	
Schulausbildung:	Achterathsfeld Grundschule, Moers, Germany	1986-1990
	Gymnasium Adolfinum, Moers, Germany Abschluss: Allgemeine Hochschulreife	1990-1999
Studium:	Biochemiestudium an der Ruhr-Universität Bochum, Germany Abschluss: Diplom	1999-2004
Auslandspraktika:	Wellcome Trust Biocentre, University of Dundee, Scotland (Praktikum 2 Monate)	2002
	University of Alberta, Edmonton, Canada (Diplomarbeit 9 Monate)	2003-2004
Promotion:	RWTH Aachen, Institut für Klinischen Chemie und Pathobiochemie des UK Aachen, Germany	2005-2008

Originalarbeiten:

Vreden, W.N., Meurer, S.K., Van de Leur, E., Gressner, A.M., Weiskirchen, R. Endoglin suppression interferes with the transdifferentiation of hepatic stellate cells to myofibroblasts. *Submitted to JBC*, **in revision**, 2008.

Buchbeiträge:

Weiskirchen, R., Borkham-Kamphorst, E., Meurer, S.K., Drews, F., Mohren, S., Hermann, J., Gressner, O.A., Scherner, O., Vreden, W., Kovalenko, E., Bomble, M., Gressner, A.M. A complex network of intra- and intercellular mediators regulate cellular activation and transdifferentiation of hepatic stellate cells. J. Bosch, A.K. Burroughs, F. Lammert, D. Lebrec, T. Sauerbruch (eds). *Springer Verlag, Heidelberg, Germany*, **in press**, 2008.

Abstrakts:

Vreden, W.N., Meurer, S.K., Weiskirchen, R., Gressner, A.M., Endoglin and its involvement in transdifferentiation of hepatic stellate cells *Zeitschrift für Gastroenterologie*, **45**, 99, 2007.

Scherner, O., Meurer, S.K., Borkham-Kamphorst, E., Sauer-Lehnen, S., Vreden, W.N., Gressner, A.M., Weiskirchen, R. Synergistic effects of Platelet-derived growth factor-BB and Transforming growth factor-β1 on profibrogenic activities in hepatic stellate cells *Zeitschrift für Gastroenterologie*, **46**, 87, 2008.

Scherner, O., Vreden, W.N., Meurer, S.K., Weiskirchen, R., Gressner A.M. BMP-7: The key antagonist of TGF-beta in liver fibrosis? *Hepatology*, **46**, 715A-716A, 2007.

Meurer, S.K., Vreden, W.N., Tihaa, L., Weiskirchen, R., Gressner A.M. Endoglin phosphorylation by TGF-beta receptors in transdifferentiating HSC *Hepatology*, **46**, 870A-871A, 2007.

Mohren, S., Vreden, W.N., Gressner, A.M., Weiskirchen, R. Gene polymorphisms in the secretory signal peptide of TGF-β1 affect the cellular synthesis, secretion and processing of TGF-β1 and secretion is modulated by the latent TGF-β binding protein-1

(LTBP-1) and furin protease *Zeitschrift für Gastroenterologie*, **45**, 854, 2007.

Meurer, S.K., Vreden, W.N., Tihaa, L., Weiskirchen, R., Gressner A.M. Endoglin is a critical regulator of the pro-fibrogenic TGF-beta signaling pathways in hepatic stellate cells *Hepatology*, **44**, 682A-682A, 2006.